Singular Value Decomposition Based Model Order Reduction Techniques

by

Ahmad Jazlan Bin Haja Mohideen

A thesis submitted to the School of Electrical, Electronic and Computer Engineering in partial fulfilment of the requirements for the degree of Doctor of Philosophy

Faculty of Engineering, Computing and Mathematics

University of Western Australia

September 2016

Statement of Originality

The content of this thesis are the results of original research and have not been submitted for a higher degree at any other institution. The content of Chapter 3 are currently under review for publication in an international refereed journal. The content of Chapter 4 and Chapter 5 have been published in international refereed journals. The content of Chapter 6 and Chapter 8 have been published in international refereed conference proceedings. The content of Chapter 7 have been presented at an international refereed conference and will appear in the conference proceedings.

Published International Refereed Journal Papers

1. Jazlan, A., Sreeram, V., Shaker, H.R.,Togneri, R. and Minh, H.B., Frequency Interval Cross Gramians for Linear and Bilinear Systems, *Asian Journal of Control*, Vol. 19, No. 1, pp. 22-34, (2016) - Chapter 4

2. Jazlan, A., Sreeram, V., Shaker, H.R. and Togneri, R., Frequency interval balanced truncation of discrete-time bilinear systems, *Cogent Engineering*, Vol. 3, No. 1, pp. 1-15, (2016) - Chapter 5

Journal Paper Submission Currently Under Review

1. Jazlan, A., Houlis, P., Sreeram, V. and Togneri, R., Comments on "A Parametrized Controller Reduction Technique via a New Frequency Weighted Model Reduction Formulation "- Under Review by *Asian Journal of Control* - Chapter 3

International Refereed Conference Papers

1. Jazlan, A., Sreeram, V., Togneri, R. and Bettayeb, M., Time weighted model reduction of flat plate solar collectors, In: *Proceedings of 4th Australian Control Conference*, pp. 107-111, Canberra, ACT (2014) - Chapter 6

2. Jazlan, A., Sreeram, V., Togneri, R. and Minh, H.B., Generalized Gramian Based Frequency Interval Model Reduction for Unstable Systems, In: *Proceedings of 6th Australian Control Conference*, Newcastle (2016) - Chapter 7

3. Kumar, D., Jazlan, A., Sreeram, V. and Togneri, R., Partial Fraction Expansion Based Frequency Weighted Balanced Singular Perturbation Approximation Model Reduction Technique with Error Bounds, In: *Proceedings of the 6th IFAC Symposium on System Structure and Control*, Vol. 49, No. 9, pp. 45-50, Istanbul (2016) - Chapter 8

The following papers represent related work which has been carried out to complement the work presented in the chapters of this thesis, however these papers have not been included as part of this thesis for brevity.

Related Journal and Conference Papers

1. Kumar, D., Jazlan, A., Sreeram, V. and Togneri, R., Partial Fraction Expansion based Frequency Weighted Model Reduction for Discrete Time Systems, *Numerical Algebra, Control and Optimization*, Vol. 6, No. 3, pp. 329-337 - Further work which complements Chapter 8.

2. Jazlan, A., Sreeram, V. and Togneri, R., Cross gramian based time interval model reduction, In: *Proceedings of the 5th Australian Control Conference*, pp. 274-276, Gold Coast, Queensland (2015) - Further work which complements Chapter 4.

3. Du, X., Jazlan, A., Sreeram, V., Togneri, R., Ghafoor, A. and Sahlan, S., A frequency limited model reduction technique for linear discrete systems, In: *Proceedings of the 3rd Australian Control Conference*, pp.421-426, Fremantle, Western Australia (2013) - Further work which complements Chapter 2.

4. Jazlan, A., Sreeram, V., Togneri, R., Mousa, W., A review on reduced order approximation for digital filters with complex coefficients using model reduction, In *Proceedings of the 3rd Australian Control Conference*, pp. 79-84, Fremantle, Western Australia (2013) - Further work which complements Chapter 2.

My doctoral studies were conducted under the guidance of Professor Dr. Victor Sreeram as my main supervisor and Professor Dr. Roberto Togneri as my co-supervisor. This research described in this thesis is the result of a collaborative effort with Professor Dr. Victor Sreeram, Professor Dr. Roberto Togneri, Associate Professor Dr. Hamid Reza Shaker from the University of Southern Denmark, Dr Pantazis Houlis, Dr. Ha Binh Minh from Banking University in Vietnam, Professor Dr. Maamar Bettayeb from Sharjah University in the United Arab Emirates and Dr Deepak Kumar from Motilal Nehru National Institute of Technology in India. The collaborators provided expertise and guidance and the main contribution to this work is my own.

Ahmad Jazlan Bin Haja Mohideen
School of Electrical, Electronic and Computer Engineering
The University of Western Australia
Crawley, W.A. 6009 Australia

Acknowledgements

First and foremost I would like to thank my main supervisor, Professor Dr. Victor Sreeram and co-supervisor Professor Dr. Roberto Togneri for giving me the opportunity to pursue my PhD studies under their supervision. Without their guidance and support I would not have been able to accomplish this major milestone.

I would also like to thank the Malaysian Ministry of Higher Education and the International Islamic University Malaysia for giving me the opportunity to pursue my studies in one of the Group of Eight Australian universities. My sincere appreciation also goes to the University of Western Australia for providing me with a six month Scholarship for International Research Fees (SIRF) which has helped me greatly in completing this thesis.

I would like to thank Associate Professor Dr. Asan Gani Abdul Muthalif, Associate Professor Dr. Shahrul Naim Sidek and all the staff of the Mechatronics Engineering Department at the International Islamic University Malaysia for supporting me throughout my stint as a graduate research student. I would also like to thank all the staff at the Kulliyah of Engineering, International Islamic University Malaysia. I look forward to producing high quality research and teaching upon my return.

I am deeply thankful to both my parents Dr. Haja Mohideen Bin Mohamed Ali and Samsunisha Yusof who have always been the pillars of strength in my life and have supported me throughout the ups and downs in my life. This thesis is dedicated to both of them. To my siblings and their spouses - Shamimah, Kamal Bacha Ibrahim, Mohamed Zafran and Nur Haslinda Harun, thank you for motivating me to achieve more each day. To my adorable nephews Mohammad Fauzan Irfan Bin Kamal Bacha and Zahin Azfar Bin Mohamed Zafran thank you for adding more happiness in my life.

I have gained a comprehensive understanding about model order reduction from many discussions with Dr. Shafishuhaza Sahlan and Dr. Wan Mariam Wan Muda.

Both of your ideas have inspired me to look at model order reduction from various angles and beyond theoretical aspects.

I have received strong support and encouragement from the Malaysian community in Perth. Thank you Safwan Samsuddin and Sharlinda Talib for supporting me during my early days in Perth. Thank you to all members of the Malaysian Postgraduate Students Association (MYPSA). Thank you Hasan Firdaus, Khairuzzaman Saudi, Mohd Hafiz Kamaruddin, Ahmad Husaini, Mohd Hafizi Abdul Rahman, Ku Ashman Ku Aziz, Azrul Azmi, Zainol Izwan Zulkifli, Ahmad Syakir, Jaffri Nasir and Ming Fook Lim.

Abstract

This thesis investigates the development of new singular value decomposition based model order reduction techniques.

Firstly a solution to the controller reduction problem via a parameterized double-sided frequency weighted controller reduction technique is developed for the feedback control of MIMO discrete time systems particularly for non-unity feedback control system configurations which have the controller located in the feedback path.

Secondly, new frequency interval cross gramians are developed for both linear and bilinear systems. New generalized Sylvester equations for calculating the frequency interval cross gramians are derived in order to be used to obtain information regarding controllability and observability of a system within a single matrix and therefore leading to increased computational efficiency.

Thirdly, a new model reduction method for discrete-time bilinear systems is developed based on newly derived frequency interval controllability and observability gramians for discrete-time bilinear systems.

Fourthly, time weighted cross gramians are developed and applied to a state space model derived from two partial differential equations representing the thermal dynamics of a flat plate solar collector.

Fifthly, generalized frequency interval controllability and observability gramians are introduced in order to obtain the frequency interval controllability and observability gramians for continuous-time linear systems which do not have a solution to the standard Lyapunov equation.

Finally, a new frequency weighted partial fraction expansion based model reduction technique is developed based on the partial fraction expansion approach. In order to further reduce the frequency weighted approximation error, singular perturbation approximation is incorporated into the algorithm.

Contents

List of Tables

List of Figures

Elementary Notations and Terminologies

Transfer function $G(s)$	$= \left[\begin{array}{c\|c} A & B \\ \hline C & D \end{array}\right] = C(sI - A)^{-1}B + D$
	$\Leftrightarrow$ State-space realization $\{A, B, C, D\}$
$\|G(s)\|_\infty$	Infinity norm of the system $G(s)$
$P > 0$	Positive definite matrix P
	Symmetric matrix P with positive eigenvalues
$P \geq 0$	Positive semidefinite matrix P
	Symmetric matrix P with non-negative eigenvalues
X^T or X'	Transpose of matrix or vector X
X^*	Complex conjugate transpose of matrix or vector X
X^{-1}	Inverse of matrix X
$\lambda_i(X)$	Eigenvalues of X
$\sigma(X)$	Singular values of X

Chapter 1

Introduction

In today's rapidly advancing technological world, mathematical models are a useful means to obtain a representation of a physical process. A physical system may be a chemical process, a multi-machine electrical power system, an attitude-control system of a space craft, a synchronous orbit satellite, a flexible space structure, very large scale integrated (VLSI) circuit, a power system, etc. Dynamical systems refer to systems in which the future behaviour depends on the past evolution. The methodology for obtaining a mathematical model which represents the characteristics of a particular dynamical system under consideration is a prerequistite for both simulation and control of the system.

Improving the accuracy of the mathematical model is essential, however as the degree of complexity of a particular process increases, the resulting mathematical model which represents the process will have a higher order which consequently becomes an obstacle to effectively analyze the system's behaviour, carry out simulations and implement control methods. In practice, one can obtain a fairly complex and a very high order model for the system upon discretizing the partial differential equations which represent a physical system. This complexity often makes it difficult to obtain a good understanding of the behaviour of the system.

Model order reduction refers to the process of approximating a high order model by a reduced order model while preserving the essential features of the original high

order model such as input-output behaviour, stability and passivity. The need to obtain such reduced order models arises due to limited computational and storage capabilities in practical applications. Similarly for simulations, performing a simulation of a high order model is commonly not feasible. Reduced order models can significantly reduce the computational complexity involved and hence enable faster simulation times.

Model order reduction methods can be divided into two broad categories, the first being moment matching techniques and the second being singular value decomposition based techniques. The concept behind moment matching techniques is that unnecessary poles are removed whereas dominant poles which have significant effects on the overall system performance are retained. The main advantage of moment matching techniques is the computational efficiency and hence these techniques are well suited to obtain reduced order models of very high order systems. However the disadvantage of moment matching techniques is that reduction errors may be large if the desired order of the the reduced order model is much smaller compared to the order of the original model.

Singular value decomposition (SVD) based techniques work by approximating a matrix by another matrix with a lower rank. The balanced truncation technique originally proposed by Moore is the foundation for singular value decomposition based model order reduction techniques [1]. In the balanced truncation technique, a given system is firstly transformed to a balanced realization such that each state is equally controllable and observable. The reduced order model is then obtained by truncating the least controllable and observable states. Two closely related singular value decomposition based methods are balanced singular perturbation approximation [2] and optimal Hankel norm approximation [3]. These singular value decomposition based model reduction methods guarantee the stability of the reduced order model and have easily computable frequency response error bounds. Singular value decomposition based model reduction techniques have been further developed and

applied to the design of single and multidimensional filters [4–8]. Another approach to address the model reduction problem is to apply optimization methods [9, 10].

In many chemical, electrical, mechanical, manufacturing and biological engineering applications the system being analyzed often exhibits non-linear behaviour. In general methods for analyzing non-linear systems are limited compared to methods for analyzing linear systems. Standard linearization methods performed on non-linear systems may not be sufficient to capture the characteristics of the non-linear system. Fortunately many non-linear systems can be represented by bilinear systems. Depending on the complexity of the system under observation, the process of deriving a bilinear mathematical model of the system may lead to a high order model which becomes an obstacle in understanding the behaviour of the system. Therefore model reduction techniques can be utilized to reduce the order of such high order bilinear systems. The essential theory of model reduction techniques for both linear and bilinear systems are also directly applicable to control configuration selection problems.

1.0.1 Organization and Contribution

In this thesis, we propose several singular value decomposition based model order reduction methods as described by Figure 1.

Chapter 2 presents an overview of of singular value decomposition based model order reduction techniques. Firstly the essential properties of balanced truncation and its closely related methods - balanced singular perturbation approximation and Hankel optimal norm approximation are presented. Several existing techniques are also reviewed in detail to provide a background understanding for the material presented in the following chapters.

In Chapter 3, a solution to the controller reduction problem via a parameterized double-sided frequency weighted controller reduction technique is developed for the feedback control of MIMO discrete time systems particularly for non-unity feedback

control system configurations which have the controller located in the feedback path. New frequency weights which are a function of a free parameter matrix are derived for the double sided frequency weighted model reduction problem. The infinity norm of the approximation error between the original closed loop system and the closed loop system with a reduced order controller can be significantly reduced by varying this free parameter matrix. The selection of an optimal value for this free parameter matrix which minimizes the infinity norm of the approximation error can be obtained by choosing a large value for the diagonal entries of this free parameter matrix without the need to construct an approximating function.

Chapter 4 focuses on the development of frequency interval cross gramians for both linear and bilinear systems. New generalized Sylvester equations for calculating the frequency interval cross gramians are derived in order to be used to obtain information regarding controllability and observability of a system within a single matrix. This information regarding the controllability and observability of a system contained within a single matrix can then be applied to both model order reduction and control configuration selection applications. The advantage of the proposed method is that it is computationally more efficient compared to existing gramian based techniques since only half of the number of equations need to be solved in order to obtain information regarding the controllability and observability of a system compared to existing techniques which require solving equations for both the controllability and observability gramians individually. Numerical examples are provided to demonstrate the computational efficiency of the proposed method which uses frequency interval cross gramians relative to existing methods in the context of control configuration selection.

Chapter 5 presents the development of a new model reduction method for discrete-time bilinear systems based on the balanced truncation framework. In many model reduction applications, it is advantageous to analyze the characteristics of the system with emphasis on particular frequency intervals of interest. In order to analyze

the degree of controllability and observability of discrete-time bilinear systems with emphasis on particular frequency intervals of interest, new generalized frequency interval controllability and observability gramians are introduced in this paper. These gramians are the solution to a pair of new generalized Lyapunov equations. The conditions for solvability of these new generalized Lyapunov equations are derived and a numerical solution method for solving these generalized Lyapunov equations is presented. Numerical examples which illustrate the usage of the new generalized frequency interval controllability and observability gramians as part of the balanced truncation framework are provided to demonstrate the performance of the proposed method.

Chapter 6 presents the application of time weighted model reduction using cross gramians on a state space model derived from two partial differential equations representing the instantaneous thermal balance of a differential element of length along the absorber plate and the absorber plate to fluid heat convection process respectively of a flat plate solar collector. Finite difference method is applied onto both these partial differential equations where discretization in time and space is performed resulting in a high order linear discrete time invariant Single Input Single Output (SISO) state space model. Numerical results are provided to demonstrate and compare the performance of time weighted model reduction relative to balanced truncation.

In Chapter 7, generalized frequency interval controllability and observability gramians are introduced in order to obtain the frequency interval controllability and observability gramians for continuous-time linear systems which do not have a solution to the Lyapunov equation. The applicability of these generalized gramians to be used in model reduction is demonstrated.

In Chapter 8, a new frequency weighted partial fraction expansion based model reduction technique is developed based on the partial fraction expansion approach. In order to further reduce the frequency weighted approximation error, singular per-

turbation approximation is incorporated into the algorithm. This technique results in stable reduced order models regardless if single sided or double sided weights are used. Error bounds are also derived for the proposed method. For minimization of the frequency weighted approximation error, free parameters are introduced into the algorithm. A numerical example is provided in order to validate the proposed algorithm.

Chapter 9 presents the conclusions of this thesis together with suggestions for future research work.

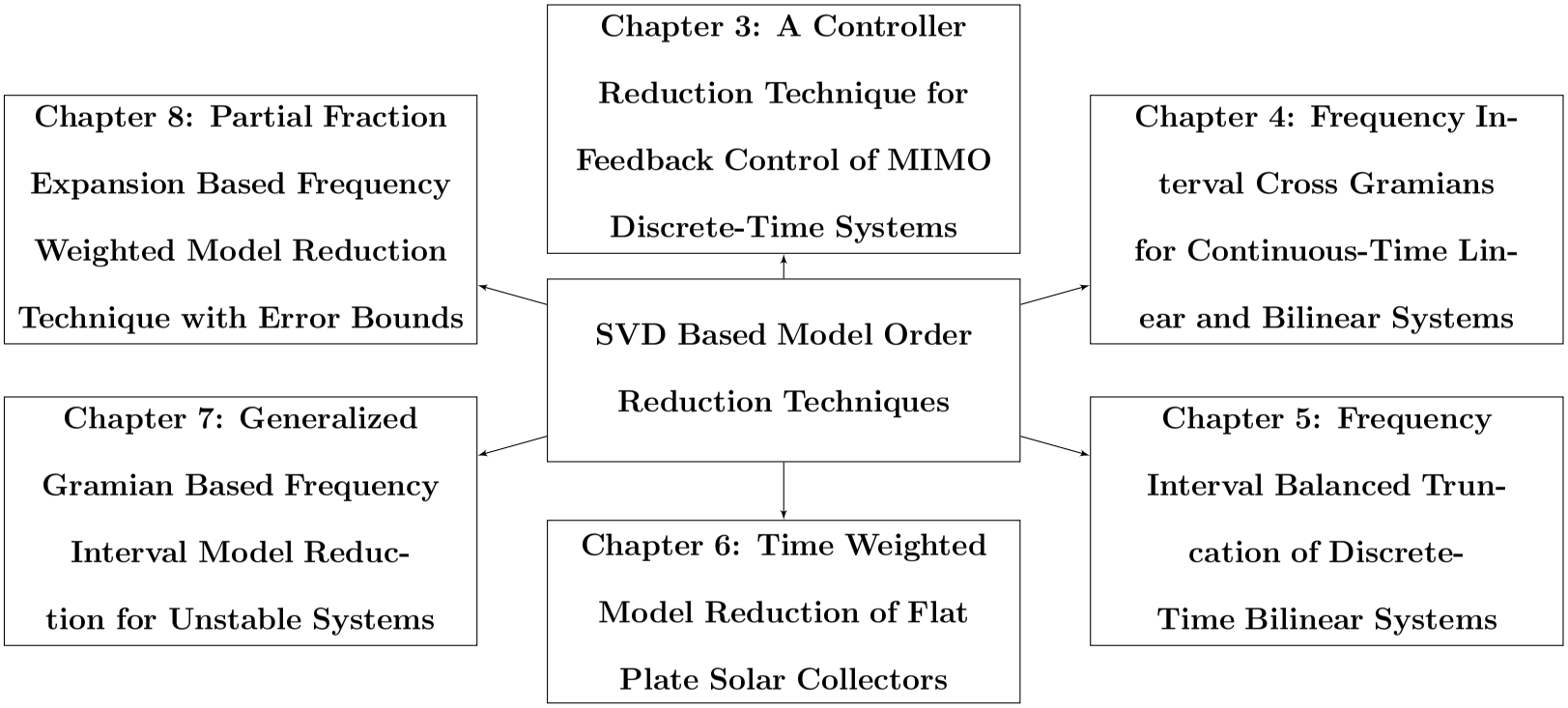

Figure 1: Proposed Singular value decomposition based model order reduction methods in this thesis.

Chapter 2

Singular Value Decomposition Based Model Order Reduction Techniques: A Review

2.1 Preliminaries

The methods described in this thesis mainly originate from the balanced truncation method [1]. A section on balanced truncation together with closely related concepts are provided in this section.

2.1.1 Singular Value Decomposition

Singular value decomposition (SVD) is a very useful tool which can be used to decompose a a matrix into its corresponding eigenvectors and eigenvalues and subsequently extracting the singular values of the matrix. The singular values obtained using SVD can then be used as part of a model reduction technique where the the degree of controllability and observability of each of the states of a particular state space model are identified and subsequently the least controllable and observable states can be truncated. Let A_{svd} be a rectangular $p \times m$ matrix with $p > m$, then

there exists a singular value decomposition factorization of A_{svd} of the form:

$$A_{svd} = U_{svd} S_{svd} V_{svd}^T$$

where U_{svd} and V_{svd} are $p \times p$ and $m \times m$ orthogonal matrices of the eigenvectors of $A_{svd}^T A_{svd}$. While S_{svd} is a diagonal matrix whose entries are the nonnegative square roots of the eigenvalues σ_i, $\{i = 1, 2, \ldots, r\}$ of $A_{svd}^T A_{svd}$. The singular values of A_{svd}, i.e. σ_i are arranged in descending order. This can be easily shown below:

$$\begin{aligned} A_{svd} &= \begin{bmatrix} A_{1,1} & \cdots & A_{1,m} \\ \vdots & \ddots & \vdots \\ A_{p,1} & \cdots & A_{p,m} \end{bmatrix} \\ &= U_{svd} S_{svd} V_{svd} \\ &= \begin{bmatrix} U_{1,1} & \cdots & U_{1,p} \\ \vdots & \ddots & \vdots \\ U_{p_s,1} & \cdots & U_{p_s,p_s} \end{bmatrix} \begin{bmatrix} \sigma_{1,1} & \cdots & 0 \\ \vdots & \ddots & \vdots \\ 0 & \cdots & \sigma_{p,m} \end{bmatrix} \begin{bmatrix} V_{1,1} & \cdots & V_{1,m} \\ \vdots & \ddots & \vdots \\ V_{m,1} & \cdots & V_{m,m} \end{bmatrix} \end{aligned}$$

where $\sigma_{1,1} > \sigma_{2,2} > \ldots > \sigma_{p,m}$.

The following section demonstrates the usage of singular value decomposition as part of the balanced truncation model order reduction method.

2.1.2 Balanced Truncation Method

A particular system under consideration can have an infinite number of possible state space realizations. Out of these different possibilities some realizations are more valuable to be used for simulation and control. A particular state space realization which is crucial for model order reduction is known as the internally balanced realization. The internally balanced realization is a realization such that the controllability and observability gramians are equal and diagonal. The degree of controllability and observability of each of the states can then be identified from the Hankel singular values. The framework of the balanced truncation method is described as follows [1].

Consider an n^{th} order, stable and minimal system $G(s)$ described by the following state space realization:

$$\dot{x}(t) = Ax(t) + Bu(t)$$
$$y(t) = Cx(t) + Du(t) \tag{2.1}$$

where $x(t) \in \mathbb{R}^n, u(t) \in \mathbb{R}^p$ and $y(t) \in \mathbb{R}^q$. The corresponding transfer function is $G(s) = C(sI - A)^{-1}B + D$ and can also be written as $G(s) = \left[\begin{array}{c|c} A & B \\ \hline C & D \end{array}\right]$.
Let P and Q be the controllability and the observability gramians which satisfy the following Lyapunov equations:

$$AP + PA^T + BB^T = 0 \tag{2.2}$$
$$A^TQ + QA + C^TC = 0 \tag{2.3}$$

Let T be a transformation matrix obtained by simultaneously diagonalizing the gramians P and Q. For a system which is both controllable and observable, both P and Q will be positive definite. P and Q can be factorized as $P = L_cL_c^T$ and $Q = L_oL_o^T$ respectively by using Cholesky factorization. The singular value decomposition of $L_o^TL_c$ is obtained such that $L_o^TL_c = USV^T$. The balancing transformation matrix T can be computed from:

$$T = L_cVS^{\frac{1}{2}}, \quad , T^{-1} = S^{\frac{-1}{2}}U^TL_o^T$$

This transformation matrix diagonalizes the controllability and observability gramians to become equal and diagonal as follows:

$$T^TQT = T^{-1}PT^{-T} = \Sigma = \begin{bmatrix} \Sigma_1 & 0 \\ 0 & \Sigma_2 \end{bmatrix}$$

where $\Sigma_1 = diag\{\sigma_1, \sigma_2, \ldots, \sigma_r\}$, $\Sigma_2 = diag\{\sigma_{r+1}, \ldots, \sigma_n\}$, $\sigma_i \geq \sigma_{i+1},\ i = 1, 2, \ldots, n-1$, $\sigma_r > \sigma_{r+1}$ and σ_i are the Hankel singular values arranged in descending order. The Hankel singular values contains valuable information about the energy corresponding to each state of the system. The original system is then transformed to obtain the internally balanced realization. The internally balanced realization is then partitioned to maintain the highly controllable and observable states in the reduced order model and discard the least controllable and observable states as follows:

$$\begin{aligned} \bar{A} &= T^{-1}AT = \begin{bmatrix} A_{11} & A_{12} \\ A_{21} & A_{22} \end{bmatrix}, \quad \bar{B} = T^{-1}B = \begin{bmatrix} B_1 \\ B_2 \end{bmatrix}, \\ \bar{C} &= CT = \begin{bmatrix} C_1 & C_2 \end{bmatrix}, \qquad \bar{D} = D \end{aligned} \tag{2.4}$$

The reduced order model is given by $G_r(s) = C_1(sI - A_{11})^{-1}B_1 + D$.

The error bounds for the balanced truncation technique are described by:

$$||G(s) - G_r(s)||_\infty \leq 2 \sum_{i=r+1}^{n} \sigma_i \tag{2.5}$$

The H_∞ norm of the error - $||G(s) - G_r(s)||_\infty$ is defined as the maximum of the highest peak of the frequency response error - $G(s) - G_r(s)$.

Remark 2.1: The concept behind the balanced truncation technique can be described as follows:

1. States that are difficult to reach, requiring a large amount of energy to reach, are in the span of the eigenvectors of the controllability gramian P which corresponds to small eigenvalues

2. States that are difficult to observe and yield a small amount of observation energy, are those that lie in the span of the eigenvectors of the observability gramians Q corresponding to small eigenvalues.

Remark 2.2: In the balanced truncation method the following important propeties apply:

1. The balanced truncation technique can only be applied to an asymptotically stable system (A, B, C, D) in order to obtained the balanced realization.

2. The subsystem $\{A_{11}, B_1, C_1, D\}$ is both controllable and observable.

In addition to reducing the order of high order models in control engineering applications such as the spatial control of mechanical vibrations [12, 14–16], balanced truncation is also effective for approximating high order Finite Impulse Response (FIR) filters by lower order Infinite Impulse Response (IIR) filters to be used in signal processing. The usage of balanced truncation to approximate a high order Finite Impulse Response (FIR) filter with complex coefficients by a lower order Infinite Impulse Response (IIR) filter used in geological signal processing has been demonstrated in [11]. Filters with complex coefficients can fulfill the requirements of having arbitrary magnitude and group delay responses [17]. The design of low order and approximately linear phase IIR filters has been described in [18].

2.1.3 Balanced Singular Perturbation Approximation

The balanced singular perturbation approximation method proposed by Liu and Anderson [2] is one of the variations to the original balanced truncation method by Moore [1]. The concept of the balanced singular perturbation approximation method is described as follows.

From the internally balanced realization described in (2.4) we have:

$$G(s) = \left[\begin{array}{c|c} \bar{A} & \bar{B} \\ \hline \bar{C} & \bar{D} \end{array}\right] = \left[\begin{array}{cc|c} A_{11} & A_{12} & B_1 \\ A_{21} & A_{22} & B_2 \\ \hline C_1 & C_2 & D \end{array}\right]$$

the transfer function $G(s)$ can be written in the form

$$G(s) = \begin{bmatrix} C_1 & C_2 \end{bmatrix} \begin{bmatrix} sI_r - A_{11} & -A_{12} \\ -A_{21} & sI_{n-r} - A_{22} \end{bmatrix}^{-1} \begin{bmatrix} B_1 \\ B_2 \end{bmatrix} + D.$$

decomposing the transfer function $G(s)$ additively as

$$G(s) = G_1(s) + G_2(s)$$

gives

$$G_1(s) = \bar{C}_{spa}(sI_r - \bar{A}_{spa}(s))^{-1}\bar{B}_{spa}(s) + D$$

$$G_2(s) = C_2(sI_{n-r} - A_{22})^{-1}B_2 \tag{2.6}$$

where

$$\bar{A}_{spa}(s) = A_{11} + A_{12}(sI_{n-r} - A_{22})^{-1}A_{21} \tag{2.7}$$

$$\bar{B}_{spa}(s) = B_1 + A_{12}(sI_{n-r} - A_{22})^{-1}B_2 \tag{2.8}$$

$$\bar{C}_{spa}(s) = C_1 + C_2(sI_{n-r} - A_{22})^{-1}A_{21.} \tag{2.9}$$

If the subsystem $G_2(s)$ is stable and its states have very fast transient dynamics in the neighbourhood of a frequency $s = \sigma_o$, then by ignoring $G_2(s)$ the reduced order model of $G(s)$ can be described by:

$$\bar{G}_{spa}(\sigma_0) = \bar{C}_{spa}(\sigma_0)[sI_r - \bar{A}_{spa}(\sigma_0)]^{-1}\bar{B}_{spa}(\sigma_0) + \bar{D}_{spa}(\sigma_0)$$

where $\bar{D}_{spa}(\sigma_0) = D + C_2(\sigma_0 I - A_{22})^{-1}B_2$. In addition $\bar{A}_{spa}(\sigma_0)$, $\bar{B}_{spa}(\sigma_0)$ and $\bar{C}_{spa}(\sigma_0)$ are as defined in (2.7), (2.8) and (2.9) by substituting s with σ_0.

There are two extreme cases of the balanced singular perturbation approximation which are presented as follows:

1. The first case occurs when $\sigma_o = 0$. The reduced order model for this case is given by

   $$\bar{G}_{spa}(s)(0) = \bar{C}_{spa}(0)[sI_r - \bar{A}_{spa}(0)]^{-1}\bar{B}_{spa}(0) + \bar{D}_{spa}(0)$$

   where

   $$\bar{A}_{spa}(0) = A_{11} - A_{12}A_{22}^{-1}A_{21}$$

   $$\bar{B}_{spa}(0) = B_1 - A_{12}A_{22}^{-1}B_2$$

   $$\bar{C}_{spa}(0) = C_1 - C_2A_{22}^{-1}A_{21}$$

   $$\bar{D}_{spa}(0) = D - C_2A_{22}^{-1}B_2$$

which is the balanced singular perturbation approximation method described by Liu and Anderson [2].

2. The second case occurs when $\sigma_0 \to \infty$. Hence we will obtain

$$\bar{A}_{spa}(\sigma_o) \to A_{11}, \quad \bar{B}_{spa}(\sigma_o) \to B_1, \quad \bar{C}_{spa}(\sigma_o) \to C_1, \quad \bar{D}_{spa}(\sigma_o) \to D$$

which is equivalent to the standard balanced truncation method by Moore [1].

Remark 2.3: Both the standard balanced truncation method and balanced singular perturbation approximation method yield minimal and stable reduced order models and both methods share the same H_∞-norm frequency response error bound formula described in (2.5).

Remark 2.4: The balanced truncation and balanced singular perturbation approximation methods are connected by a frequency inversion $s \to \frac{1}{s}$ as shown below

1. Given $G(s)$ in the balanced form, define $H(s) = G(\frac{1}{s})$
2. Define a reduced order model $H_r(s)$ obtained using the balanced truncation method from $H(s)$
3. Define $G_r(s) = H_r(\frac{1}{s})$ where $G_r(s)$ is the reduced order model from the balanced truncation of $G(s)$.

Remark 2.5: Balanced truncation and singular perturbation approximation have the following reciprocal property [2]:

1. The balanced truncation technique tends to have smaller errors at high frequencies and larger errors at low frequencies.
2. The singular perturbation approximation technique tends to have large errors at high frequencies and smaller errors at low frequencies.

In addition to model order reduction, singular perturbations have been widely applied in many aspects of control theory [19–23].

2.1.4 Controller Reduction

Let $G(s)$ be a transfer function matrix of a linear time-invariant plant and $K(s)$ be the transfer function matrix of the corresponding high order controller for the closed loop system shown in Figure 2.1. The reduced order controller which approximates the original high order controller $K(s)$ is denoted by $K_r(s)$. This reduced order controller $K_r(s)$ can then be placed into the closed loop configuration as shown in the Figure 2.2 to substitute the original high order controller. The following conditions are applicable to controller reductions:

1. $K(s)$ and $K_r(s)$ have the same number of poles in the open right half plane and no poles on the imaginary axis.

2. Either

$$\left\|[K(s) - K_r(s)]G(s)[I + K(s)G(s)^{-1}]\right\|_\infty < 1$$

or

$$\left\|[I + G(s)K(s)]^{-1}G(s)[K(s) - K_r(s)]\right\|_\infty < 1$$

where $G(s)(I - K(s)G(s))^{-1} = (I + G(s)K(s))^{-1}G(s)$.

2.1.4.1 Closed-loop Transfer Functions Obtained by Considering Frequency Weightings

The closed-loop transfer function matrices for the configurations in Figure 2.1 and Figure 2.2 which employ the high order controller $K(s)$ and the low order controller $K_r(s)$ respectively are described by:

$$W(s) = G(s)K(s)[I + G(s)K(s)]^{-1} = I - [I + G(s)K(s)]^{-1}$$

and

$$W_r(s) = G(s)K_r(s)[I + G(s)K_r(s)]^{-1} = I - [I + G(s)K_r(s)]^{-1}$$

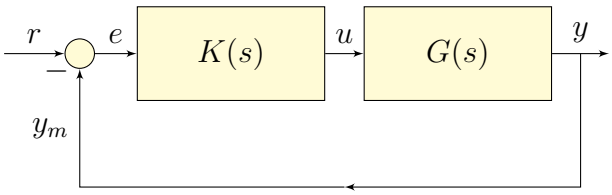

Figure 2.1: Closed-Loop System Configuration with Full Order Controller $K(s)$.

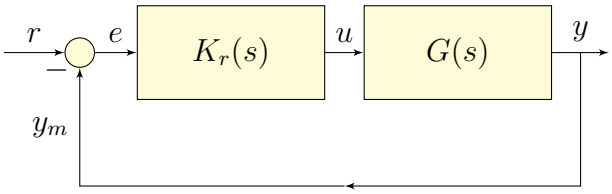

Figure 2.2: Closed-Loop System Configuration with Reduced Order Controller $K_r(s)$.

Finding the difference between the $W(s)$ and $W_r(s)$ yields [24]:

$$\begin{aligned} W(s) - W_r(s) &= G(s)K(s)[I + G(s)K(s)]^{-1} - G(s)K_r(s)[I + G(s)K_r(s)]^{-1} \\ &\approx (I + G(s)K(s))^{-1}G(s)(K(s) - K_r(s))(I + G(s)K(s))^{-1} \end{aligned}$$

which is in the form of a double-sided frequency weighted model reduction problem where the input weight is given by $V_1(s) = (I + G(s)K(s))^{-1}G(s)$ and the output weight is given by $V_2(s) = (I + G(s)K(s))^{-1}$. Hence, the objective of this frequency weighted model reduction problem is to find the reduced order controller $K_r(s)$ such that:

1. $K(s)$ and $K_r(s)$ have the same number of poles in the open right half plane and no poles on the imaginary axis,

2. and the index

$$\left\| G(s)K(s)[I + G(s)K(s)]^{-1} - G(s)K_r(s)[I + G(s)K_r(s)]^{-1} \right\|_\infty$$

is minimized.

2.2 Frequency Weighted Model Reduction Technique

The original balanced truncation technique was further developed by Enns [25]. This further development incorporated frequency weighting into the original balanced truncation technique resulting in the frequency weighted model reduction problem formulation. Incorporating frequency weighting as part of the model reduction framework was motivated by the controller reduction problem described previously in section 2.1.4. The following section describes the usage of frequency weighting to form an augmented system. This augmented system is the basis for the frequency weighted model reduction methods by Enns, Lin and Chiu, Varga and Anderson and also Wang, Sreeram and Liu [25–28] which are also described in this chapter.

2.2.1 Frequency Weighting

Let the transfer function of the original stable system be given by $G(s) = \left[\begin{array}{c|c} A & B \\ \hline C & D \end{array}\right]$ where $\{A, B, C, D\}$ is a minimal state-space realization. Let the transfer functions of the stable input and output weights be $V(s) = \left[\begin{array}{c|c} A_V & B_V \\ \hline C_V & D_V \end{array}\right]$ and $W(s) = \left[\begin{array}{c|c} A_W & B_W \\ \hline C_W & D_W \end{array}\right]$ where $\{A_V, B_V, C_V, D_V\}$ and $\{A_W, B_W, C_W, D_W\}$ are minimal realizations. The state-space realization of the augmented system $W(s)G(s)V(s)$ (as shown in Figure 2.3) is given by

$$\left[\begin{array}{c|c} \tilde{A} & \tilde{B} \\ \hline \tilde{C} & \tilde{D} \end{array}\right] = \left[\begin{array}{ccc|c} A_W & B_W C & B_W D C_V & B_W D D_V \\ 0 & A & B C_V & B D_V \\ 0 & 0 & A_V & B_V \\ \hline C_W & D_W C & D_W D C_V & D_W D D_V \end{array}\right] \tag{2.10}$$

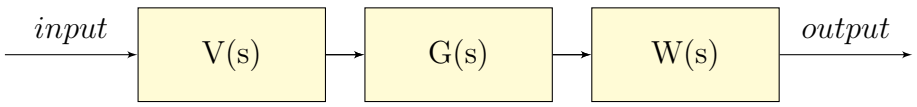

Figure 2.3: Input/Output augmented system

The controllability and observability Gramians of the augmented realization $\left\{\tilde{A}, \tilde{B}, \tilde{C}, \tilde{D}\right\}$ are given by

$$\tilde{P} = \begin{bmatrix} P_W & P_{12} & P_{13} \\ P_{12}^T & P_E & P_{23} \\ P_{13}^T & P_{23}^T & P_V \end{bmatrix} \text{ and } \tilde{Q} = \begin{bmatrix} Q_W & Q_{12} & Q_{13} \\ Q_{12}^T & Q_E & Q_{23} \\ Q_{13}^T & Q_{23}^T & Q_V \end{bmatrix} \tag{2.11}$$

where P_E and Q_E are the frequency weighted controllability and observability Gramians defined by Enns [25] which satisfies the following Lyapunov equations:

$$\tilde{A}\tilde{P} + \tilde{P}\tilde{A}^T + \tilde{B}\tilde{B}^T = 0 \tag{2.12}$$

$$\tilde{A}^T\tilde{Q} + \tilde{Q}\tilde{A} + \tilde{C}^T\tilde{C} = 0 \tag{2.13}$$

Assuming that there are no pole-zero cancellations in $W(s)G(s)V(s)$, the gramians, $\tilde{P}$ and $\tilde{Q}$ are positive definite.

2.2.2 Enns Method

Enns technique [25] is based on expanding the (2,2) blocks of equations (2.12) and (2.13) for controllability and observability Gramian respectively. This yields the following equations:

$$AP_E + P_E A^T + X = 0 \tag{2.14}$$

$$A^T Q_E + Q_E A + Y = 0 \tag{2.15}$$

where

$$X = BC_V P_{23}^T + P_{23} C_V^T B^T + BD_V D_V^T B^T \tag{2.16}$$

$$Y = C^T B_W^T Q_{12} + Q_{12}^T B_W C + C^T D_W^T D_W C \tag{2.17}$$

The Gramians P_E and Q_E are then diagonalized simultaneously

$$T^{-1}P_E T^{-T} = T^T Q_E T = \Sigma = diag(\sigma_1, \sigma_2, .., \sigma_n)$$

where $\sigma_1 > \sigma_2 > ... > \sigma_n > 0$ are the frequency weighted Hankel singular values. Transforming and partitioning the original system yields the following:

$$\left[\begin{array}{c|c} T^{-1}AT & T^{-1}B \\ \hline CT & D \end{array}\right] = \left[\begin{array}{cc|c} A_{11} & A_{12} & B_1 \\ A_{21} & A_{22} & B_2 \\ \hline C_1 & C_2 & D \end{array}\right] \tag{2.18}$$

where A_{11} depends on the order of the required truncated model. Hence this gives the Enns reduced order model $G_r(s)$:

$$G_r(s) = \left[\begin{array}{c|c} A_{11} & B_1 \\ \hline C_1 & D \end{array}\right] \tag{2.19}$$

The main concept behind Enns method is based on simultaneously diagonalizing the solutions of the Lyapunov equations as given by equations (2.14) and (2.15). However, Enns method cannot guarantee the stability of reduced order models as both of the matrices X and Y are not guaranteed to be positive semidefinite. Several modifications to the Enns technique are proposed in the literature to overcome this stability problem.

2.2.3 Lin and Chiu's Technique

Lin and Chiu [26] proposed the following technique to overcome the stability problem in Enns technique. Firstly by using the following transformation matrix:

$$\tilde{T} = \begin{bmatrix} I & -Q_W^{-1}Q_{12} & 0 \\ 0 & I & P_{23}P_V^{-1} \\ 0 & 0 & I \end{bmatrix} \tag{2.20}$$

the gramians of the augmented system (2.10) are first transformed using the transformation matrix $\tilde{T}$ to yield the following forms $\hat{P}$ and $\hat{Q}$ which have block diagonal

structures:

$$\hat{P} = \begin{bmatrix} \hat{P}_W & \hat{P}_{12} & P_{13} \\ \hat{P}_{12}^T & P_{LC} & 0 \\ P_{13}^T & 0 & P_V \end{bmatrix}, \quad \hat{Q} = \begin{bmatrix} \hat{Q}_W & 0 & Q_{13} \\ 0 & Q_{LC} & \hat{Q}_{23} \\ \hat{Q}_{13}^T & \hat{Q}_{23}^T & Q_V \end{bmatrix} \tag{2.21}$$

where $P_{LC} = P_E - P_{23}P_V^{-1}P_{23}^T$ and $Q_{LC} = Q_E - Q_{12}^T Q_W^{-1} Q_{12}$.

The corresponding state-space realizations have the following structures:

$$\hat{G}(s) = \left[\begin{array}{c|c} \hat{A} & \hat{B} \\ \hline \hat{C} & \hat{D} \end{array}\right] = \left[\begin{array}{c|c} \tilde{T}^{-1}\tilde{A}\tilde{T} & \tilde{T}^{-1}\tilde{B} \\ \hline \tilde{C}\tilde{T} & \tilde{D} \end{array}\right]$$

$$= \left[\begin{array}{ccc|c} A_W & X_{12} & X_{13} & X_1 \\ 0 & A & X_{23} & X_2 \\ 0 & 0 & A_V & B_V \\ \hline C_W & Y_1 & Y_2 & D_W D D_V \end{array}\right]$$

where

$$X_{12} = Q_W^{-1}Q_{12}A - A_W Q_W^{-1}Q_{12} + B_W C \tag{2.22}$$

$$X_{23} = AP_{23}P_V^{-1} - P_{23}P_V^{-1}A_V + BC_V \tag{2.23}$$

$$X_{13} = B_W C P_{23} P_V^{-1} + Q_W^{-1}Q_{12}AP_{23}P_V^{-1} + B_W D C_V + Q_W^{-1}Q_{12}BC_V - Q_W^{-1}Q_{12}P_{23}P_V^{-1}A_V \tag{2.24}$$

$$X_1 = B_W D D_V + Q_W^{-1}Q_{12}BD_V - Q_W^{-1}Q_{12}P_{23}P_V^{-1}B_V \tag{2.25}$$

$$X_2 = BD_V - P_{23}P_V^{-1}B_V \tag{2.26}$$

$$Y_1 = D_W C - C_W Q_W^{-1}Q_{12} \tag{2.27}$$

$$Y_2 = D_W C P_{23} P_V^{-1} + D_W D C_V \tag{2.28}$$

$$\hat{D} = D_W D D_V \tag{2.29}$$

Note that the transformation matrix $\tilde{T}$ does not change the diagonal blocks of the system matrix $\tilde{A}$.

The new realizations $\hat{G}(s) = \left\{\hat{A}, \hat{B}, \hat{C}, \hat{D}\right\}$ now satisfy the following Lyapunov

equations:

$$\hat{A}\hat{P} + \hat{P}\hat{A}^T + \hat{B}\hat{B}^T = 0 \tag{2.30}$$

$$\hat{A}^T\hat{Q} + \hat{Q}\hat{A} + \hat{C}^T\hat{C} = 0. \tag{2.31}$$

Diagonalizing the weighted gramians $\{P_{LC}, Q_{LC}\}$ of the system $\{A, X_2, Y_1\}$ which satisfy:

$$AP_{LC} + P_{LC}A^T + X_2X_2^T = 0$$

$$A^TQ_{LC} + Q_{LC}A + Y_1^TY_1 = 0$$

yields

$$T_{LC}^{-1}P_{LC}T_{LC}^{-T} = T_{LC}^TQ_{LC}T_{LC} = diag(\sigma_1, \sigma_2 \ldots, \sigma_r, \sigma_{r+1}, \ldots, \sigma_n) \tag{2.32}$$

where $\sigma_1 \geq \sigma_2 \geq \cdots \geq \sigma_n > 0$ and $\sigma_r > \sigma_{r+1}$. The reduced order model is then obtained by transforming, partitioning and truncating the original system realization. Since the realization $\{A, X_2, Y_1\}$ satisfies the Lyapunov equation, this method guarantees the stability of the reduced order models for the case of double sided weightings.

2.2.4 Varga and Anderson's modification to Lin and Chiu's Technique

In controller reduction applications, the input and outputs weights applied in a double sided frequency weighting are of the form $(I+G(s)K(s))^{-1}$ and $(I+G(s)K(s)^{-1}G(s))$ where $K(s)$ is the controller for the plant $G(s)$. For these weights it is inevitable that Lin and Chiu's requirement of no pole/zero cancellation between the weights and the controller will not be fullfilled.

To address this problem, Varga and Anderson [28] proposed a frequency weighted model reduction method based on simultaneously diagonalizing another pair of controllability and observability gramians denoted by P_{VA} and Q_{VA}

$$T^TQ_{VA}T = T^{-1}P_{VA}T^{-T} = diag(\sigma_1, \sigma_2, \ldots, \sigma_n)$$

where

$$P_{VA} = P_E - \alpha_c^2 P_{23} P_V^{-1} P_{23}^T \quad (2.33)$$

$$Q_{VA} = Q_E - \alpha_o^2 Q_{12}^T Q_W^{-1} Q_{12} \quad (2.34)$$

$0 \leq \alpha_c \leq 1, 0 \leq \alpha_o \leq 1$, where $\sigma_i \geq \sigma_{i+1}$, $i = 1, 2, \cdots, n-1$ and $\sigma_r \geq \sigma_{r+1}$. Reduced order models are then obtained by transforming and partitioning the original system.

Remark 2.6: For the case $\alpha_c = \alpha_o = 0$, it follows that this method is equivalent to Enns technique and the stability of the reduced order model is not guaranteed.

Remark 2.7: For the case $\alpha_c = \alpha_o = 1$, it follows that this method is equivalent to Lin and Chiu's technique and the stability of the reduced order model is guaranteed.

2.2.5 Wang, Sreeram and Liu's Technique

Another method that addresses the stability problem associated with Enns' [25] method was proposed by Wang, Sreeram and Liu [27]. The main concept of this method is to guarantee the positive semidefiniteness of the X and Y matrices defined in (2.16) and (2.17). New controllability and observability gramians denoted by P_{WSL} and Q_{WSL} are obtained by solving the following Lyapunov equations:

$$AP_{WSL} + P_{WSL}A^T + B_{WSL}B_{WSL}^T = 0 \quad (2.35)$$

$$A^T Q_{WSL} + Q_{WSL}A + C_{WSL}^T C_{WSL} = 0 \quad (2.36)$$

Both of these gramians P_{WSL} and Q_{WSL} are simultaneously diagonalized. The matrices B_{WSL} and C_{WSL} in (2.35) and (2.36) are fictitious input and output matrices determined by:

$$B_{WSL} = U_{WSL}|S_{WSL}|^{\frac{1}{2}}$$

$$C_{WSL} = |R_{WSL}|^{\frac{1}{2}} V_{WSL}^T$$

The terms on the RHS of the above equations, U_{WSL}, S_{WSL}, V_{WSL}, and R_{WSL} are obtained from the following orthogonal eigenvalue decompositions of the symmetric

matrices X and Y:

$$\begin{aligned} X &= U_{WSL} S_{WSL} U_{WSL}^T \\ Y &= V_{WSL} R_{WSL} V_{WSL}^T \end{aligned}$$

where $S_{WSL} = diag(s_1, s_2, ...s_n)$, $R_{WSL} = diag(r_1, r_2, ...r_n)$, $R_{WSL} = diag(r_1, r_2, ...r_n)$, $|s_1| \geq s_2 \geq ...|s_n| \geq 0$ and $|r_1| \geq |r_2| \geq ... \geq |r_n| \geq 0$

Since

$$\begin{aligned} X &\leq B_{WSL} B_{WSL}^T \geq 0 \\ Y &\leq C_{WSL}^T C_{WSL} \geq 0 \end{aligned}$$

and $\{A, B_{WSL}, C_{WSL}\}$ is minimal, the stability of the reduced order models for the case of double-sided weighting is guaranteed.

Remark 2.8: If $X \geq 0$ and $Y \geq 0$ then Wang, Sreeram and Liu's technique is equivalent to Enns technique.

Remark 2.9: The following error bound holds true for Wang, Sreeram and Liu's technique:

$$\|W(s)\left(G(s) - G_r(s)\right)V(s)\|_\infty \leq k \sum_{i=r+1}^{n} \sigma_i$$

where $k = 2\|W(s)L\|_\infty \|KV(s)\|_\infty$ with

$$L = CV_{WSL} diag(|r_1|^{-1/2}, |r_2|^{-1/2}, \ldots, |r_{ni}|^{-1/2}, 0, \ldots, 0)$$

$$K = diag(|s_1|^{-1/2}, |s_2|^{-1/2}, \ldots, |s_{no}|^{-1/2}, 0, \ldots, 0) U_{WSL}^T B$$

such that $ni = rank(X)$ and $ni = rank(Y)$

2.2.6 Varga and Anderson's modification to Wang, Sreeram and Liu's Technique

Varga and Anderson [28] proposed a modification to Wang, Sreeram and Liu's [27] technique such that the difference between $P_{WSL} - P_E$ and $Q_{WSL} - Q_E$ is reduced.

This is accomplished by simultaneously diagonalizing the Gramians $\hat{P}_{VA}$ and $\hat{Q}_{VA}$ as follows

$$T^T \hat{Q}_{VA} T = T^{-1} \hat{P}_{VA} T^{-T} = diag(\sigma_1, \sigma_2, \ldots, \sigma_n)$$

where the pair of Lyapunov equations are given as

$$A\hat{P}_{VA} + \hat{P}_{VA}A^T + B_{VA}B_{VA}^T = 0 \tag{2.37}$$

$$A^T\hat{Q}_{VA} + \hat{Q}_{VA}A + C_{VA}^T C_{VA} = 0 \tag{2.38}$$

and $\sigma_i \geq \sigma_{i+1}$, $i = 1, 2, \cdots, n-1$ and $\sigma_r > \sigma_{r+1}$. The new pseudo input and output matrices B_{VA} and C_{VA} are defined as $B_{VA} = U_{VA_1} S_{VA_1}^{1/2}$ and $C_{VA} = R_{VA_1}^{1/2} V_{VA}^T$ respectively and the terms U_{VA_1}, S_{VA_1}, R_{VA_1} and V_{VA_1} are obtained from the orthogonal eigenvalue decomposition of the symmetric matrices X and Y as follows

$$X = \begin{bmatrix} U_{VA_1} & U_{VA_2} \end{bmatrix} \begin{bmatrix} S_{VA_1} & 0 \\ 0 & S_{VA_2} \end{bmatrix} \begin{bmatrix} U_{VA_1}^T \\ U_{VA_2}^T \end{bmatrix}$$

$$Y = \begin{bmatrix} V_{VA_1} & V_{VA_2} \end{bmatrix} \begin{bmatrix} R_{VA_1} & 0 \\ 0 & R_{VA_2} \end{bmatrix} \begin{bmatrix} V_{VA_1}^T \\ V_{VA_2}^T \end{bmatrix}$$

where $\begin{bmatrix} S_{VA_1} & 0 \\ 0 & S_{VA_2} \end{bmatrix} = diag\{s_1, s_2, \cdots, s_n\}$, $\begin{bmatrix} R_{VA_1} & 0 \\ 0 & R_{VA_2} \end{bmatrix} = diag\{r_1, r_2, \cdots, r_n\}$

and $S_{VA_1} > 0$, $S_{VA_2} \leq 0$, $R_{VA_1} > 0$ and $R_{VA_2} \leq 0$. The reduced order model is then obtained by transforming and partitioning the original system. Since

$$X \leq B_{VA}B_{VA}^T \leq B_{WSL}B_{WSL}^T \geq 0$$

$$Y \leq C_{VA}^T C_{VA} \leq C_{WSL}^T C_{WSL} \geq 0$$

and the realization $\{A, B_{VA}, C_{VA}\}$ is minimal, stability of the reduced order model for the case of double sided frequency weighting is guaranteed.

Remark 2.10: An error bound for this method exists which is similar to the error bound for Wang, Sreeram and Liu's method provided that $rank \begin{bmatrix} B_{VA} & B \end{bmatrix} = rank \begin{bmatrix} B_{VA} \end{bmatrix}$ and $rank \begin{bmatrix} C_{VA} \\ C \end{bmatrix} = rank \begin{bmatrix} C_{VA} \end{bmatrix}$.

2.2.7 Frequency Interval Gramian Based Model Order Reduction

Gawronski and Juang [29] had introduced the concept of using frequency interval controllability and observability gramians such that a particular frequency interval of interest is emphasized. However the stability of the reduced order model obtained by using this technique is not guaranteed. To address this stability issue Gugercin and Antoulas [30] had proposed a modification to the method by Gawronski and Juang by incorporating the method proposed by Wang, Sreeram and Liu [27]. Both the methods by Gawronski and Juang and also by Gugercin and Antoulas are described in this section. In addition to these methods another frequency interval model reduction has been previously developed based on Impulse Response Gramians for both continuous and discrete time systems. [31, 32].

2.2.7.1 Gawronski and Juang's Method

Considering the linear state space model $\{A, B, C, D\}$ in the form of (2.1) and emphasizing a particular frequency interval of interest denoted by $[\omega_1, \omega_2]$ where $\omega_2 > \omega_1$, the frequency interval controllability and observability gramians have been defined by Gawronski and Juang as follows [29]

$$P_\Omega = P(\omega_2) - P(\omega_1)$$

$$Q_\Omega = Q(\omega_2) - Q(\omega_1),$$

$P(\omega)$ and $Q(\omega)$ are defined as

$$P(\omega) = \frac{1}{2\pi}\int_{-\omega}^{+\omega}(j\omega I - A)^{-1}BB^T(-j\omega I - A^T)^{-1}d\omega$$

$$Q(\omega) = \frac{1}{2\pi}\int_{-\omega}^{+\omega}(-j\omega I - A^T)^{-1}C^TC((j\omega I - A)^{-1}d\omega,$$

The gramians P_Ω and Q_Ω satisfy the following Lyapunov equations

$$AP_\Omega + P_\Omega A^T + X_\Omega = 0$$

$$A^T Q_\Omega + Q_\Omega A + Y_\Omega = 0,$$

where

$$X_\Omega = (S(\omega_2) - S(\omega_1))BB^T + BB^T(S^*(\omega_2) - S^*(\omega_1)) \tag{2.39}$$

$$Y_\Omega = (S^*(\omega_2) - S^*(\omega_1))C^TC + C^TC(S(\omega_2) - S(\omega_1)) \tag{2.40}$$

$$S(\omega) = \tfrac{j}{2\pi} ln((j\omega I + A)(-j\omega I + A)^{-1}).$$

and $S^*(\omega)$ is the conjugate transpose of $S(\omega)$. Simultaneously diagonalizing the gramians P_Ω and Q_Ω yields:

$$T^T Q_\Omega T = T^{-1} P_\Omega T^{-T} = diag\{\sigma_1, \sigma_2, ..., \sigma_n\}$$

where $\sigma_i \geq \sigma_{i+1}, i = 1, 2, ...n-1, \sigma_r > \sigma_{r+1}$. The corresponding reduced order model is then obtained by transforming and partitioning the original system.

Remark 2.11: It is also possible to emphasize more than one frequency interval at a time. For example, suppose two frequency intervals are emphasized - $[\omega_1, \omega_2]$ and $[\omega_3, \omega_4]$, $\omega_1 < \omega_2, \omega_3 < \omega_4$, the symmetric matrices X_Ω and Y_Ω will become

$$X_\Omega = (S(\omega_2) - S(\omega_1) + S(\omega_4) - S(\omega_3))BB^T + ...$$

$$BB^T(S^*(\omega_2) - S^*(\omega_1) + S^*(\omega_4) - S^*(\omega_3))$$

$$Y_\Omega = (S^*(\omega_2) - S^*(\omega_1) + S^*(\omega_4) - S^*(\omega_3))C^TC + ...$$

$$C^TC(S(\omega_2) - S(\omega_1) + S(\omega_4) - S(\omega_3))$$

Remark 2.12: The symmetric matrices X_Ω and Y_Ω are not guaranteed to be positive semidefinite, therefore the stability of the reduced order model obtained using Gawronski and Juang's method is not guaranteed.

2.2.7.2 Gugercin and Antoulas's Method

To overcome the stability issue associated with Gawronski and Juang's method, Gugercin and Antoulas [30] had proposed the following modification based in the method by Wang, Sreeram and Liu [27]. The symmetric matrices defined in (2.39) and (2.40) are made to be positive semidefinite by using the method described by Wang, Sreeram and Liu [27]. The new controllability and observability gramians are denoted by P_{GA} and Q_{GA} are obtained by solving the following Lyapunov equations where:

$$AP_{GA} + P_{GA}A^T + B_{GA}B_{GA}^T = 0 \tag{2.41}$$

$$A^TQ_{GA} + Q_{GA}A + C_{GA}^TC_{GA} = 0. \tag{2.42}$$

These controllability and observability gramians P_{GA} and Q_{GA} are then simultaneously diagonalized

$$T^TQ_{GA}T = T^{-1}P_{GA}T^{-T} = diag\{\sigma_1, \sigma_2, ...\sigma_n\}$$

where $\sigma_i \geq \sigma_{i+1},\ i = 1, 2, ..., n-1,\ \sigma_r > \sigma_{r+1}$. The matrices B_{GA} and C_{GA} in the Lyapunov equations in (2.41) and (2.42) are pseudo-input and output matrices such that $B_{GA} = U_{GA}|S_{GA}|^{\frac{1}{2}}$ and $C_{GA} = |R_{GA}|^{\frac{1}{2}}V_{GA}^T$ respectively. The terms U_{GA}, S_{GA}, V_{GA} and R_{GA} are obtained from the orthogonal eigenvalue decomposition of the symmetric matrices $X_\Omega = U_{GA}S_{GA}U_{GA}^T$ and $Y_\Omega = V_{GA}R_{GA}V_{GA}^T$ where $S_{GA} = diag(s_1, s_2, ...s_n),\ R_{GA} = diag(r_1, r_2, ...r_n),\ |s_1| \geq |s_2| \geq ... \geq |s_n| \geq 0$ and $|r_1| \geq |r_2| \geq ... \geq |r_n| \geq 0$. The reduced order models are then obtained by transforming and partitioning the original system. Since

$$X_\Omega \geq B_{GA}B_{GA}^T \geq 0$$

$$Y_\Omega \geq C_{GA}^TC_{GA} \geq 0$$

and the realization $\{A, B_{GA}, C_{GA}\}$ is minimal, the stability of the reduced order model is guaranteed.

2.3 Time Weighted Model Reduction

In addition to the frequency weighting and frequency interval gramian based model reduction methods described in the previous sections, another enhancement to the balanced truncation method can be achieved by incorporating time weighting. The concept of model reduction based on time weighted balanced truncation was first introduced by Schelfhout and De Moor [33]. For a linear time-invariant continuous-time system with the state space realization (A, B, C, D) in the form of (2.1), the time weighted controllability and observability gramians P_f and Q_f are given by

$$P_f = \int_0^\infty f(t) e^{A\tau} B B^* e^{A^*\tau} d\tau \tag{2.43}$$

$$Q_f = \int_0^\infty f(t) e^{A^*\tau} C^* C e^{A\tau} d\tau \tag{2.44}$$

where $f(t)$ is the corresponding time weighting function. By selecting the time weighting function as $f(t) = t^i$, the time weighted controllability and observability gramians are given by

$$P_i = \int_0^\infty t^i e^{A\tau} B B^* e^{A^*\tau} d\tau \tag{2.45}$$

$$Q_i = \int_0^\infty t^i e^{A^*\tau} C^* C e^{A\tau} d\tau \tag{2.46}$$

Schelfhout and De Moor had proposed a recursive method for the computation of the time-weighted controllability and observability gramians. By using this recursive method the time weighted controllability and observability gramians are defined as [33]

$$P_{r+1} = \frac{1}{r!}\int_0^\infty t^r e^{At} BB^* e^{A^* t} dt, \quad r = 0, 1, 2, ... \tag{2.47}$$

$$Q_{r+1} = \frac{1}{r!}\int_0^\infty t^r e^{A^* t} C^* C e^{At} dt, \quad r = 0, 1, 2... \tag{2.48}$$

The time weighted controllability and observability gramians P_{r+1} and Q_{r+1} can then be obtained by solving the following continuous time recursive Lyapunov equations

$$AP_{r+1} + P_{r+1}A^* = -P_r, \quad r = 0, 1, 2, ... \tag{2.49}$$

$$A^* Q_{r+1} + Q_{r+1}A = -Q_r, \quad r = 0, 1, 2, ... \tag{2.50}$$

where

$$P_o = BB^*,$$

$$Q_o = C^* C$$

As for the discrete time case, the controllability and observability gramians are defined as

$$P_{r+1} = \sum_{k=0}^{\infty} \frac{(k+r)!}{k!} A^k BB^* (A^*)^k, \quad r = 0, 1, 2, ... \tag{2.51}$$

$$Q_{r+1} = \sum_{k=0}^{\infty} \frac{(k+r)!}{k!} (A^*)^k C^* C A^k, \quad r = 0, 1, 2, ... \tag{2.52}$$

these discrete time gramians can be obtained by solving the following discrete time recursive Lyapunov equations

$$AP_{r+1}A^* - P_{r+1} = -P_r, \quad r = 0, 1, 2, ... \tag{2.53}$$

$$A^* Q_{r+1}A - Q_{r+1} = -Q_r, \quad r = 0, 1, 2, ... \tag{2.54}$$

where

$$P_o = BB^*,$$

$$Q_o = C^*C$$

Upon obtaining the continuous or discrete time weighted controllability and observability gramians, both of these gramians can then be simultaneously diagonalized and the balanced truncation model reduction procedure can be applied to obtain the reduced order model. A frequency response error bound for this technique by Schelfhout and De Moor [33] was developed by Sreeram [34]. In addition to balanced truncation, balanced stochastic singular perturbation approximation has also been applied as part of the time weighted model reduction process [35]. In previous studies related to time weighted model reduction, the emphasis was on the theoretical aspects of obtaining a reduced order model which closely approximates the full order model [33–35]. In chapter 6 we will present both the theoretical aspects of obtaining a reduced order model and also the applicability of the proposed time weighted model order reduction technique to be used in a practical application which involves determining the cross sectional fluid temperature of a flat plate solar collector.

2.4 Bilinear Systems

Bilinear systems are an important class of nonlinear systems which have well-established theories and are applicable to many practical applications. Mathematical models in the form of bilinear systems can be found in a variety of fields such as the mathematical models which describe the processes of electrical networks, hydraulic systems, heat transfer and chemical processes. Many nonlinear systems can be modelled as bilinear systems with appropriate state feedback or can be approximated as bilinear systems by using the bilinearization process [36, 37].

Similar to the case of linear systems, high order models of bilinear systems can also benefit from model order reduction techniques. The following section provides a

description of the controllability and observability gramians which are used in the balanced truncation technique for continuous-time bilinear systems. On the other hand the description of the controllability and observability gramians which are used in the balanced truncation technique of discrete-time bilinear systems is described in chapter 5.

2.4.1 Balanced Truncation of Bilinear Systems

Let Σ be a continuous-time bilinear system described by the following state space model formulation

$$\Sigma = \begin{cases} \dot{x}(t) = Ax(t) + \sum_{j=1}^{m} N_j x(t) u_j(t) + Bu(t) \\ y(t) = Cx(t) \end{cases} \tag{2.55}$$

where $x(t) \in \mathbb{R}^n$,$u(t) \in \mathbb{R}^m$, $y(t) \in \mathbb{R}^m$

The controllability gramian for this system is given by [38, 39]

$$P = \sum_{i=0}^{\infty} \int_0^{\infty} \dots \int_0^{\infty} P_i P_i^* dt_1 \dots dt_i \tag{2.56}$$

where

$$P_1(t_1) = e^{At_1} B,$$
$$P_1(t_1, ..., t_i) = e^{At_i} \begin{bmatrix} N_1 P_{i-1} & N_2 P_{i-1} \dots N_m P_{i-1} \end{bmatrix}$$

the observability gramian is given by [38, 39]

$$Q = \sum_{i=0}^{\infty} \int_0^{\infty} \dots \int_0^{\infty} P_i^* Q_i dt_1 \dots dt_i \tag{2.57}$$

where

$$Q_1(t_1) = Ce^{At_1}$$

$$Q_1(t_1, ..., t_i) = \begin{bmatrix} Q_{i-1}N_1 \\ Q_{i-1}N_2 \\ \vdots \\ Q_{i-1}N_m \end{bmatrix} \tag{2.58}$$

The solutions to (2.56) and (2.57) can be obtained by solving the following generalized Lyapunov equations [40].

$$AP + PA^* + \sum_{j=1}^{m} N_j P N_j^* + BB^* = 0 \tag{2.59}$$

$$A^*Q + QA + \sum_{j=1}^{m} N_j^* Q N_j + C^*C = 0 \tag{2.60}$$

The generalized Lyapunov equation in (2.59) can be solved iteratively. The controllability gramian P is obtained by [40]

$$P = \lim_{i \to +\infty} \hat{P}_i \tag{2.61}$$

where

$$\begin{aligned} A\hat{P}_1 + \hat{P}_1 A^* + BB^* = 0, \\ A\hat{P}_i + \hat{P}_i A^* + \sum_{j=1}^{m} N_j \hat{P}_{i-1} N_j^* + BB^* = 0, \\ i = 2, 3, ... \end{aligned} \tag{2.62}$$

Similarly the generalized Lyapunov equation in (2.60) can be solved iteratively. The observability gramian is obtained by [40]

$$Q = \lim_{i \to +\infty} \hat{Q}_i \tag{2.63}$$

$$A^*\hat{Q}_1 + \hat{Q}_1 A + C^*C = 0,$$

$$A^*\hat{Q}_i + \hat{Q}_i A + \sum_{j=1}^{m} N_j^* \hat{Q}_{i-1} N_j + C^*C = 0,$$

$$i = 2, 3, ... \tag{2.64}$$

Upon obtaining the generalized controllability and observability gramians of the bilinear system, the balanced truncation procedure for bilinear systems is similar to that of linear systems.

2.4.2 Control Configuration Selection

The same techniques for gramian based model order reduction are directly applicable to control configuration selection. Continuous technological advancement of industrial control processes have resulted in the development of complex multivariable high order systems. Dealing with such multivariable high order systems requires increased computational effort and places higher demands on the overall control system of the plant. There are two main approaches for designing a suitable controller structure for a multivariable plant. The first approach is to design a centralized controller whereas the second approach is to design a decentralized control structure. Decentralized controllers are generally more robust to uncertainties and controller failures [41]. It has been established in previous studies that it is advantageous to decompose a multivariable system into separate subsystems and implement decentralized controller designs corresponding to the dynamic behaviour of the subsystem and also incorporating information regarding interaction between subsystems [42]. Control configuration selection is a prerequisite for effective decentralized control of industrial processes [43–45]. The Hankel interaction index matrix which depicts the degree of controllability and observability of each elementary linear SISO subsystem was originally developed by Wittenmark, Salgado and Conley [46, 47] and these are the pioneering gramian based methods for determining the most suitable input-

output pairing in control configuration selection of linear systems. The following section describes the control configuration selection procedure for both linear and bilinear systems through numerical examples.

2.4.2.1 Control Configuration Selection Procedure for Linear Systems

Consider the following linear 3×3 multivariable plant $G(s)$ together with its corresponding subsystems $G_{ij}(s), i = 1, 2, 3, j = 1, 2, 3$ originally presented in [47].

$$G(s) = \begin{bmatrix} \frac{0.4}{(s+1)^2} & \frac{4(s+3)}{(s+2)(s+5)} & \frac{-2}{s+4} \\ \frac{2}{(s+2)(s+1)} & \frac{2}{(s+2)^2} & \frac{1}{(s+2)} \\ \frac{6(-s+1)}{(s+5)(s+4)} & \frac{4}{(s+3)^2} & \frac{8}{(s+2)(s+5)} \end{bmatrix}$$

The procedure to obtain a control configuration structure for this system is described as follows [46, 47]:

i Firstly the outputs are denoted by y_1 to y_3 and the inputs are denoted by u_1 to u_3. Each of the 9 elementary SISO subsystem in the transfer function matrix $G(s)$ is then denoted by $G_{ij}(s)$ as follows:

$$G(s) = \begin{array}{c} \\ y_1 \\ y_2 \\ y_3 \end{array} \begin{array}{c} \begin{array}{ccc} u_1 & u_2 & u_3 \end{array} \\ \begin{bmatrix} G_{11}(s) & G_{12}(s) & G_{13}(s) \\ G_{21}(s) & G_{22}(s) & G_{23}(s) \\ G_{31}(s) & G_{32}(s) & G_{33}(s) \end{bmatrix} \end{array} \tag{2.65}$$

For each of these elementary subsystems $G_{ij}(s)$, the corresponding state space realizations are obtained. The state space realizations of the elementary subsystems in the form of (2.1) are denoted by

$$G_{ij}(s) = \{A_{y_i,u_j}, B_{y_i,u_j}, C_{y_i,u_j}\},$$

$$(i = 1, 2, 3, j = 1, 2, 3)$$

ii Secondly in order to determine the degree of controllability and observability of each of these subsystems $G_{ij}(s)$, the controllability and observability gramians corresponding to each of the subsystems denoted by P_{y_i,u_j} and Q_{y_i,u_j} respectively are calculated as follows

$$A_{y_i,u_j}P_{y_i,u_j} + P_{y_i,u_j}A^*_{y_i,u_j} + B_{y_i,u_j}B^*_{y_i,u_j} = 0$$

$$A^*_{y_i,u_j}Q_{y_i,u_j} + Q_{y_i,u_j}A_{y_i,u_j} + C^*_{y_i,u_j}C_{y_i,u_j} = 0$$

It has been shown in [47] that the controllability and observability gramians of the MIMO system $G(s)$ is equal to the summation of the controllability and observability gramians of the subsystems as follows

$$P = \sum_{j=1}^{3}\sum_{i=1}^{3} P_{y_i,u_j}$$

$$Q = \sum_{j=1}^{3}\sum_{i=1}^{3} Q_{y_i,u_j}$$

iii Thirdly the participation matrix which depicts the degree of controllability and observability of each subsystem is formed by using the following formula [47]

$$\Phi = \left[\phi_{ij}\right]$$

where

$$\phi_{ij} = \frac{trace(P_{y_i,u_j}Q_{y_i,u_j})}{trace(PQ)}$$

It follows that the participation matrix for this system is

$$\Phi = \begin{bmatrix} 0.0370 & 0.2018 & 0.0385 \\ 0.2226 & 0.0578 & 0.0385 \\ 0.2193 & 0.0457 & 0.1389 \end{bmatrix}$$

Subsystems which have a larger value of ϕ_{ij} in this participation matrix indicate that the pair $(u_i - y_j)$ subsystem is easier to control and observe and therefore should be prioritized to be included in the nominal model whereas subsystems which have a lower value of ϕ_{ij} indicates that the pair $(u_i - y_j)$ is more difficult to control and observe. The suitability of the pairing and the performance of the designed controller structure depend on how large the total of ϕ_{ij} is for all the subsystems in the nominal model. When the total of ϕ_{ij} for the selected subsystems is large, the original model and nominal model are close to each other and the error is small. Refering to this participation matrix, in order to construct the structure of the nominal model for completely decentralized control only one element per row and one element per column can be selected. Selecting the pairs $(u_1, y_2), (u_2, y_1)$ and (u_3, y_3) results in the following structure of the nominal model denoted as $\mathcal{L}_n$ for implementing decentralized control:

$$struct(\mathcal{L}_n) = \begin{array}{c} \\ y_1 \\ y_2 \\ y_3 \end{array} \begin{array}{c} \begin{array}{ccc} u_1 & u_2 & u_3 \end{array} \\ \begin{bmatrix} 0 & * & 0 \\ * & 0 & 0 \\ 0 & 0 & * \end{bmatrix} \end{array}$$

2.4.2.2 Control Configuration Selection Procedure for Bilinear Systems

Considering the numerical example of a 3×3 MIMO bilinear system presented in [48]:

$$\Sigma = \begin{cases} \dot{x}(t) = Ax(t) + \sum_{j=1}^{3} N_j x(t) u_j(t) +, Bu(t) \\ y(t) = Cx(t) \end{cases} \tag{2.66}$$

where

$$A = \begin{bmatrix} -30 & 0 & 0 \\ 0 & -70 & 0 \\ 0 & 0 & -15 \end{bmatrix}, N_1 = N_2 = \begin{bmatrix} 0 & -0.07 & 0 \\ 30 & 0 & 0 \\ 0 & 0 & 0 \end{bmatrix}, N_3 = \begin{bmatrix} 0 & 0 & -0.07 \\ 0 & 0 & 0 \\ 30 & 0 & 0 \end{bmatrix}$$
$$B = \begin{bmatrix} 20 & 0 & 0 \\ 0 & 60 & 0 \\ 0 & 0 & 50 \end{bmatrix}, C = \begin{bmatrix} 1 & 0 & 0 \end{bmatrix} \tag{2.67}$$

The procedure to obtain a control configuration structure for this system is described as follows [48]

i Firstly this 3×3 MIMO bilinear system is decomposed into its 9 elementary SISO bilinear subsystems denoted by the state space matrices $\Sigma = \{A, B_{u_i,y_j}, C_{u_i,y_j}, N_1, N_2, N_3\}$, $(i = 1, 2, 3, j = 1, 2, 3)$ respectively:

$$\Sigma_{ij} = \begin{cases} \dot{x}(t) = Ax(t) + \sum_{j=1}^{3} N_j x(t) u_j(t) +, B_{u_i,y_j} u(t) \\ y(t) = C_{u_i,y_j} x(t) \end{cases} \tag{2.68}$$

$$\Sigma = \begin{array}{c} \\ y_1 \\ y_2 \\ y_3 \end{array} \begin{array}{c} \begin{array}{ccc} u_1 & u_2 & u_3 \end{array} \\ \begin{bmatrix} \Sigma_{11}(s) & \Sigma_{12}(s) & \Sigma_{13}(s) \\ \Sigma_{21}(s) & \Sigma_{22}(s) & \Sigma_{23}(s) \\ \Sigma_{31}(s) & \Sigma_{32}(s) & \Sigma_{33}(s) \end{bmatrix} \end{array}$$

ii Secondly the controllability and observability gramians for each of these elementary SISO subsystems are obtained by solving the following Lyapunov equations

$$AP_{u_i,y_j} + P_{u_i,y_j} A^* + \sum_{j=1}^{m} N_j P_{u_i,y_j} N_j^* + B_{u_i,y_j} B_{u_i,y_j}^* = 0$$
$$A^* Q_{u_i,y_j} + Q_{u_i,y_j} A + \sum_{j=1}^{m} N_j^* Q_{u_i,y_j} N_j + C_{u_i,y_j}^* C_{u_i,y_j} = 0$$

It has been shown in [48] that the controllability and observability gramians of the MIMO system Σ is equal to the summation of the controllability and observability of the subsystems as follows

$$P = \sum_{j=1}^{3} \sum_{i=1}^{3} P_{y_i,u_j}$$
$$Q = \sum_{j=1}^{3} \sum_{i=1}^{3} Q_{y_i,u_j}$$

iii Thirdly the participation matrix which depicts the degree of controllability and observability of each subsystem is formed by using the following formula

$$\Phi = \left[\phi_{ij}\right]$$

where

$$\phi_{ij} = \frac{trace(P_{u_i,y_j} Q_{u_i,y_j})}{trace(PQ)}$$

It follows that the participation matrix for this system is

$$\Phi = \begin{bmatrix} 0.00133 & 0.219 & 0.744 \\ 0.000000133 & 0.00219 & 0.0000595 \\ 0.000000648 & 0.0000857 & 0.033 \end{bmatrix} \tag{2.69}$$

Subsystems which have a larger value of ϕ_{ij} in this participation matrix indicate that the pair $(u_i - y_j)$ subsystem is easier to control and observe and therefore should be prioritized to be included in the nominal model whereas subsystems which have a lower value of ϕ_{ij} indicates that the pair $(u_i - y_j)$ is more difficult to control and observe. The suitability of the pairing and the performance of the designed controller structure depend on how large the total of ϕ_{ij} is for all the subsystems in the nominal model. When the total of ϕ_{ij} for the selected

subsystems is large, the original model and nominal model are close to each other and the error is small. Refering to this participation matrix, in order to construct the structure of the nominal model for completely decentralized control only one element per row and one element per column can be selected. Selecting the pairs $(u_3, y_1), (u_2, y_2)$ and (u_1, y_3) results in the following structure of the nominal model denoted as $\mathcal{L}_n$ for implementing decentralized control:

$$struct(\mathcal{L}_n) = \begin{array}{c} \\ y_1 \\ y_2 \\ y_3 \end{array} \begin{array}{c} \begin{array}{ccc} u_1 & u_2 & u_3 \end{array} \\ \begin{bmatrix} 0 & 0 & * \\ 0 & * & 0 \\ * & 0 & 0 \end{bmatrix} \end{array}$$

2.5 Conclusion

In this chapter, the essential properties of balanced truncation and balanced singular perturbation approximation have been presented. Several frequency and time weighted model reduction techniques have been reviewed and their important characteristics have been highlighted. The balanced truncation procedure for bilinear systems has also been described. Finally examples are provided to demonstrate the control configuration selection procedure for both linear and bilinear systems.

Chapter 3

A Controller Reduction Technique for Feedback Control of MIMO Discrete-Time Systems

3.1 Introduction

Frequency weighted model reduction (FWMR) was originally developed by Enns [25] to solve controller reduction problems. Controller reduction problems can be formulated as FWMR problems and the same procedure can be used to solve compensator reduction problems. Recent works on FWMR have been developed in [49–57]. FWMR can be classified into single-sided or double-sided cases. Figure 3.1 shows a feedback closed loop configuration with the discrete time plant $G(z)$ and a discrete time controller/compensator $K(z)$ connected in series in the forward path. Both single and double sided FWMR techniques attempt to find a discrete time reduced order controller/compensator $K_r(z)$ which minimizes an error of the form [28]:

$$e = \|V_1(z)(K(z) - K_r(z))V_2(z)\|_\infty$$

Single sided FWMR enforces closed loop stability by using the following output and input weight pairs:

$$V_1(z) = (I + G(z)K(z))^{-1}G(z), \quad V_2(z) = I \ \ or$$
$$V_1(z) = I, \quad V_2(z) = (I + G(z)K(z))^{-1}G(z)$$

Performance preserving considerations lead to the following double sided weights:

$$V_1(z) = (I + G(z)K(z))^{-1}G(z),$$
$$V_2(z) = (I + G(z)K(z))^{-1}$$

Note that throughout this chapter $G(z)$, $K(z)$ and $K_r(z)$ refer to discrete time transfer function matrices and I is an identity matrix. The transfer function of the feedback closed-loop system in Figure 3.1 denoted as $W(z)$ is given by:

$$W(z) = G(z)K(z)(I + G(z)K(z))^{-1} \tag{3.1}$$

If the original controller/compensator $K(z)$ in Figure 3.1 is replaced by a reduced-order controller/compensator $K_r(z)$, then the closed-loop system transfer function is given by

$$W_r(z) = G(z)K_r(z)(I + G(z)K_r(z))^{-1} \tag{3.2}$$

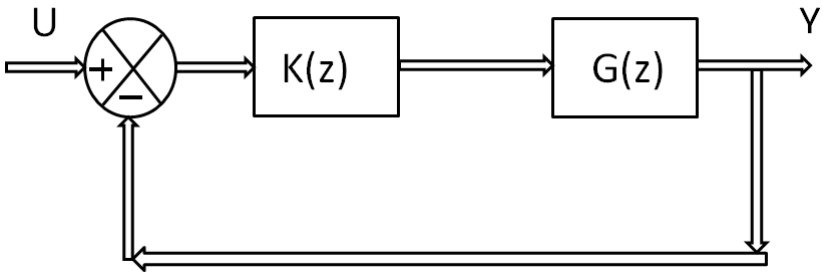

Figure 3.1: Closed Loop Configuration with the Plant $G(z)$ and Controller $K(z)$ in the forward path.

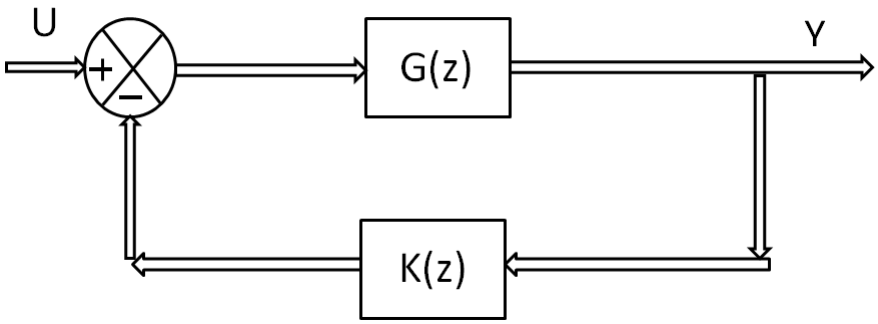

Figure 3.2: Closed Loop Configuration with the Plant $G(z)$ in the Forward Path and Controller $K(z)$ Located in the Feedback Path.

The infinity norm of the approximation error $||W(z) - W_r(z)||_\infty$ obtained using existing FWMR methods [27, 28, 58, 59] are at best equal to or slightly lower than Enns Method. Furthermore more recent theoretical developments for FWMR techniques are still relatively less compared to unweighted model reduction techniques [60–64]. Therefore FWMR techniques which further reduce the infinity norm of $||W(z) - W_r(z)||_\infty$ are highly desired. Houlis and Sreeram proposed a parametrized controller/compensator reduction problem formulation based on deriving a new set of weights by considering a continuous time unity feedback closed-loop system with the controller/compensator and plant connected in series as shown in Figure 3.1 [65–67]. This method was extended to work with controllers and plants connected in the Linear Fractional Transformation (LFT) configuration [68]. The advantage of this formulation is that one of the frequency weights becomes a function of a free parameter matrix which can be varied to reduce the infinity norm $||W(z) - W_r(z)||_\infty$ by using any standard double sided FWMR technique [25, 27, 28, 58, 59]. However the disadvantage of this technique is that determining the optimal value of the free parameter matrix requires an extensive search over a wide range of values, therefore an approximating function is required to locate an optimal value. In addition this technique is not applicable for the closed loop configuration in Figure 3.2 which is useful especially for certain compensator design configurations which have the compensator located in the feedback path. A compensator $K(z)$ can be placed either in

series with the plant in the forward path (cascade or series compensation) as shown in Figure 3.1 or in the feedback path as shown in Figure 3.2 (feedback or parallel compensation). The selection of the location for the compensator depends on the characteristics of the control system and the desired results. The cascade compensator $K(z)$ is placed at the low energy point along the forward path. As a result the plant $G(z)$ needs to have high input impedance. Isolation amplifiers may be required to avoid loading towards or by the compensator. Along the forward path the signal propagates from a low to a high energy level whereas the reverse is true along the feedback path [69–71]. Generally an amplifier may not be necessary for a compensator located in the feedback path however the compensator located in the forward path may require an amplifier for gain and/or isolation [69–71].

In this chapter, a parameterized controller/compensator reduction method is developed for MIMO discrete time feedback control systems where the controller/ compensator is located in the feedback path as shown in Figure 3.2 to address the need for lower order controllers/compensators which approximate the behaviour of high order controllers/compensators located in the feedback path. New parameterized weights which are a function of a free parameter matrix are derived. These new weights are applicable with standard double sided FWMR technique [25,27,28,58,59] and variation of the free parameter matrix plays a significant role in reducing the approximation error $||W(z) - W_r(z)||_\infty$ relative to the standard FWMR technique. For the proposed FWMR problem formulation the procedure to obtain an optimal value of the free parameter matrix does not require an approximating function to locate an optimal value as in the previous works by Houlis and Sreeram [65–67], since it has a superior and easier searching method. The preliminary results that were presented by Houlis and Sreeram [72] were only applicable for SISO continuous time systems. The method presented in this thesis is a further development which enables the applicability of the proposed method to a variety of practical problems which involve MIMO discrete time systems.

3.2 Preliminaries

In this section the parameterized controller reduction method originally presented by Houlis and Sreeram in [65–67] for both SISO and MIMO continuous time feedback control systems with the controller in the forward path is further developed to be applicable to discrete time systems. Although the main focus of this chapter is on feedback control systems with the controller in the feedback path, it is also essential to present the theory for feedback control systems with the controller in the forward path in order to gain a comprehensive understanding of the proposed method.

3.2.1 Controller Reduction Technique for MIMO Discrete Time Feedback Control Systems with the Plant and Controller in the Forward Path: Overview

Lemma 3.1: Given a discrete time plant $G(z)$ and a discrete time controller/compensator $K(z)$ which have the dimensions $m \times n$ and $n \times m$ respectively (where m and n refer to the number of input and outputs of $G(z)$ respectively) as shown in Figure 3.1 and the reduced order discrete time controller/compensator $K_r(z)$, subtracting (3.2) from (3.1) and assuming that the second order terms are negligible in $[K(z)-K_r(z)]$, we will obtain:

$$W(z) - W_r(z) = (I + G(z)K(z))^{-1}G(z)\,[K(z) - K_r(z)]\,(I + G(z)K(z))^{-1} \quad (3.3)$$

Proof: This has been shown by Liu and Anderson in [73] and is the standard double sided frequency weighted controller reduction problem formulation with the weights $V_1(z) = (I + G(z)K(z))^{-1}G(z)$ and $V_2(z) = (I + G(z)K(z))^{-1}$. Note that I is an identity matrix with dimension $m \times m$.

In this section we present a generalization of the FWMR problem formulation described by (3.3) based on the augmented closed loop feedback configuration shown in Figure 3.3 which incorporates a free parameter matrix $C = cI$ (where the parameter c is a constant) as described in Lemma 3.2 in the following section. As

for continuous time systems, a generalization of the FWMR problem formulation derived from an augmented closed loop feedback configuration which incorporate a free parameter matrix have been previously presented in [65–67].

3.2.1.1 Relationship Between Original and Augmented Closed Loop Configurations

Let $W(z) = G(z)K(z)(I + G(z)K(z))^{-1}$ and $\bar{W}(z) = \bar{G}(z)\bar{K}(z)(I + \bar{G}(z)\bar{K}(z))$ be closed loop systems with plants $G(z)$, $\bar{G}(z)$ and controllers/compensators $K(z)$, $\bar{K}(z)$ respectively.

Definition 3.1:

$$H_c(z) = I + G(z)K(z)(I - C) \tag{3.4}$$

$$H(z) = I + G(z)K(z) \tag{3.5}$$

$$\bar{H}(z) = I + \bar{G}(z)\bar{K}(z) \tag{3.6}$$

$$\bar{K}(z) = K(z)C \tag{3.7}$$

$$\bar{K}_r(z) = K_{rc}(z)C \tag{3.8}$$

$$\bar{G}(z) = H_c^{-1}(z)G(z) \tag{3.9}$$

It follows that if $H^{-1}(z)$ exists, it can be shown that $H_c^{-1}(z)$ also exists for a given value of the free parameter matrix $C = cI$ except for a finite number of values of c which can be disregarded [67].

Lemma 3.2: Based on the original and augmented closed loop feedback configuration shown in Figure 3.1 and Figure 3.3 respectively, the equivalence between both these configurations is given by:

$$\bar{W}(z) = W(z)C \tag{3.10}$$

Proof: Firstly we have:

$$\begin{aligned}
\bar{H}(z) &= I + \bar{G}(z)\bar{K}(z) \\
&= I + (H_c^{-1}(z)G(z)K(z)C) \\
&= H_c^{-1}(z)[H_c(z) + G(z)K(z)C] \\
&= H_c^{-1}(z)[I + G(z)K(z) - G(z)K(z)C + G(z)K(z)C] \\
&= H_c^{-1}(z)H(z)
\end{aligned}$$

Since the inverses of $H_c^{-1}(z)$ and $H(z)$ both exists, it follows that $\bar{H}^{-1}(z)$ also exists such that:

$$\bar{H}^{-1}(z) = H^{-1}(z)H_c(z) \tag{3.11}$$

Note that when $C = I$, the configuration in Figure 3.3 becomes identical to the configuration in Figure 3.1. For any closed loop systems configuration with the form shown in Figure 3.1, the commutative property $G(z)K(z)H^{-1}(z) = H^{-1}(z)G(z)K(z)$ holds true [74]. With reference to Figure 3.3, there is an outer and inner feedback loop denoted by $W(z)$ and $\bar{W}(z)$ respectively. $\bar{W}(z)$ has the same form as $W(z)$ the only difference being the augmented controller $\bar{K}(z)$ and plant $\bar{G}(z)$ instead of the original controller $K(z)$ and plant $G(z)$. Therefore the commutative property $\bar{G}(z)\bar{K}(z)\bar{H}^{-1}(z) = \bar{H}^{-1}(z)\bar{G}(z)\bar{K}(z)$ holds true. This property is then applied together with equation (3.11) and Definition 3.1 as follows:

$$\begin{aligned}
\bar{W}(z) &= \bar{G}(z)\bar{K}(z)\bar{H}^{-1}(z) \\
&= \bar{H}^{-1}(z)\bar{G}(z)\bar{K}(z) \\
&= H^{-1}(z)H_c(z)\bar{G}(z)\bar{K}(z) \\
&= H^{-1}(z)H_c(z)H_c^{-1}(z)G(z)K(z)C \\
&= H^{-1}(z)G(z)K(z)C \\
&= G(z)K(z)H^{-1}(z)C \\
&= W(z)C \qquad \blacksquare
\end{aligned}$$

Remark 3.1: Note that by applying block diagram simplification to the closed loop configuration in Figure 3.1 and Figure 3.3, the same closed loop transfer functions is obtained algebraically provided that the free parameter matrix C is a diagonal matrix with equal entries along the diagonal.

If the reduced order controllers K_r and $\bar{K}_r$ are used instead, (3.10) can be written as follows:

$$\bar{W}_r(z) = W_r(z)C \tag{3.12}$$

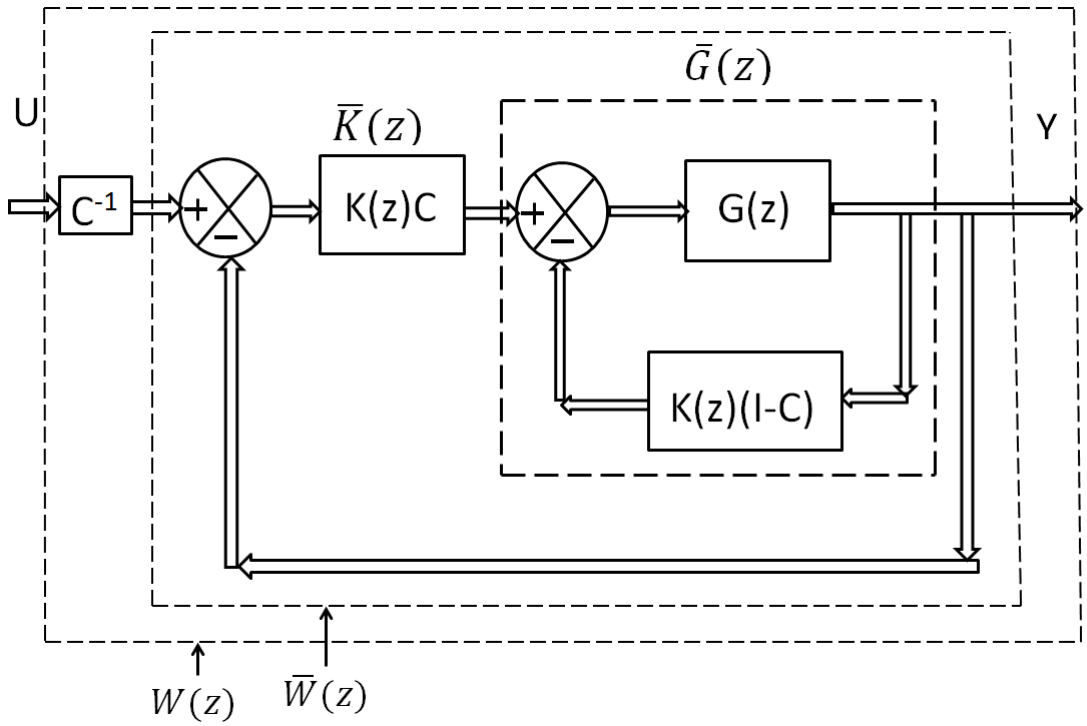

Figure 3.3: Augmented Closed Loop Feedback Configuration

3.2.1.2 Derivation of New Frequency Weights

In this subsection, new double sided frequency weights are derived based on the augmented feedback closed loop configuration shown in Figure 3.3. This derivation is based on approximating the error between the closed loop systems $\bar{W}(z)$, $\bar{W}_r(z)$, $W(z)$ and $\bar{W}(z)$ respectively. Subtracting (3.12) from (3.10) yields:

$$[W(z) - W_r(z)]C = \bar{W}(z) - \bar{W}_r(z) \tag{3.13}$$

From Lemma 3.1 we have:

$$W(z) - W_r(z) = H^{-1}(z)G(z)[K(z) - K_r(z)]H^{-1}(z)$$

$$\bar{W}(z) - \bar{W}_r(z) = \bar{H}^{-1}(z)\bar{G}(z)[\bar{K}(z) - \bar{K}_r(z)]\bar{H}^{-1}(z)$$

Therefore equation (3.13) may be written as:

$$[H^{-1}(z)G(z)[K(z) - K_r(z)]H^{-1}(z)]C = \bar{H}^{-1}(z)\bar{G}(z)[\bar{K}(z) - \bar{K}_r(z)]\bar{H}^{-1}(z) \quad (3.14)$$

Theorem 3.1: Based on the definitions described in Definition 3.1, we have:

$$W(z) - W_r(z) = H^{-1}(z)G(z)[K(z) - K_{rc}(z)]H^{-1}(z)H_c(z) \quad (3.15)$$

Proof: To prove this theorem, equations (3.11) and (3.9) are substituted into the right hand side of equation (3.14) which gives:

$$\begin{aligned}
&[H^{-1}(z)G(z)[K(z) - K_r(z)]H^{-1}(z)]C \\
&= H^{-1}(z)G(z)[K(z)C - K_{rc}(z)C]H^{-1}(z)H_c(z) \\
&= H^{-1}(z)G(z)[K(z) - K_{rc}(z)]CH^{-1}(z)H_c(z) \qquad (3.16)
\end{aligned}$$

Finally, cancelling the free parameter matrix C which occurs on the left and right hand side of equation (3.16) gives:

$$H^{-1}(z)G(z)[K(z) - K_r(z)]H^{-1}(z) = H^{-1}(z)G(z)[K(z) - K_{rc}(z)]H^{-1}(z)H_c(z) \ \blacksquare$$

The new input and output frequency weights $V_1(z)$ and $V_2(z)$ immediately follow from the right hand side of (3.15) where $V_1(z) = H^{-1}(z)G(z)$ and $V_2(z) = H^{-1}(z)H_c(z)$. $V_1(z)$ is a fixed weight whereas $V_2(z)$ varies with respect to the value of c, therefore by solving the double sided FWMR problem with these weights different reduced order controllers $K_{rc}(z)$ are obtained which correspond to each value of c. The reduced order controller obtained - $K_{rc}(z)$ obtained which corresponds to each value of c is replaced into (3.3) to establish the frequency weighted approximation error denoted as E_c as a function of the free parameter matrix $C = cI$ as follows:

$$E_c = H^{-1}(z)G(z)\left[K(z) - K_{rc}(z)\right]H^{-1}(z) \quad (3.17)$$

Definition 3.2:

$$e_c = ||E_c||_\infty \tag{3.18}$$

$$W(z) - W_r(z) = E_1 \tag{3.19}$$

$$E_1 = H^{-1}(z)G(z)\left[K(z) - K_r(z)\right]H^{-1}(z) \tag{3.20}$$

$$e_1 = ||E_1||_\infty \tag{3.21}$$

The following section describes how varying the diagonal entries of the free parameter matrix $C = cI$ in this new double sided frequency weighted model reduction problem formulation minimizes the infinity norm of the approximation error described by equation (3.17).

3.2.1.3 Error Analysis

Based on the theory derived in the previous sections, the proposed technique aims to minimize the norm of the approximation error between the original closed loop system and closed loop system with a reduced order controller by using the weights $V_1(z)$ and $V_2(z)$ from the right hand side of (3.15). The effect of varying the diagonal entries of the free parameter matrix $C = cI$ towards reducing the infinity norm of the approximation error in (3.17) is described in Lemma 3.3 as follows:

Lemma 3.3: Let $h_c = ||H_c(z)||_\infty$ and $\hat{h}_c = ||H_c^{-1}(z)||_\infty$ and both e_c and e_1 be as defined in (3.18) and (3.21), Then we will have:

$$e_1 h_c^{-1} \leq e_c \leq e_1 \hat{h}_c \tag{3.22}$$

Proof: Firstly the left part of (3.22) which represents the lower bound of the approximation error e_c is proven. By substituting (3.20) and (3.17) into (3.15), we

have:

$$
\begin{aligned}
E_1 &= E_c H_c(z) \\
||E_1||_\infty &= ||E_c H_c(z)||_\infty \\
||E_1||_\infty &\leq ||E_c||_\infty ||H_c(z)||_\infty \\
e_1 &\leq e_c h_c \\
e_1 h_c^{-1} &\leq e_c
\end{aligned} \tag{3.23}
$$

As for the right part of (3.22) which represents the upper bound of the approximation error e_c, substituting (3.20) and (3.17) into (3.15) and rearranging, we have:

$$
\begin{aligned}
E_c &= E_1 H_c^{-1}(z) \\
||E_c||_\infty &= ||E_1 H_c^{-1}(z)||_\infty \\
||E_c||_\infty &\leq ||E_1||_\infty ||H_c^{-1}(z)||_\infty \\
e_c &\leq e_1 \hat{h}_c
\end{aligned} \tag{3.24}
$$

By combining (3.23) and (3.24), the upper and lower bounds of e_c is obtained as shown in (3.22). From (3.22), it can be observed that determining the optimal value c for the diagonal entries of the free parameter matrix $C = cI$ requires a computationally extensive search since the optimal value of c which minimizes the approximation error can be located anywhere between the lower bound $e_1 h_c^{-1} \leq e_c$ and upper bound $e_c \leq e_1 \hat{h}_c$. In the following sections of this chapter we will demonstrate that for feedback control systems with the controller/compensator located in the feedback path, the optimal value of c can be determined by choosing a large absolute value of c and therefore a computationally extensive search and the construction of an approximating function is not required as in the case for feedback control systems with the controller in the forward path [65–67].

3.2.2 Feedback Control System with the Compensator Located in the Feedback Path

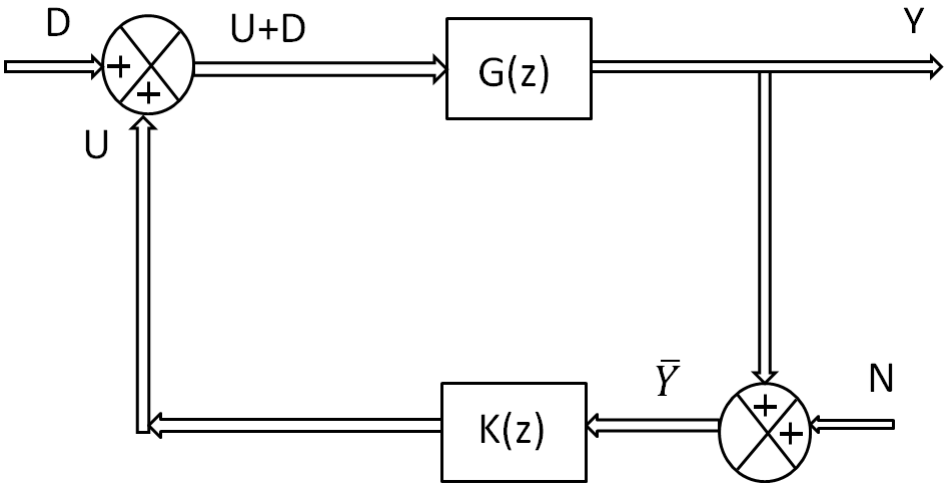

Figure 3.4: Basic LQG Disturbance rejection loop

The basic LQG compensation loop in Figure 3.4 is an example of a feedback control system with the compensator located in the feedback path. The compensator $K(z)$ uses the measurements of the plant output Y to generate a control signal U which regulates Y to be around zero while the system is subject to an input disturbance D and measurement noise N. Feedback compensation as shown in Figure 3.4 is beneficial in disturbance rejection which requires that the output Y must not be affected by the disturbance input D such that the steady state response Y_{ss} is such that $Y_{ss} = 0_{m\times m}$ for the disturbance input $D \neq 0_{m\times m}$ [69–71]. The presence of noise within the control system may also be a deciding factor for compensator location. An amplifier located along the forward path in a cascade configuration may also amplify noise in addition to the input signal therefore using feedback compensation as shown in Figure 3.4 without an amplifier may be more suitable [69]. Placing the compensator in the feedback path may eliminate the need for additional amplifiers in the control system configuration and therefore can be beneficial in applications such as aircraft and spacecraft control designs where minimum size and weight of the components are essential [69–71].

3.3 Main Contribution

In this section we present a new double sided frequency weighted controller/compensator reduction problem formulation for MIMO discrete time feedback control systems with the controller/compensator located in the feedback path. The equivalence between the closed-loop configurations shown in Figures 3.2 and proposed configuration in Figure 3.5 are first established. This equivalence is then used to derive new input and output weights for the new double sided frequency weighted model reduction formulation which is applicable to MIMO discrete time feedback control systems which have the controller/compensator located in the feedback path. A useful characteristic of this developed problem formulation is that the optimal values for the diagonal entries of the free parameter matrix $C = cI$ which minimize the infinity norm of the approximation error can be obtained by selecting a large value of the diagonal entries of the free parameter matrix C without the need for an approximating function as with the problem formulation by Houlis and Sreeram in [65–67].

3.3.1 Double-Sided Feedback Control System with the Controller in the Feedback Path

Consider the feedback system shown in Figure 3.2, with the plant $G(z)$ and controller/compensator $K(z)$. The transfer function of the closed-loop system is given by:

$$W(z) = (I + G(z)K(z))^{-1}G(z) \tag{3.25}$$

If the original controller/compensator $K(z)$ is replaced by a reduced-order controller $K_r(z)$, then the closed-loop system transfer function is given by:

$$W_r(z) = (I + G(z)K_r(z))^{-1}G(z) \tag{3.26}$$

Subsequently the error between both the closed loop systems is:

$$W(z) - W_r(z) = (I + G(z)K(z))^{-1}G(z) - (I + G(z)K_r(z))^{-1}G(z) \tag{3.27}$$

(3.27) can be formulated as a double sided frequency weighted model reduction problem as described in Lemma 3.4.

Lemma 3.4: Given a plant $G(z)$, controller/compensator $K(z)$ and a reduced order controller/compensator $K_r(z)$ subtracting (3.26) from (3.25) and assuming that the second order terms in $[K(z) - K_r(z)]$ are negligible, we will have:

$$W(z) - W_r(z) = (I + G(z)K(z))^{-1}G(z)\,[K(z) - K_r(z)]\,(I + G(z)K(z))^{-1}G(z) \tag{3.28}$$

Proof:

$$\begin{aligned}
&W(z) - W_r(z) \\
&= (I + G(z)K(z))^{-1}G(z) - (I + G(z)K_r(z))^{-1}G(z) \\
&= \left[(I + G(z)K(z))^{-1} - (I + G(z)K_r(z))^{-1}\right] G(z) \\
&= \left[I - (I + G(z)K_r(z))^{-1}(I + G(z)K(z))\right] (I + G(z)K(z))^{-1}G(z) \\
&= (I + G(z)K_r(z))^{-1}[(I + G(z)K_r(z)) - (I + G(z)K(z))](I + G(z)K(z))^{-1}G(z) \\
&= (I + G(z)K_r(z))^{-1}\,[G(z)K_r(z) - G(z)K(z)]\,(I + G(z)K(z))^{-1}G(z)
\end{aligned}$$

Replacing $K_r(z)$ by $K(z)$ in the first term $(I+G(z)K_r(z))^{-1}$ is equivalent to neglecting second order terms of $K(z) - K_r(z)$ whose norm is small and can be neglected. Thus, we have:

$$\begin{aligned}
&W(z) - W_r(z) \\
&= (I + G(z)K(z))^{-1}G(z)\,[K(z) - K_r(z)]\,(I + G(z)K(z))^{-1}G(z) \qquad \blacksquare
\end{aligned}$$

The output and input weights immediately follow from (3.28) where both the output and input weights are $V_1(z) = V_2(z) = (I + G(z)K(z))^{-1}G(z)$. Therefore, the controller reduction problem can be reduced to a double-sided frequency weighted

model reduction problem, which aims to minimize an index of the form $e = \|W(z) - W_r(z)||_\infty$.

3.3.2 Augmented Closed Loop Configuration

In order to derive the parameterized FWMR formulation for the feedback configuration shown in Figure 3.2, The closed loop configuration in Figure 3.2 firstly needs to be expressed in another augmented closed-loop configuration which incorporates a free parameter matrix $C = cI$ shown in Figure 3.5. A more detailed view of the new configuration of Figure 3.5 is shown in Figure 3.6. The new configuration consists of the original plant $G(z)$ and two controllers $C^2K(z)$ and $K(z)(I - CH_c(z))$. Note that the closed-loop configurations in Figures 3.2, 3.5 and 3.6 yield the same closed-loop system transfer functions algebraically.

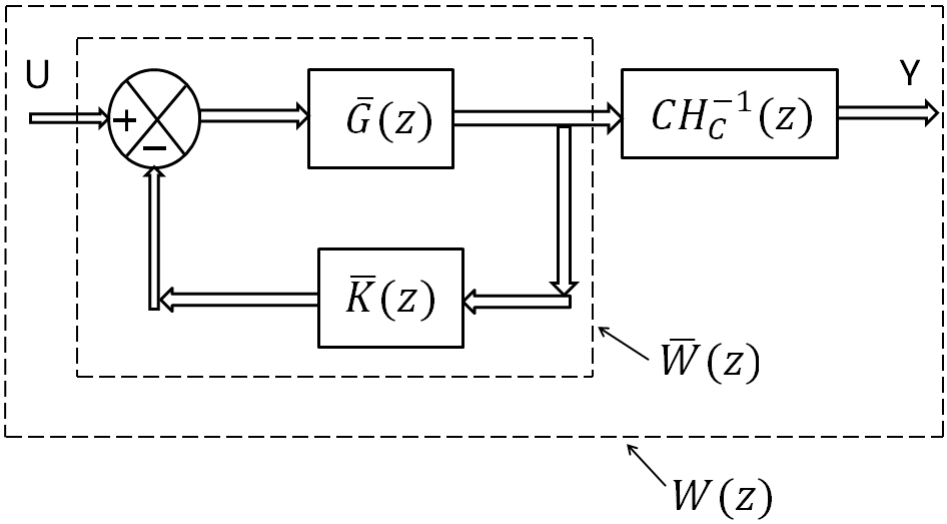

Figure 3.5: Augmented closed loop configuration

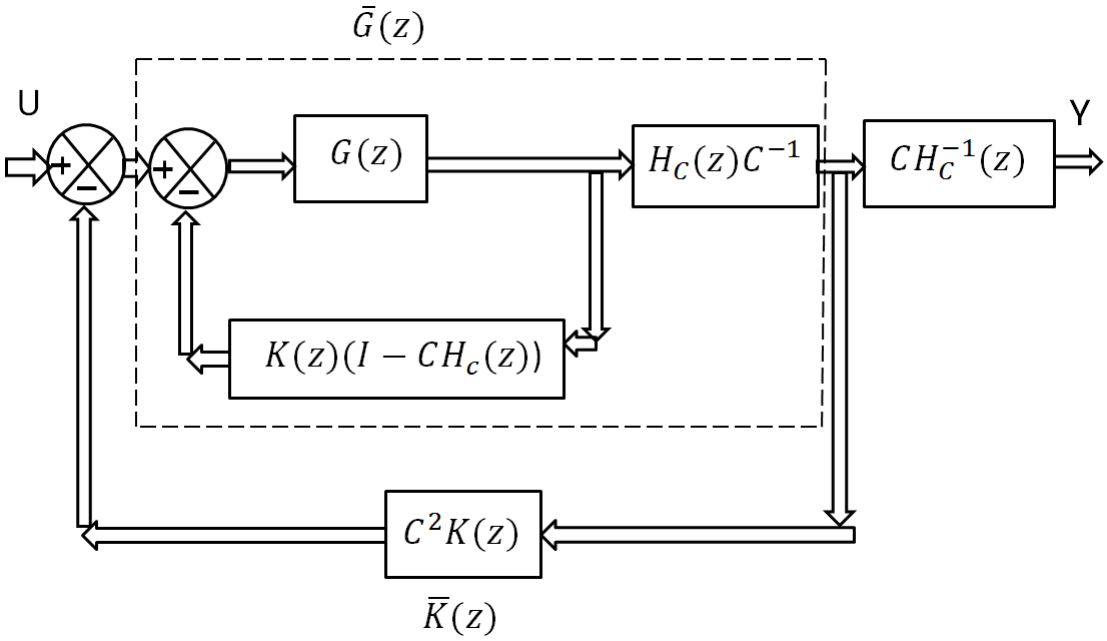

Figure 3.6: Detailed view of $\bar{G}(z)$ and $\bar{K}(z)$ in Figure 3.5

3.3.3 Relationship between Closed Loop Configurations

In this subsection we derive the relationships between the closed-loop configurations shown in Figures 3.2, 3.5 and 3.6. The transfer function matrices $G(z)$ and $K(z)$ have dimensions $m \times n$ and $n \times m$ respectively. The free matrix parameter $C = cI$ used in this paper has a dimension of $m \times m$ and has equal entries along the diagonal (denoted as c) which ensures that the commutative properties of the expressions $CG(z)K(z) = G(z)K(z)C$ and $H^{-1}(z)H_c(z) = H_c(z)H^{-1}(z)$ holds true [74]. Let $W(z) = (I + G(z)K(z))^{-1}G(z)$, $\bar{W}(z) = (I + \bar{G}(z)\bar{K}(z))^{-1}\bar{G}(z)$ be two closed-loop transfer functions with plants and controllers $G(z)$, $K(z)$ and $\bar{G}(z)$, $\bar{K}(z)$ respectively.

Definition 3.3:

$$H_c(z) = I + G(z)K(z)(I - C)$$

$$H_c'(z) = I + K(z)G(z)(I - C)$$

$$J_c(z) = I + (I - CH_c(z))G(z)K(z).$$

$$\bar{H}(z) = I + \bar{G}(z)\bar{K}(z)$$

$$H(z) = I + G(z)K(z) \tag{3.29}$$

Remark 3.2: By assuming that $(I + G(z)K(z))^{-1}$ exists, it can be shown that $(I+G(z)K(z)(I-C))^{-1}$ and $(I+(I-CH_c(z))G(z)K(z))^{-1}$ also exist for a given c, except for a finite number of values of c which will be disregarded [67]. Assume now that we have the closed-loop systems $W(z) = H^{-1}(z)G(z)$ and $\bar{W}(z) = \bar{H}^{-1}(z)\bar{G}(z)$ as defined above. Then the following lemma applies:

Lemma 3.5: If we are given $\bar{K}(z) = C^2K(z)$ and $\bar{G}(z) = J_c^{-1}(z)H_c(z)C^{-1}G(z)$ (where $C \neq 0_{m\times m}$), then the relationship between $W(z)$ and $\bar{W}(z)$ becomes:

$$W(z) = H_c^{-1}(z)C\bar{W}(z) \tag{3.30}$$

Proof: Note that the commutative property $G(z)K(z)H^{-1}(z) = H^{-1}(z)G(z)K(z)$ holds, as a consequence the property $H^{-1}(z)H_c(z) = H_c(z)H^{-1}(z)$ also holds true [74]. Now we have $\bar{W}(z)$:

$$= (I + \bar{G}(z)\bar{K}(z))^{-1}\bar{G}(z)$$

$$= (I + J_c^{-1}(z)H_c(z)G(z)C^{-1}C^2K(z))^{-1}J_c^{-1}(z)H_c(z)C^{-1}G(z)$$

$$= (J_c(z) + J_c(z)J_c^{-1}(z)CH_c(z)G(z)K(z))^{-1}$$

$$H_c(z)C^{-1}G(z)$$

$$= (I + (I - CH_c(z))G(z)K(z) + CH_c(z)G(z)K(z))^{-1}H_c(z)C^{-1}G(z)$$

$$= (I + G(z)K(z))^{-1}H_c(z)C^{-1}G(z)$$

$$= H^{-1}(z)H_c(z)C^{-1}G(z)$$

$$= H_c(z)C^{-1}H^{-1}(z)G(z) = H_c(z)C^{-1}W(z) \qquad \blacksquare$$

It follows that

$$W(z) = H_c^{-1}(z)C\bar{W}(z) \tag{3.31}$$

If the reduced order controllers K_r and $\bar{K}_r$ are used instead, (3.31) becomes:

$$W_r(z) = H_c^{-1}(z)C\bar{W}_r(z) \tag{3.32}$$

We have shown that the closed-loop system $W(z)$ in Figure 3.2 can be replaced by the augmented closed-loop system $H_c^{-1}(z)C\bar{W}(z)$ in Figure 3.5. It can be easily shown that when $C = I$ the closed loop block diagram in Figure 3.2 is identical with the closed loop block diagram in Figure 3.5.

Remark 3.3: The relationship between $W(z)$ and $\bar{W}(z)$ as described by equation (3.30) which is essential in the theoretical development in the following sections holds true provided that the free parameter matrix C is a diagonal matrix with equal entries along the diagonal and $C \neq 0_{m\times m}$.

Remark 3.4: Although $W(z)$ and $\bar{W}(z)$ are related algebraically by (3.30) and Figures 3.2, 3.5 and 3.6 yield the same closed loop transfer algebraically, applying state space modelling and simplifying the augmented closed loop configuration in Figure 3.5 computationally may inflate the order of $\bar{W}(z)$ due to additional pole/zero dynamics being introduced due to the block diagram algebra. Extensive simulations have shown that very large absolute values of the diagonal entries of the free parameter matrix C ($|c| \geq 100$) can effect the equality of (3.30) where the frequency response of $\bar{W}(z)$ deteriorates at low frequencies. Therefore in this paper the range of absolute values considered for c is restricted to the interval $c = [-20, 20]$.

3.3.4 Derivation of New Double Sided Frequency Weights

In this section we derive new double sided frequency weights based on the augmented configuration in Figure 3.5. The system $\bar{W}(z)$ has a plant $\bar{G}(z) = J_c^{-1}(z)H_c(z)C^{-1}G(z)$ and a controller $\bar{K}(z) = C^2K(z)$ and similarly the system $\bar{W}_r(z)$ has a plant

$\bar{G}(z) = J_c^{-1}(z)H_c(z)C^{-1}G(z)$ and controller $\bar{K}_r(z) = C^2K_{rc}(z)$. The relationship between the error of $W(z) - W_r(z)$ and $\bar{W}(z) - \bar{W}_r(z)$ is used to derive the new weights and this relationship is expressed by subtracting (3.32) from (3.31)

$$W(z) - W_r(z) = H_c^{-1}(z)C(\bar{W}(z) - \bar{W}_r(z)) \tag{3.33}$$

where $W(z) - W_r(z)$ refers to the standard double sided frequency weighted model reduction problem formulation with the weights as shown in (3.28).

Theorem 3.2: Based on the definitions described in Definition 2, we have:

$$W(z) - W_r(z) = CH^{-1}(z)G(z)[K(z) - K_{rc}(z)]H_c(z)H^{-1}(z)G(z) \tag{3.34}$$

Proof:

Firstly $\bar{W}(z) - \bar{W}_r(z)$ is obtained by generalizing (3.28) as follows:

$$\begin{aligned}
&\bar{W}(z) - \bar{W}_r(z) \\
&= (I + \bar{G}(z)\bar{K}(z))^{-1}\bar{G}(z)\left[\bar{K}(z) - \bar{K}_r(z)\right](I + \bar{G}(z)\bar{K}(z))^{-1}\bar{G}(z) \\
&= H_c(z)C^{-1}H^{-1}(z)G(z)[C^2K(z) - C^2K_{rc}(z)]H_c(z)C^{-1}H^{-1}(z)G(z) \\
&= H_c(z)H^{-1}(z)G(z)[K(z) - K_{rc}(z)]H_c(z)H^{-1}(z)G(z)
\end{aligned} \tag{3.35}$$

Substituting $\bar{W}(z) - \bar{W}_r(z)$ from (3.35) into (3.33) yields:

$$W(z) - W_r(z) = CH^{-1}(z)G(z)[K(z) - K_{rc}(z)]H_c(z)H^{-1}(z)G(z) \quad \blacksquare$$

The new weights follow directly from (3.34) where $V_1(z) = CH^{-1}(z)G(z)$ and $V_2(z) = H_c(z)H^{-1}(z)G(z)$. Equation (3.34) is a generalized version of equation (3.28) which incorporates a free parameter matrix $C = cI$ such that a different controller denoted as $K_{rc}(z)$ is obtained which corresponds the variation of the diagonal entries of the free parameter matrix $C = cI$. When $C = I$, equation (3.34) reduces to the original form as shown in equation (3.28). Upon solving the double sided FWMR problem with the double sided weights as described in (3.34) and obtaining the reduced order controller - $K_{rc}(z)$, this reduced order controller - $K_{rc}(z)$ is replaced into (3.28) to establish the frequency weighted approximation error denoted

as E_c as a function of the free parameter matrix $C = cI$ as follows:

$$W_{rc}(z) = E_c$$

$$E_c = H^{-1}(z)G(z)\left[K(z) - K_{rc}(z)\right]H^{-1}(z)G(z) \tag{3.36}$$

Definition 3.4:

$$e_c = ||E_c||_\infty \tag{3.37}$$

$$W(z) - W_r(z) = E_1 \tag{3.38}$$

$$E_1 = H^{-1}(z)G(z)\left[K(z) - K_r(z)\right]H^{-1}(z)G(z) \tag{3.39}$$

$$e_1 = ||E_1||_\infty \tag{3.40}$$

The following section describes how varying the diagonal entries of the free parameter matrix $C = cI$ in this new double sided frequency weighted model reduction problem formulation minimizes the infinity norm of the approximation error described by equation (3.36)

3.3.5 Error Analysis

Based on the theory derived in section 3.1 - 3.4, the proposed technique aims to minimize the norm of the approximation error between the original closed loop system and closed loop system with a reduced order controller by using the weights $V_1(z)$ and $V_2(z)$ from (3.34) together with a large value of the diagonal entries of the free parameter matrix $C = cI$. The effect of varying the diagonal entries of the free parameter matrix $C = cI$ towards reducing the infinity norm of the approximation error in (3.36) is described in Lemma 3.6 as follows:

Lemma 3.6: Let e_c and e_1 be as defined in (3.37) and (3.40), Then we will have:

$$e_c = ||E_1 H_c'^{-1}(z)C^{-1}||_\infty \tag{3.41}$$

Proof: Note that:

$H_c(z)H^{-1}(z)G(z) = H^{-1}(z)H_c(z)G(z) = H^{-1}(z)G(z)H_c'(z)$,

where $H'_c(z) = I + K(z)G(z)(I - C)$. Substituting (3.38) into (3.34) yields:

$$\begin{aligned} E_1 &= CH^{-1}(z)G(z)[K(z) - K_{rc}(z)]H_c(z)H^{-1}(z)G(z) \\ &= CH^{-1}(z)G(z)[K(z) - K_{rc}(z)]H^{-1}(z)G(z)H'_c(z) \\ &= CE_cH'_c(z) \end{aligned} \tag{3.42}$$

Rearranging (3.42) and applying the infinity norm to both sides of the equation yields:

$$||E_c||_\infty = ||E_1 H'^{-1}_c(z)C^{-1}||_\infty \qquad \blacksquare$$

If the absolute value of the diagonal entries of the free parameter matrix $C = cI$ increases, the right hand side of (3.41) becomes smaller. To compensate for this, the left hand side of (3.41) is forced to produce a reduced order controller $K_{rc}(z)$ which is closer to $K(z)$ than the original reduced order controller $K_r(z)$ which is obtained using standard techniques.

3.3.6 Comparison of the Variation of the Approximation Error e_c between Feedback Control Systems with the Controller in the Forward Path and Feedback Paths

There is a difference between the behaviour of the approximation error e_c for the proposed parameterized controller reduction technique for feedback control systems with the controller in the feedback path (Case 1) compared to the parameterized controller reduction technique for feedback control systems with the plant and controller connected in series in the forward path (Case 2) as described previously by Houlis and Sreeram in [65–67]. The additional parameter C^{-1} in equation (3.41) only exists for Case 1. Due to the existence of this additional parameter, choosing a large value of the diagonal entries of the free parameter matrix $C = cI$ produces a reduced order controller $K_{rc}(z)$ which gives a reduced approximation error e_c without the need to construct an approximating function to locate the optimal value of

c as in [65–67]. There is however a limit on how much the absolute value of c can be increased due to the constraint mentioned in Remark 3.4. This characteristic can be illustrated by comparing both equation (3.41) and equation (3.22) which correspond to Case 1 and Case 2 respectively.

$$e_c \approx ||E_1 H_c'^{-1}(z) C^{-1}||_\infty \qquad \text{(Case1)}$$

$$e_1 h_c^{-1} \leq e_c \leq e_1 \hat{h}_c \qquad \text{(Case2)}$$

For Case 1 it is clear that whenever c is increased (to a certain limit) e_c becomes smaller and the value of c which results in a reduced order controller which yields low approximation error e_c can be determined by choosing a large absolute value of c. However for Case 2 the approximation error e_c is bounded by two quantities, each of which has a constant part e_1 and a function which depends on $H_c(z)$. Therefore selecting a value of c which will give an optimal reduced order controller with low approximation error e_c requires the construction of an approximation function to locate the value of c which will give an optimal reduced order controller as described in [65–67].

3.4 Computational Procedure and Numerical Example

The following 6th order MIMO plant $G(z) = \{A_G, B_G, C_G, D_G\}$ is obtained by discretizing a continuous time plant representing a Turbo Generator System [75] using a zero-order hold on the inputs and a sampling rate of 0.01 sec. A corresponding 6th order MIMO LQG compensator $K(z) = \{A_K, B_K, C_K, D_K\}$ is designed and connected in the feedback path as shown in Figure 3.4.

$$A_G = \begin{bmatrix} 0.8307 & 0.03725 & -0.01946 & 0.00198 & 0.003445 & -0.0007797 \\ -0.03589 & 0.9407 & 0.0548 & -0.006994 & -0.01145 & 0.002712 \\ 0.01274 & 0.014 & 0.9741 & 0.006247 & 0.008582 & -0.002234 \\ -0.0001502 & 0.002298 & -0.005087 & 0.9962 & -0.06288 & 0.001241 \\ -0.0003139 & -0.003263 & 0.006872 & 0.06284 & 0.9912 & 0.003656 \\ -0.0004889 & -0.002277 & 0.002195 & -0.0004889 & -0.002277 & 0.002195 \end{bmatrix}$$

$$B_G = \begin{bmatrix} -0.002503 & 0.02584 \\ -0.0004749 & -0.0885 \\ -0.001553 & 0.07212 \\ 0.0007442 & -0.04608 \\ -0.0007918 & -0.1031 \\ 0.0002449 & 0.1381 \end{bmatrix}$$

$$C_G = \begin{bmatrix} 0.5971 & -0.7697 & 4.885 & 4.861 & -9.818 & -8.861 \\ 3.101 & 9.342 & -5.6 & -0.749 & 2.997 & 10.57 \end{bmatrix}$$

$$D_G = \begin{bmatrix} 0 & 0 \\ 0 & 0 \end{bmatrix}$$

$$A_K = \begin{bmatrix} 0.8035 & -0.02234 & -0.02285 & -0.04204 & 0.083 & -0.01892 \\ -0.2989 & 0.3133 & 0.1484 & -0.2402 & 0.3481 & -0.1251 \\ -0.07798 & -0.165 & 0.9178 & -0.1754 & 0.3457 & 0.03183 \\ 0.1137 & 0.2065 & 0.1121 & 1.252 & -0.5418 & -0.1629 \\ 0.2312 & 0.4262 & 0.2123 & 0.5575 & 0.06873 & -0.2626 \\ -0.1443 & -0.4776 & 0.3576 & 0.07943 & -0.2295 & 0.2205 \end{bmatrix}$$

$$B_K = \begin{bmatrix} 0.008386 & 0.007144 \\ 0.06522 & 0.07225 \\ 0.03584 & 0.02234 \\ -0.05345 & -0.02641 \\ -0.1031 & -0.05479 \\ -0.01804 & 0.04983 \end{bmatrix}$$

$$C_K = \begin{bmatrix} 0.007095 & 0.02788 & 0.0912 & -0.0271 & 0.03801 & -0.02741 \\ -0.000525 & 0.02949 & -0.08547 & -0.3357 & 0.7247 & -0.6575 \end{bmatrix}$$

$$D_K = \begin{bmatrix} 0 & 0 \\ 0 & 0 \end{bmatrix}$$

3.4.1 Effect of Varying the Diagonal Entries of the Free Parameter Matrix towards the Infinity Norm of the Approximation Error

By using the Enns double sided frequency weighted model reduction technique [25] with the following input and output weights - $V_1(z) = CH^{-1}(z)G(z)$ and $V_2(z) = H_c(z)H^{-1}(z)G(z)$, the resulting reduced order controllers $K_{rc}(z)$ obtained for various values of the diagonal entries of the free parameter matrix $C = cI$ ranging from $c = [-20, 20]$ (with the exception of $c = 0$) are then replaced into equation (3.28). The corresponding infinity norms of the approximation error $e_c = ||W(z) - W_{rc}(z)||_\infty = ||H^{-1}(z)G(z)\left[K(z) - K_{rc}(z)\right]H^{-1}(z)G(z)||_\infty$ are calculated with respect to the variation of the diagonal entries of the free parameter matrix $C = cI$. e_1 denotes the standard Enns Method whereas e_{20} denotes the proposed method where a large absolute value of c is used ($c = 20$). Figure 3.7 and 3.8 show the plots of the infinity norm of the approximation error $e_c = ||W(z) - W_{rc}(z)||_\infty$ vs variation of the diagonal entries of the free parameter matrix $C = cI$ for a second

and third reduced order controller respectively. Controller reduction up to the first order was not considered due to the fact that $K(z)$ and $K_r(z)$ can be drastically different for very low orders and as a result (3.28) is no longer a good approximation of (3.27) [76]. Table 3.1 displays these approximation errors of the proposed technique denoted as e_{20} relative to the standard Enns technique denoted as e_1 [25].

The effect of varying the diagonal entries of the free parameter matrix $C = cI$ towards the behaviour of the approximation error $e_c = ||W(z) - W_{rc}(z)||_\infty$ for Case 1 is shown in Figures 3.7 and Figure 3.8 and can be described by equation (3.41). Table 3.1 shows the approximation error $e_c = ||W(z) - W_{rc}(z)||_\infty$ for both the standard Enns method and the proposed method. Increasing the the absolute value of the diagonal entries of C^{-1} (to a certain limit) on the right hand side of (3.41) forces the left hand side of (3.41) to produce a controller $K_{rc}(z)$ which yields a lower approximation error relative to the standard Enns method. On the contrary for Case 2, in order to locate the optimal value for the diagonal entries of the free parameter matrix, a searching procedure is required due to the behaviour of $e_c = ||W(z) - W_{rc}(z)||_\infty$ as depicted by equation (3.22).

Table 3.1: $e_c = ||W(z) - W_{rc}(z)||_\infty$ for Case 1

Order	$\|\|W(z) - W_{r1}(z)\|\|_\infty$	$\|\|W(z) - W_{r20}(z)\|\|_\infty$
5	0.009985	0.002462
4	0.03543	0.03157
3	5.379	1.569
2	8.331	6.866

Remark 3.5: The closed loop configurations with the controller in the forward path (Figure 3.1) differ from the closed loop configurations with the controller in the feedback path (Figure 3.2) in terms of the closed loop transfer function as shown in (3.1) and (3.25) and also the double sided weights for standard FWMR techniques

as shown in (3.3) and (3.28). The parameterized double sided weights described in Theorem 3.1 and Theorem 3.2 also differ. Due to these inherent differences, the infinity norm of the approximation error $e_c = ||W(z) - W_{rc}(z)||_\infty$ obtained by varying the diagonal entries of the free parameter matrix $C = cI$ for the closed loop system with the controller in the forward path and the controller in the feedback path are not directly comparable.

3.4.2 Computational Procedure of the Proposed Method

1. Given a plant $G(z)$ and controller $K(z)$ connected in the feedback path as shown in Figure 2, define the stable output and input weights $V_1(z) = CH^{-1}(z)G(z)$ and $V_2(z) = H_c(z)H^{-1}(z)G(z)$. (Note that if positive feedback is used as in Figure 4, $H(z) = I - G(z)K(z)$).

2. Solve the double sided frequency weighted model reduction problem $V_1(z)(K(z) - K_{rc}(z))V_2(z)$ for a large value of c to obtain the desired controller $K_{rc}(z)$

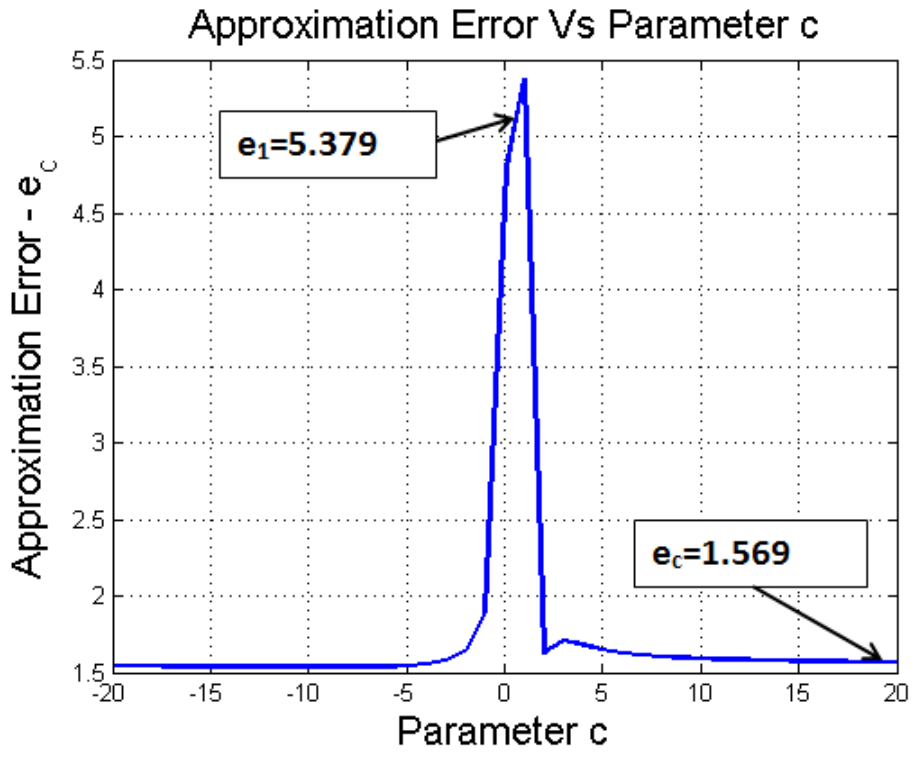

Figure 3.7: e_c for a 3rd order controller.

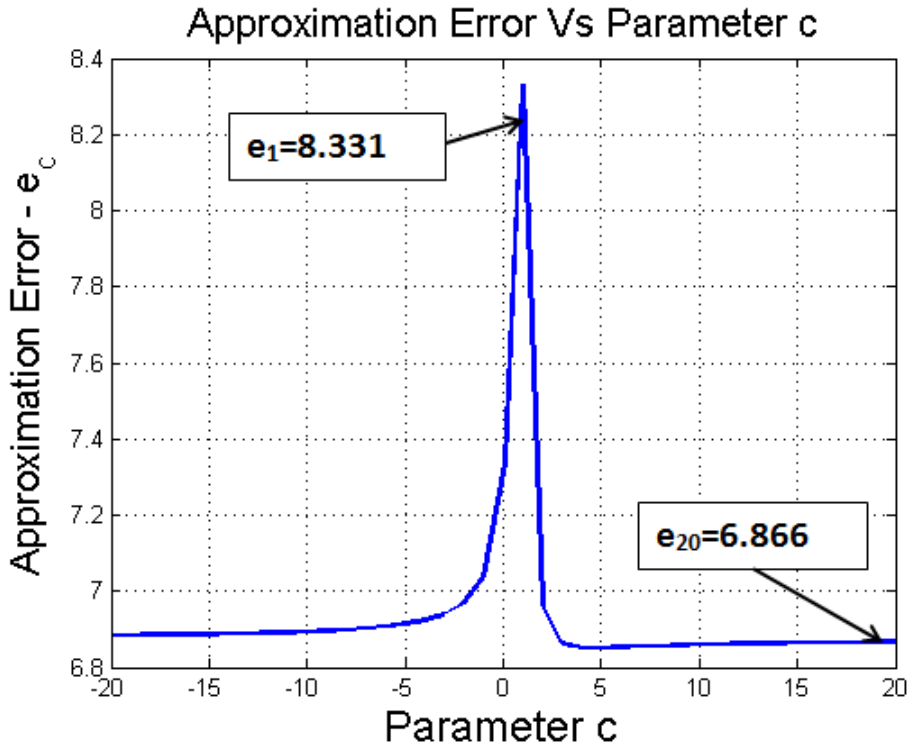

Figure 3.8: e_c for a 2nd order controller.

3.5 Conclusion

Formulas for a new pair of double sided frequency weights for the frequency weighted model reduction problem have been derived for a non-unity MIMO discrete time feedback control system with the controller in the feedback path. The advantage of the proposed formulation is that the optimal values for the diagonal entries of the free parameter matrix $C = cI$ which minimize the infinity norm of the approximation error $e_c = ||W(z) - W_{rc}(z)||_\infty$ can be obtained by selecting a large value for the diagonal entries of the free parameter matrix without the need to use an approximating function. In addition the new weights in this proposed problem formulation which are a function of a free parameter matrix are compatible with any of the standard double sided frequency weighted model reduction techniques.

Chapter 4

Frequency Interval Cross Gramians for Continuous-Time Linear and Bilinear Systems

4.1 Introduction

Many control engineering problems which involve the computation of gramians are inherently frequency dependent, for example Gawronski and Juang had emphasized that no realistic sensor or actuator can operate over an infinite frequency interval [29]. Similarly Varga et al. had described that the models which represent the aerodynamics and structural mechanics of aircraft flexible structures are only valid up to specific frequency intervals [77]. These inherent constraints have led to extensive theoretical developments in robust control techniques which emphasize particular frequency intervals and extensive developments in this area have been presented in [49–54, 78].

It is a common occurrence in many control applications that the processes under consideration are nonlinear. Linearization methods are often insufficient to capture the characteristics of the nonlinear process. Bilinear systems are an important category of nonlinear systems which have well established theories and many nonlinear

systems can be represented as bilinear systems [40, 64].

Controllability and observability gramians are matrices which contain information regarding controllability and observability of a system. Similar to the case of linear systems, information regarding the controllability and observability of bilinear systems is a prerequisite for understanding the characteristics of a system and controller design. The theory for obtaining frequency interval controllability and observability gramians for bilinear systems have been presented in [56, 79]. Another type of gramian matrix known as cross gramians contains combined information regarding controllability and observability in a single matrix and requires solving only one Sylvester equation and is therefore useful in reducing computational complexity associated with solving two Lyapunov equations for obtaining the controllability and observability gramians [80, 81]. There also exists yet another type of matrix known as the Gram matrix which is related to the controllability, observability and cross gramians [83, 84].

Decentralized control is an established control strategy for industrial processes [42–45]. A prerequisite for implementing decentralized control is to select appropriate input and output pairs for the control design and this process is known as control configuration selection. The control configuration selection method is based on firstly decomposing a MIMO system into its elementary SISO subsystems and subsequently a participation matrix which indicates the degree of controllability and observability of each SISO subsystem is constructed. In order to form a nominal model, highly controllable and observable subsystems can be identified from the participation matrix and subsequently can be retained whereas the least controllable and observable subsystems can be discarded [46, 47]. Previous studies have demonstrated the computational efficiency of using unweighted cross gramians as part of the control configuration selection framework [42, 85–87]. The preliminary findings regarding the usage of frequency interval controllability and observability gramians for input-output interactions in control configuration selection for linear

systems was first reported in [88]. Control configuration selection using frequency interval controllability and observability gramians for bilinear systems have been developed in [79]. Both these works in [79, 88] incorporate the control configuration selection input-output pairing procedure originally presented in [46, 47].

The contributions presented in this chapter are as follows. Firstly a new generalized Sylvester equation for obtaining the frequency interval cross gramian is derived for linear SISO systems. This method is then further developed to obtain a new generalized Sylvester equation for obtaining the frequency interval cross gramian for bilinear SISO systems. The computational efficiency of using frequency interval cross gramians derived in this study is demonstrated by numerical examples which present the application of frequency interval cross gramians for constructing a participation matrix as part of the control configuration selection procedure for both linear and bilinear systems.

The notation used in this paper is as follows. M^* denotes the transpose of matrix. The $\otimes$ symbol represents the Kronecker product. $Struct(L_n) = [\phi_{ij}]_{p\times p}$ shows the structure of the system L_n which is a symbolic matrix where $\phi_{ij} = \star$ if there exists a subsystem in L_n with input u_i and output y_j. Otherwise $\phi_{ij} = 0$.

4.2 Preliminaries

In this section preliminary material on controllability, observability and cross gramians are presented in section 4.2.1, frequency interval controllability and observability gramians for linear and bilinear systems are presented in section 4.2.2 and section 4.2.3 respectively.

4.2.1 Controllability, Observability and Cross Gramians

Assuming that a linear continuous time, controllable, observable and stable SISO system Σ is defined by:

$$\Sigma = \begin{cases} \dot{x}(t) = Ax(t) + Bu(t) \\ y(t) = Cx(t) \end{cases} \tag{4.1}$$

SISO systems have symmetric transfer functions such that $H(s) = H^*(s)$ [89] where:

$$C(sI - A)^{-1}B = B^*((sI - A)^*)^{-1}C^* \tag{4.2}$$

For these SISO systems, the matrices A and A^*, C and B^* are related by a similarity transformation matrics T which is invertible such that:

$$A^* = T^{-1}AT, C^* = T^{-1}B, B^* = CT \tag{4.3}$$

For the SISO system defined in (4.1), the time and frequency domain controllability gramian (P), observability gramian (Q) and cross gramian (R) can be defined as follows:

$$\begin{aligned} P &= \int_0^\infty e^{A\tau}BB^*e^{A^*\tau}d\tau \\ &= \frac{1}{2\pi}\int_{-\infty}^{\infty}(j\omega I - A)^{-1}BB^*(-j\omega I - A^*)^{-1}d\omega \end{aligned} \tag{4.4}$$

$$\begin{aligned} Q &= \int_0^\infty e^{A^*\tau}C^*Ce^{A\tau}d\tau \\ &= \frac{1}{2\pi}\int_{-\infty}^{\infty}(-j\omega I - A^*)^{-1}C^*C(j\omega I - A)^{-1}d\omega \end{aligned} \tag{4.5}$$

$$\begin{aligned} R &= \int_0^\infty e^{A\tau}BCe^{A\tau}d\tau \\ &= \frac{1}{2\pi}\int_{-\infty}^{\infty}(j\omega I - A)^{-1}BC(-j\omega I - A)^{-1}d\omega \end{aligned} \tag{4.6}$$

where $H(\omega) = (j\omega I - A)^{-1}$, $H^*(\omega) = (-j\omega I - A^*)^{-1}$, $H_R(\omega) = (-j\omega I - A)^{-1}$ and I denotes an identity matrix. (4.4),(4.5) and (4.6) can be determined by solving the following Lyapunov and Sylvester equations:

$$AP + PA^* + BB^* = 0 \tag{4.7}$$

$$A^*Q + QA + C^*C = 0 \tag{4.8}$$

$$AR + RA + BC = 0 \tag{4.9}$$

The fundamental property which relates the cross gramian to the controllability and observability gramians for systems with symmetric transfer functions is defined by Fernando and Nicholson as follows [80]:

$$R^2 = PQ \tag{4.10}$$

Cross gramian matrices contain combined information regarding controllability and observability in a single matrix and have been applied previously in a variety of applications such as for the model order reduction of large scale dynamical systems and systems with complex hyperbolic networks [81] and control configuration selection. However the usage of cross gramians are limited only to SISO or symmetric MIMO systems [82]. In this chapter the frequency interval cross gramians are derived for both linear and bilinear SISO systems. The computational efficiency associated with the usage of frequency interval cross gramians are demonstrated in the numerical examples section in which frequency interval cross gramians are applied as part of the framework of control configuration selection for both linear and bilinear systems.

4.2.2 Frequency Interval Controllability and Observability Gramians for Linear Systems

Definition 4.1 ([29]). The frequency interval controllability and observability gramians within the interval $\Omega = [\omega_1, \omega_2]$ for the stable linear system in (4.1) are defined as:

$$\hat{P}_\Omega = \hat{P}(\omega_2) - \hat{P}(\omega_1) \tag{4.11}$$

$$\hat{Q}_\Omega = \hat{Q}(\omega_2) - \hat{Q}(\omega_1), \tag{4.12}$$

where

$$\hat{P}(\omega) = \frac{1}{2\pi}\int_{-\omega}^{\omega} H(\omega)BB^*H^*(\omega)d\omega \tag{4.13}$$

$$= \frac{1}{2\pi}\int_{-\infty}^{+\infty} H(\mu)\left[S(\omega)BB^* + BB^*S^*(\omega)\right]H^*(\mu)d\mu$$

$$= S(\omega)P + PS^*(\omega) \tag{4.14}$$

$$\hat{Q}(\omega) = \frac{1}{2\pi}\int_{-\omega}^{\omega} H^*(\omega)C^*CH(\omega)d\omega \tag{4.15}$$

$$= \frac{1}{2\pi}\int_{-\infty}^{+\infty} H^*(\mu)\left[S(\omega)C^*C + C^*CS(\omega)\right]H(\mu)d\mu$$

$$= S^*(\omega)Q + QS(\omega) \tag{4.16}$$

and

$$S(\omega) = \frac{1}{2\pi}\int_{-\omega}^{+\omega} H(\omega)d\omega$$

$$= \frac{1}{2\pi}\int_{-\omega}^{+\omega} (j\omega I - A)^{-1}d\omega \tag{4.17}$$

$$= \frac{j}{2\pi}\ln[(j\omega I + A)(-j\omega I + A)^{-1}] \tag{4.18}$$

It follows that $\hat{P}(\omega)$ and $\hat{Q}(\omega)$ are the solutions to the following Lyapunov equations [29]:

$$A\hat{P}(\omega) + \hat{P}(\omega)A^* + S(\omega)BB^* + BB^*S^*(\omega) = 0 \tag{4.19}$$

$$A^*\hat{Q}(\omega) + \hat{Q}(\omega)A + S^*(\omega)C^*C + C^*CS(\omega) = 0. \tag{4.20}$$

4.2.3 Frequency Interval Controllability and Observability Gramians for Bilinear Systems

Let Σ be a stable SISO bilinear dynamical system described by:

$$\Sigma = \begin{cases} \dot{x}(t) = Ax(t) + \sum_{j=1}^{m} N_j x(t)u_j(t) + Bu(t) \\ y(t) = Cx(t) \end{cases} \tag{4.21}$$

where $x(t) \in \mathbb{R}^n$,$u(t) \in \mathbb{R}^m$, $y(t) \in \mathbb{R}^m$

Definition 4.2 ([56, 79]). The frequency interval controllability gramian for the bilinear system defined in (4.21) for the frequency interval $\Omega = [\gamma_1, \gamma_2]$ is as follows:

$$\hat{P}_\Omega = \hat{P}(\gamma_2) - \hat{P}(\gamma_1) \tag{4.22}$$

where

$$\begin{aligned}
&\hat{P}(\omega) = \\
&\sum_{i=1}^{\infty} \frac{1}{(2\pi)^i} \int_{-\omega}^{+\omega} ... \int_{-\omega}^{+\omega} \hat{P}_i(\omega_1, ..., \omega_i) \hat{P}_i^*(\omega_1, ..., \omega_i) ... d\omega_i \qquad (4.23)\\
&\hat{P}_1(\omega_1) = (j\omega_1 I - A)^{-1} B \\
&\vdots \\
&\hat{P}_i(\omega_1, ..., \omega_i) \\
&= (j\omega_i I - A)^{-1} \begin{bmatrix} N_1 \hat{P}_{i-1} & N_2 \hat{P}_{i-1} ... & N_m \hat{P}_{i-1} \end{bmatrix}, \qquad (4.24)
\end{aligned}$$

The gramian $\hat{P}(\omega)$ in (4.23) is the solution to the following Lyapunov equation [56, 79]:

$$\begin{aligned}
&A\hat{P}(\omega) + \hat{P}(\omega)A^* + S(\omega) \left(\sum_{j=1}^{m} N_j \hat{P}(\omega) N_j^* \right) + ... \\
&\left(\sum_{j=1}^{m} N_j \hat{P}(\omega) N_j^* \right) S^*(\omega) + S(\omega) BB^* + BB^* S^*(\omega) = 0. \qquad (4.25)
\end{aligned}$$

The Lyapunov equation in (4.25) can be solved by using the iterative numerical solution method described in [40]. The controllability gramian $\hat{P}(\omega)$ is obtained by

$$\hat{P}(\omega) = \lim_{i \to +\infty} \hat{P}_i(\omega) \tag{4.26}$$

where

$$\begin{aligned}
&A\hat{P}_1(\omega) + \hat{P}_1(\omega)A^* + S(\omega)BB^* + BB^* S^*(\omega) = 0, \qquad (4.27)\\
&A\hat{P}_i(\omega) + \hat{P}_i(\omega)A^* + S(\omega)(\sum_{j=1}^{m} N_j \hat{P}_{i-1} N_j^*) + (\sum_{j=1}^{m} N_j \hat{P}_{i-1} N_j^*) S^*(\omega) + ... \\
&S(\omega)BB^* + BB^* S^*(\omega) = 0 \quad i \geq 2. \qquad (4.28)
\end{aligned}$$

Dually the frequency interval observability gramians for the bilinear system presented in [56, 79] is as follows:

$$\hat{Q}_\Omega = \hat{Q}(\gamma_2) - \hat{Q}(\gamma_1) \tag{4.29}$$

where

$$\hat{Q}(\omega) =$$

$$\sum_{i=1}^{\infty} \frac{1}{(2\pi)^i} \int_{-\omega}^{+\omega} ... \int_{-\omega}^{+\omega} \hat{Q}_i^*(\omega_1, ..., \omega_i) \hat{Q}_i(\omega_1, ..., \omega_i) ... d\omega_i \tag{4.30}$$

$$\hat{Q}_1(\omega_1) = C(j\omega_1 I - A)^{-1}$$

$$\vdots$$

$$\hat{Q}_i(\omega_1, ..., \omega_i) = \begin{bmatrix} \hat{Q}_{i-1} N_1 \\ \hat{Q}_{i-1} N_2 \\ \vdots \\ \hat{Q}_{i-1} N_m \end{bmatrix} (j\omega_i I - A)^{-1} \tag{4.31}$$

The gramian $\hat{Q}(\omega)$ in (4.30) is the solution to the following Lyapunov equation [56, 79]:

$$A^* \hat{Q}(\omega) + \hat{Q}(\omega) A + S^*(\omega) \left(\sum_{j=1}^{m} N_j^* \hat{Q}(\omega) N_j \right) + ...$$

$$\left(\sum_{j=1}^{m} N_j^* \hat{Q}(\omega) N_j \right) S(\omega) + S^*(\omega) C^* C + C^* C S(\omega) = 0. \tag{4.32}$$

The Lyapunov equation in (4.32) can also be solved by using the iterative numerical solution method described in [40]. The observability gramian $\hat{Q}(\omega)$ is obtained by

$$\hat{Q}(\omega) = \lim_{i \to +\infty} \hat{Q}_i(\omega) \tag{4.33}$$

where

$$A^* \hat{Q}_1(\omega) + \hat{Q}_1(\omega) A + S^*(\omega) C^* C + C^* C S(\omega) = 0, \tag{4.34}$$

$$A^* \hat{Q}_i(\omega) + \hat{Q}_i(\omega) A + S^*(\omega) (\sum_{j=1}^{m} N_j^* \hat{Q}_{i-1} N_j) + (\sum_{j=1}^{m} N_j^* \hat{Q}_{i-1} N_j) S(\omega) + ...$$

$$S^*(\omega) C^* C + C^* C S(\omega) = 0 \quad i \geq 2. \tag{4.35}$$

4.3 Main Work

4.3.1 Generalized Sylvester Equation for Obtaining Frequency Interval Cross Gramians for Continuous-Time Linear SISO Systems

In this section, a generalized Sylvester equation is derived in which solving this equation yields the frequency interval cross gramian in a specified frequency interval $\Omega = [\omega_1, \omega_2]$ for the SISO linear system.

Definition 4.3: The frequency interval cross gramian for the stable linear system defined in (4.1) is as follows:

$$\hat{R}_\Omega = \hat{R}(\omega_2) - \hat{R}(\omega_1), \tag{4.36}$$

where $\hat{R}(\omega)$ satisfies:

$$\hat{R}(\omega) = \frac{1}{2\pi}\int_{-\omega}^{+\omega}(j\omega I - A)^{-1}BC(-j\omega I - A)^{-1}d\omega. \tag{4.37}$$

Theorem 4.1: $\hat{R}(\omega)$ defined in (4.37) is the solution to the following Sylvester equation:

$$A\hat{R}(\omega) + \hat{R}(\omega)A + S(\omega)BC + BCS(\omega) = 0. \tag{4.38}$$

Proof

(4.9) can be re-written as:

$$\begin{aligned} BC &= -AR - RA \\ &= (j\omega I - A)R + R(-j\omega I - A), \end{aligned} \tag{4.39}$$

Substituting $BC = (j\omega I - A)R + R(-j\omega I - A)$ from (4.39) into (4.37) yields:

$$\hat{R}(\omega) = \frac{1}{2\pi}\int_{-\omega}^{+\omega}(j\omega I - A)^{-1}R + R(-j\omega I - A)^{-1}d\omega, \tag{4.40}$$

Note that

$$\begin{aligned} S(\omega) &= \frac{1}{2\pi}\int_{-\omega}^{+\omega}(j\omega I - A)^{-1}d\omega \\ &= \frac{1}{2\pi}\int_{-\omega}^{+\omega}(-j\omega I - A)^{-1}d\omega \end{aligned}$$

Hence

$$\hat{R}(\omega) = S(\omega)R + RS(\omega), \tag{4.41}$$

Taking into consideration the following property [29, 30]

$$H(\omega_1)H(\omega_2) = H(\omega_2)H(\omega_1), \tag{4.42}$$

and substituting both (4.17) and (4.6) into (4.41) yields

$$\begin{aligned}
&\hat{R}(\omega) = \\
&\frac{1}{2\pi}\int_{-\omega}^{+\omega} H(\omega)d\omega \cdot \frac{1}{2\pi}\int_{-\infty}^{+\infty} H(\mu)BCH_R(\mu)d\mu + ... \\
&\frac{1}{2\pi}\int_{-\infty}^{+\infty} H(\mu)BCH_R(\mu)d\mu \cdot \frac{1}{2\pi}\int_{-\omega}^{+\omega} H(\omega)d\omega \\
&= \frac{1}{2\pi}\int_{-\infty}^{+\infty} \left(\frac{1}{2\pi}\int_{-\omega}^{+\omega} H(\omega)d\omega\right) H(\mu)BCH_R(\mu)d\mu + ... \\
&\frac{1}{2\pi}\int_{-\infty}^{+\infty} H(\mu)BCH_R(\mu)\left(\frac{1}{2\pi}\int_{-\omega}^{+\omega} H(\omega)d\omega\right) d\mu \\
&= \frac{1}{2\pi}\int_{-\infty}^{+\infty} H(\mu)\left(\frac{1}{2\pi}\int_{-\omega}^{+\omega} H(\omega)d\omega\right) BCH_R(\mu)d\mu + ... \\
&\frac{1}{2\pi}\int_{-\infty}^{+\infty} H(\mu)BC\left(\frac{1}{2\pi}\int_{-\omega}^{+\omega} H_R(\omega)d\omega\right) H_R(\mu)d\mu \\
&= \frac{1}{2\pi}\int_{-\infty}^{+\infty} H(\mu)\left[S(\omega)BC + BCS(\omega)\right] H_R(\mu)d\mu,
\end{aligned} \tag{4.43}$$

Since A is stable we can conclude that $\hat{R}(\omega)$ expressed in the form of (4.43) is the solution to the following Sylvester equation:

$$A\hat{R}(\omega) + \hat{R}(\omega)A + S(\omega)BC + BCS(\omega) = 0$$

■

This concludes the proof of Theorem 1. In the following section it is shown that Theorem 1 is instrumental for deriving the Sylvester equation corresponding to frequency interval cross gramians for continuous-time bilinear SISO systems.

4.3.2 Sylvester Equation for Obtaining Frequency Interval Cross Gramians for Continuous-Time Bilinear SISO Systems

In this section, a generalized Sylvester equation is derived in which solving this equation yields the frequency interval cross gramian for a specified frequency interval $\Omega = [\gamma_1, \gamma_2]$ for the SISO bilinear system.

Definition 4.4: The frequency interval cross gramian $\hat{R}_\Omega$ of the bilinear systems defined in (4.21) for the interval $\Omega = [\gamma_1, \gamma_2]$ is as follows:

$$\hat{R}_\Omega = \hat{R}(\gamma_2) - \hat{R}(\gamma_1) \tag{4.44}$$

where

$$\begin{aligned}
&\hat{R}(\omega) = \\
&\sum_{i=1}^{\infty} \frac{1}{(2\pi)^i} \int_{-\omega}^{+\omega} ... \int_{-\omega}^{+\omega} \hat{P}_i(\omega_1, ..., \omega_i)\bar{Q}_i(\omega_1, ..., \omega_i)d\omega_1...d\omega_i \qquad (4.45)\\
&\hat{P}_1(\omega_1) = (j\omega_1 I - A)^{-1}B \\
&\vdots \\
&\hat{P}_i(\omega_1, ..., \omega_i) = (j\omega_i I - A)^{-1}\begin{bmatrix} N_1\hat{P}_{i-1} & N_2\hat{P}_{i-1}...N_m\hat{P}_{i-1} \end{bmatrix} \qquad (4.46)\\
&\bar{Q}_1(\omega_1) = C(-j\omega_1 I - A)^{-1} \\
&\vdots \\
&\bar{Q}_i(\omega_1, ..., \omega_i) = \begin{bmatrix} \bar{Q}_{i-1}N_1 \\ \bar{Q}_{i-1}N_2 \\ \vdots \\ \bar{Q}_{i-1}N_m \end{bmatrix} (-j\omega_i I - A)^{-1} \qquad (4.47)
\end{aligned}$$

Theorem 4.2: $\hat{R}(\omega)$ in (4.45) is the solution to the following generalized Sylvester equation

$$\begin{aligned}
&A\hat{R}(\omega) + \hat{R}(\omega)A + S(\omega)\left(\sum_{j=1}^{m} N_j\hat{R}(\omega)N_j\right) + ... \\
&\left(\sum_{j=1}^{m} N_j\hat{R}(\omega)N_j\right)S(\omega) + S(\omega)BC + BCS(\omega) = 0. \qquad (4.48)
\end{aligned}$$

Proof:

Let

$$\tilde{R_1}(\omega) = \frac{1}{2\pi}\int_{-\omega}^{\omega} \hat{P}_1(\omega_1)\bar{Q}_1(\omega_1)d\omega_1, \tag{4.49}$$

$$\vdots$$

$$\tilde{R_i}(\omega) = \frac{1}{(2\pi)^i}\int_{-\omega}^{\omega}...\int_{-\omega}^{\omega} \hat{P}_i(\omega_1,...,\omega_i)\bar{Q}_i(\omega_1,...,\omega_i)d\omega_1...d\omega_i, \tag{4.50}$$

we have

$$\hat{R}(\omega) = \sum_{i=1}^{\infty} \tilde{R_i}(\omega), \tag{4.51}$$

From Theorem 4.1 and its corresponding proof, it is clear that $\tilde{R_1}(\omega)$ is the solution to:

$$A\tilde{R_1}(\omega) + \tilde{R_1}(\omega)A + S(\omega)BC + BCS(\omega) = 0, \tag{4.52}$$

For $\tilde{R_2}(\omega)$, we have:

$$\begin{aligned}
&\tilde{R_2}(\omega) = \\
&\frac{1}{(2\pi)^2}\int_{-\omega}^{+\omega}\int_{-\omega}^{+\omega} \hat{P}_2(\omega_1,\omega_2)\bar{Q}_2(\omega_1,\omega_2)d\omega_1 d\omega_2 \\
&= \frac{1}{(2\pi)^2}\int_{-\omega}^{+\omega}\int_{-\omega}^{+\omega} (j\omega_2 I - A)^{-1}\left[N_1\hat{P}_1...N_m\hat{P}_1\right]\begin{bmatrix}\bar{Q}_1N_1\\ \bar{Q}_1N_2\\ \vdots \\ \bar{Q}_1N_m\end{bmatrix}(-j\omega_2 I - A)^{-1}d\omega_1 d\omega_2 \\
&= \frac{1}{2\pi}\int_{-\omega}^{+\omega}(j\omega_2 I - A)^{-1}\left(\sum_{j=1}^{m} N_j\left(\frac{1}{2\pi}\int_{-\omega}^{+\omega}\hat{P}_1(\omega_1)\bar{Q}_1(\omega_1)d\omega_1\right)N_j\right)(-j\omega_2 I - A)^{-1}d\omega_2 \\
&= \frac{1}{2\pi}\int_{-\omega}^{\omega}(j\omega_2 I - A)^{-1}\left(\sum_{j=1}^{m} N_j\tilde{R_1}(\omega)N_j\right)(-j\omega_2 I - A)^{-1}d\omega_2
\end{aligned} \tag{4.53}$$

By substituting the term BC in (4.37) with $\sum_{j=1}^{m} N_j\tilde{R_1}(\omega)N_j$ and applying Theorem 4.1, $R_2(\omega)$ will be the solution to:

$$A\tilde{R_2}(\omega) + \tilde{R_2}(\omega)A + S(\omega)\sum_{j=1}^{m} N_j\tilde{R_1}(\omega)N_j + \sum_{j=1}^{m} N_j\tilde{R_1}(\omega)N_jS(\omega) = 0, \tag{4.54}$$

Following the same procedure as described for the derivations of (4.53) and (4.54), $R_i(\omega)$ will be the solution to:

$$A\tilde{R}_i(\omega) + \tilde{R}_i(\omega)A + S(\omega)\sum_{j=1}^{m} N_j\tilde{R}_{i-1}(\omega)N_j + \sum_{j=1}^{m} N_j\tilde{R}_{i-1}(\omega)N_jS(\omega) = 0 \quad i \geq 2, \tag{4.55}$$

Adding (4.52) and (4.55) and applying (4.51) yields:

$$A\sum_{i=1}^{\infty}\tilde{R}_i(\omega) + \sum_{i=1}^{\infty}\tilde{R}_i(\omega)A + S(\omega)\left(\sum_{j=1}^{m} N_j\sum_{i=2}^{\infty}\tilde{R}_{i-1}(\omega)N_j\right) + \ldots$$
$$\left(\sum_{j=1}^{m} N_j\sum_{i=2}^{\infty}\tilde{R}_{i-1}(\omega)N_j\right)S(\omega) + S(\omega)BC + BCS(\omega) = 0, \tag{4.56}$$

Equivalently we have

$$A\sum_{i=1}^{\infty}\tilde{R}_i(\omega) + \sum_{i=1}^{\infty}\tilde{R}_i(\omega)A + S(\omega)\left(\sum_{j=1}^{m} N_j\sum_{i=1}^{\infty}\tilde{R}_i(\omega)N_j\right) + \ldots$$
$$\left(\sum_{j=1}^{m} N_j\sum_{i=1}^{\infty}\tilde{R}_i(\omega)N_j\right)S(\omega) + S(\omega)BC + BCS(\omega) = 0, \tag{4.57}$$

Finally applying (4.51) to (4.57) gives:

$$A\hat{R}(\omega) + \hat{R}(\omega)A + S(\omega)\left(\sum_{j=1}^{m} N_j\hat{R}(\omega)N_j\right) + ...$$
$$\left(\sum_{j=1}^{m} N_j\hat{R}(\omega)N_j\right)S(\omega) + S(\omega)BC + BCS(\omega) = 0.$$

■

4.3.3 Conditions for Solvability of the Generalized Sylvester Equation for Bilinear Systems

The solvability of the generalized Sylvester equation in (4.48) is described in Theorem 4.3 as follows:

Theorem 4.3:

The generalized Sylvester equation in (4.48) is solvable and has a unique solution if and only if:

$$W = (I \otimes A) + (A^* \otimes I) + \sum_{j=1}^{m} N_j^* \otimes S(\omega)N_j + \sum_{j=1}^{m} S^*(\omega)N_j^* \otimes N_j \tag{4.58}$$

is non-singular.

Proof:

Let $vec(.)$ be an operator which takes a matrix and converts it to a vector by stacking its columns on top of each other. This operator has the following property [90]:

$$vec(M_1, M_2, M_3) = (M_3^* \otimes M_1)vec(M_2), \tag{4.59}$$

Applying $vec(.)$ to (4.48) and using the the property in (4.59) yields

$$\begin{aligned}&((I \otimes A) + (A^* \otimes I) + \sum_{j=1}^{m} N_j^* \otimes S(\omega)N_j + \dots \\ &\sum_{j=1}^{m} S^*(\omega)N_j^* \otimes N_j)vec(\hat{R}(\omega) = -vec(S(\omega)BC + BCS(\omega)),\end{aligned} \tag{4.60}$$

The Sylvester equation in (4.48) is solvable and has a unique solution if this linear equation in (4.60) is solvable and has a unique solution. (4.60) has a unique solution if and only if:

$$W = (I \otimes A) + (A^* \otimes I) + \sum_{j=1}^{m} N_j^* \otimes S(\omega)N_j + \sum_{j=1}^{m} S^*(\omega)N_j^* \otimes N_j. \tag{4.61}$$

is non-singular. This completes the proof that (4.48) is solvable and has a solution if and only if W in equation (4.61) is non-singular. ■

Remark 4.1: In this paper the rank of the square matrix W in (4.61) is calculated in order to check its singularity. It follows that the matrix W needs to have full rank for equation (4.48) to be solvable.

4.3.4 Numerical Solution Method for the New Generalized Sylvester Equation for Bilinear Systems

The same iterative procedure of solving bilinear Lyapunov equations in previous studies [40,56,79] can also be applied to obtain the solution of the Sylvester equation in (4.48) - $\hat{R}(\omega)$ as follows

$$\hat{R}(\omega) = \lim_{i \to +\infty} \tilde{R}_i(\omega), \tag{4.62}$$

where

$$A\hat{R}_1(\omega) + \hat{R}_1(\omega)A + S(\omega)BC + BCS(\omega) = 0, \tag{4.63}$$

$$A\hat{R}_i(\omega) + \hat{R}_i(\omega)A + S(\omega)(\sum_{j=1}^{m} N_j\hat{R}_{i-1}N_j) + (\sum_{j=1}^{m} N_j\hat{R}_{i-1}N_j)S(\omega) + ...$$

$$S(\omega)BC + BCS(\omega) = 0 \quad i \geq 2. \tag{4.64}$$

4.4 Numerical Examples

4.4.1 Application of Frequency Interval Cross Gramians for the Model Reduction of Linear Systems

The computational procedure for model reduction based on frequency interval cross gramians is as follows.

1. For a given symmetric or SISO state space model (A, B, C) as defined in (4.1) determine the cross gramian matrix by solving (4.9)

2. Determine the frequency interval cross gramian by solving (4.36).

3. By using eigenvalue decomposition, obtain a matrix U which diagonalizes the frequency limited cross gramian matrics, $\hat{R}_\Omega$ resulting in the following diagonal matrix S.

$$S = U^{-1}\hat{R}_\Omega U$$

4. The diagonal entries of the matrix S in the previous step need to be arranged in decending order. If the diagonal entries of the matrix S are not in descending order permutation matrices are used to reorder the states as described in [89]

5. Similarity transformation is applied onto A, B and C using the transformation matrics U obtained from the diagonalization of the frequency limited cross

gramian as follows

$$\hat{A} = U^{-1}AU, \hat{B} = U^{-1}B, \hat{C} = CU$$

6. Finally after truncating the least controllable and observable states, the resulting reduced order model is obtained with state space matrices $A_r^{r\times r}, B_r^{r\times 1}$ and $C_r^{1\times r}$.

Revisiting the spring-mass-damper example in [29],

$$G(s) = \frac{-2.118s^4 - 0.2481s^3 - 24.83s^2 - 0.906s - 45.36}{s^6 + 0.3295s^5 + 32.97s^4 + 3.609s^3 + 180.6s^2 + 3.566s + 119.1}$$

Obtaining the frequency limited cross gramians for the frequency interval of $\Omega = [0.7, 3.2]$ and $\Omega = [1.5, 3.2]$ and applying the described computational procedure yields the following 4^{th} order reduced order models shown in (4.65) and (4.66). The reduced order models obtained using frequency limited cross gramians is identical to the reduced order models obtained using Gawronski and Juang's method [29] and this is expected since the frequency interval cross gramian contains combined information regarding controllability and observability. Figure 4.1 shows the frequency response of the original as well as reduced order model for the frequency interval of $\Omega = [0.7, 3.2]$ whereas Figure 4.2 shows the frequency response of the original and reduced order model for the frequency interval of $\Omega = [1.5, 3.2]$.

$$G_r(s) = \frac{-0.0109s^3 - 0.4758s^2 - 0.02831s - 1.444}{s^4 + 0.0685s^3 + 6.7s^2 + 0.09151s + 4.532} \tag{4.65}$$

$$G_r(s) = \frac{-0.002372s^3 - 0.254s^2 + 0.02358s - 1.167}{s^4 - 0.05969s^3 + 10.48s^2 - 0.4328s + 27.03} \tag{4.66}$$

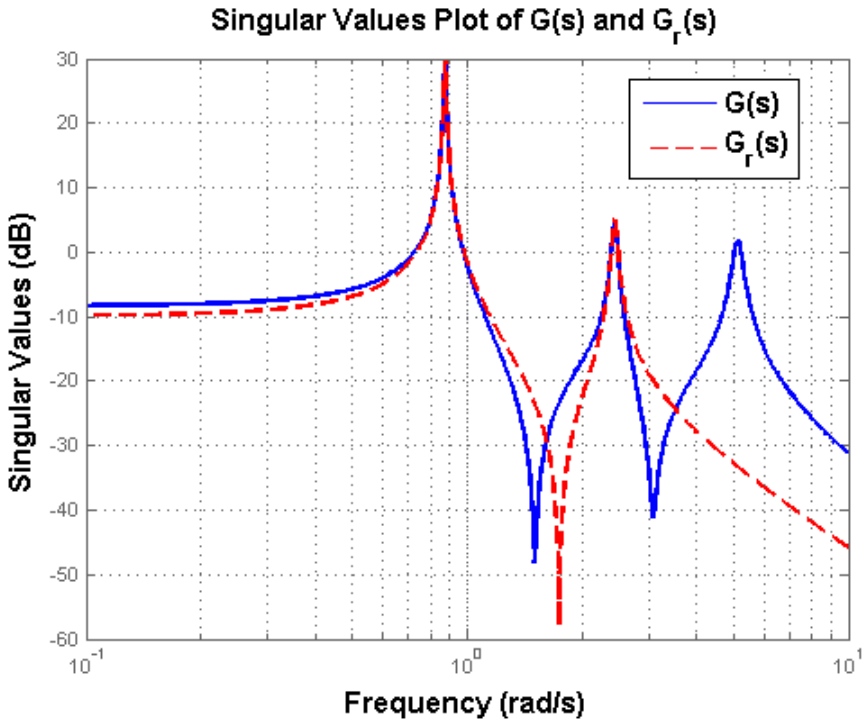

Figure 4.1: Singular Values for $G(s)$ and $G_r(s)$ for $\Omega = [0.7, 3.2]$

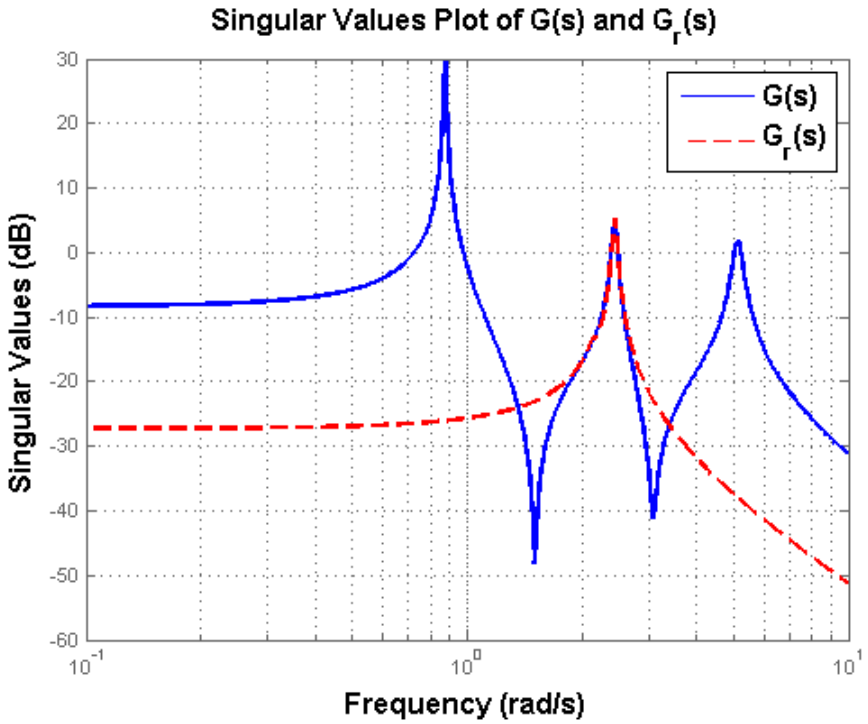

Figure 4.2: Singular Values for $G(s)$ and $G_r(s)$ for $\Omega = [1.5, 3.2]$

4.4.2 Application of Frequency Interval Cross Gramians for the Model Reduction of Bilinear Systems

Considering the following continuous time bilinear system originally from [56]

$$A = \begin{bmatrix} -0.81 & 0.47 & -0.43 & 1.6 & 0.26 & -0.4 & 0.92 \\ -0.61 & -1.9 & 0.8 & -1.6 & 2.0 & 0.98 & -0.9 \\ 0.5 & -1.2 & -2.1 & -1.6 & -1.1 & 0.14 & -0.87 \\ -1.3 & 2.1 & 0.47 & -1.2 & 3.7 & -1.2 & -1.3 \\ -0.24 & -0.081 & 1.6 & -3.6 & 1.3 & 1.7 & -2.6 \\ 1.3 & -0.96 & -1.3 & -0.57 & -2.4 & -2.4 & -0.36 \\ -0.16 & 1.5 & -0.99 & 1.5 & 0.61 & -2.2 & -3.3 \end{bmatrix} \quad B = \begin{bmatrix} 0 \\ 0 \\ -0.196 \\ 1.42 \\ 0.292 \\ 0.198 \\ 1.59 \end{bmatrix}$$

$$N = \begin{bmatrix} -1.0 & 0 & 0 & 0 & 0 & 0 & 0 \\ 0 & -1.0 & 0 & 0 & 0 & 0 & 0 \\ 0 & 0 & -1.0 & 0 & 0 & 0 & 0 \\ 0 & 0 & 0 & -1.0 & 0 & 0 & 0 \\ 0 & 0 & 0 & 0 & -1.0 & 0 & 0 \\ 0 & 0 & 0 & 0 & 0 & -1.0 & 0 \\ 0 & 0 & 0 & 0 & 0 & -0 & -1.0 \end{bmatrix}$$

$$C = \begin{bmatrix} -0.804 & 0 & 0.835 & -0.244 & 0.216 & -1.17 & -1.15 \end{bmatrix}$$

The computational procedure for model reduction based on frequency interval cross gramians for bilinear systems is described as follows

1. Firstly the frequency interval cross gramian for a particular bilinear system is obtained by solving (4.44)

2. By using eigenvalue decomposition, obtain a matrix U which diagonalizes the frequency limited cross gramian matrics, $\hat{R}_\Omega$ resulting in the following diagonal

matrix S.

$$S = U^{-1}\hat{R}_{\Omega}U$$

3. The diagonal entries of the matrix S in the previous step need to be arranged in decending order. If the diagonal entries of the matrix S are not in descending order permutation matrices are used to reorder the states as described in [89].

4. Similarity transformation is applied onto A, N, B and C using the transformation matrics U obtained from the diagonalization of the frequency limited cross gramian as follows

$$\hat{A} = U^{-1}AU,\ \ \hat{N} = U^{-1}NU,\ \ \hat{B} = U^{-1}B,\ \ \hat{C} = CU$$

5. Finally after truncating the least controllable and observable states, the resulting reduced order model is obtained.

Obtaining the frequency limited cross gramians for the frequency interval of $\Omega = [0, 0.2]$ and applying the described computational procedure yields the following 2^{nd} order reduced order model:

$$\bar{A} = \begin{bmatrix} -1.2 & 0.36 \\ 0.422 & -0.485 \end{bmatrix}, \bar{B} = \begin{bmatrix} 0.337 \\ -0.1227 \end{bmatrix} \tag{4.67}$$

$$\bar{N} = \begin{bmatrix} -1.0 & -0.000000000000000069 \\ 0.00000000000000000555 & -1.0 \end{bmatrix}, \quad \bar{C} = \begin{bmatrix} -2.56 & 2.1 \end{bmatrix} \tag{4.68}$$

For comparison, the 2^{nd} order reduced order model obtained using the method by Zhang and Lam [40] is

$$\tilde{A} = \begin{bmatrix} -0.299 & -6.15 \\ 6.15 & -0.299 \end{bmatrix}, \tilde{B} = \begin{bmatrix} 1.1 \\ 0.684 \end{bmatrix} \tag{4.69}$$

$$\tilde{N} = \begin{bmatrix} -1.0 & -0.0000000000000000688 \\ 0.0000000000000000397 & -1.0 \end{bmatrix}, \quad \tilde{C} = \begin{bmatrix} 1.1 & 0.684 \end{bmatrix} \tag{4.70}$$

Figure 4.3 and Figure 4.4 show the responses of the original and reduced order models respectively.

Although the usage of frequency interval cross gramians is applicable to both model reduction and control configuration selection, the computational efficiency associated with using frequency interval cross gramians is more prevalent in control configuration selection and this will be demonstrated in the following sections.

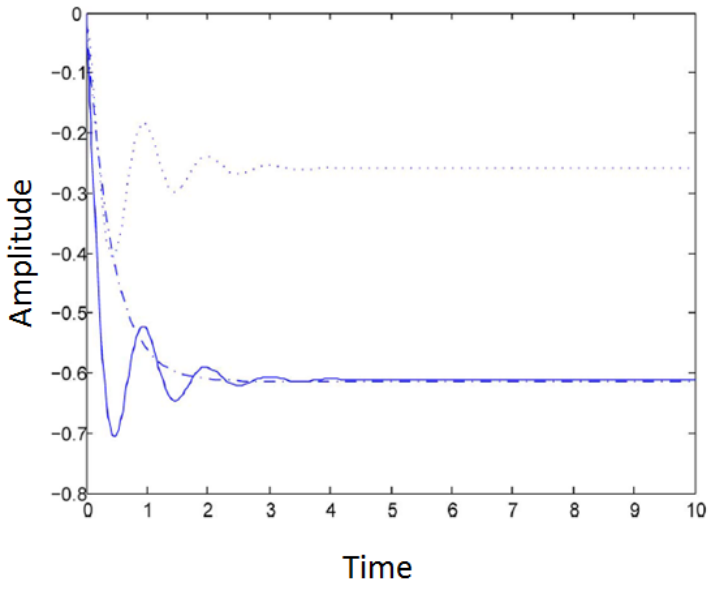

Figure 4.3: Step responses of the original model (solid line), 2^{nd} order reduced model obtained using the method by [40] (dotted) and 2^{nd} order reduced model obtained using the proposed technique (dash-dotted) for a frequency interval $\Omega = [0, 0.2]$

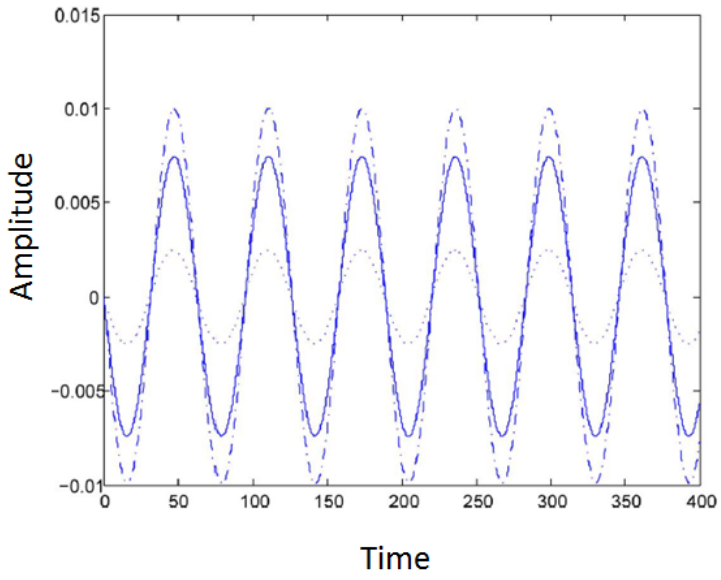

Figure 4.4: Responses of the original model (solid line), 2^{nd} order reduced model obtained using the method by [40] (dotted) and 2^{nd} order reduced model obtained using the proposed technique (dash-dotted) for a frequency interval $\Omega = [0, 0.2]$ to the input $u = 0.01sin(0.1t)$.

4.4.3 Application of Frequency Interval Cross Gramians for the Control Configuration Selection of Linear Systems

In this section the computational efficiency associated with applying frequency interval cross gramians derived in the previous sections is demonstrated by the construction of a participation matrix which is essential for the formation of a nominal model and subsequently solving the control configuration selection problem for linear systems. The procedure used for the control configuration selection using frequency interval cross gramians is consistent with previous works which use other types of gramian matrices [42, 46, 47, 85] and is described in section 4.4.3.1 with the help of a numerical example.

4.4.3.1 Example 1

Considering the 4×4 transfer function matrix $G(s)$ representing a stripper distillation system which was originaly presented in [91]. We denote the outputs as y_1 to y_4 and the inputs as u_1 to u_4. The procedure to obtain a control configuration structure for this system is as follows:

i Firstly each of the 16 elementary SISO subsystem in the transfer function matrix $G(s)$ is denoted by $G_{ij}(s)$ as follows:

$$G(s) = \begin{array}{c} \\ y_1 \\ y_2 \\ y_3 \\ y_4 \end{array} \begin{array}{c} \begin{array}{cccc} u_1 & u_2 & u_3 & u_4 \end{array} \\ \begin{bmatrix} G_{11}(s) & G_{12}(s) & G_{13}(s) & G_{14}(s) \\ G_{21}(s) & G_{22}(s) & G_{23}(s) & G_{24}(s) \\ G_{31}(s) & G_{32}(s) & G_{33}(s) & G_{34}(s) \\ G_{41}(s) & G_{42}(s) & G_{43}(s) & G_{44}(s) \end{bmatrix} \end{array}$$

For each of these elementary subsystems $G_{ij}(s)$, the corresponding state space realizations are obtained by applying 10th order Pade approximations to the transfer functions of these elementary subsystems in the form of (4.1) respectively such that:

$$G_{ij}(s) = \{A_{y_i,u_j}, B_{y_i,u_j}, C_{y_i,u_j}\},$$
$$(i = 1, 2, 3, 4, j = 1, 2, 3, 4)$$

ii Secondly in order to determine the degree of controllability and observability of each of these subsystems $G_{ij}(s)$, the frequency interval cross gramians matrices - $\hat{R}_{\Omega ij}$ are calculated for each elementary subsystem by using equation (4.36). In this example the frequency interval emphasized for the subsystems $G_{1j}(s)$ is $\Omega_{1j} = [0.7, 3.2]$, $G_{2j}(s)$ is $\Omega_{2j} = [70, 100]$, $G_{3j}(s)$ is $\Omega_{3j} = [1, 20]$, $G_{4j}(s)$ is Ω_{4j} , where $j = 1, 2, 3, 4$.

iii Thirdly the norm of the frequency interval cross gramian matrices (denoted as $\phi(\hat{R}_{ij})$) corresponding to each subsystems is calculated and the following

participation matrix denoted as Σ_{GH} is formed as follows:

$$\Sigma_{GH} =$$

$$\begin{array}{c} \\ y_1 \\ y_2 \\ y_3 \\ y_4 \end{array} \begin{array}{c} \begin{array}{cccc} u_1 & u_2 & u_3 & u_4 \end{array} \\ \begin{bmatrix} \phi(\hat{R}_{\Omega 11}) & \phi(\hat{R}_{\Omega 12}) & \phi(\hat{R}_{\Omega 13}) & \phi(\hat{R}_{\Omega 14}) \\ \phi(\hat{R}_{\Omega 21}) & \phi(\hat{R}_{\Omega 22}) & \phi(\hat{R}_{\Omega 23}) & \phi(\hat{R}_{\Omega 24}) \\ \phi(\hat{R}_{\Omega 31}) & \phi(\hat{R}_{\Omega 32}) & \phi(\hat{R}_{\Omega 33}) & \phi(\hat{R}_{\Omega 34}) \\ \phi(\hat{R}_{\Omega 41}) & \phi(\hat{R}_{\Omega 42}) & \phi(\hat{R}_{\Omega 43}) & \phi(\hat{R}_{\Omega 44}) \end{bmatrix} \end{array}$$

$$= \begin{array}{c} \\ y_1 \\ y_2 \\ y_3 \\ y_4 \end{array} \begin{array}{c} \begin{array}{cccc} u_1 & u_2 & u_3 & u_4 \end{array} \\ \begin{bmatrix} 2.9353 & 6.5847 & 0.1534 & 0.3581 \\ 2.6652 & 3.7638 & 0.0499 & 0.9470 \\ 3.1941 & 6.2127 & 2.5929 & 3.2555 \\ 8.9006 & 19.2396 & 0.0753 & 2.93 \end{bmatrix} \end{array} \tag{4.71}$$

Subsystems which have a larger value of $\hat{R}_{\Omega ij}$ indicates that the pair $(u_i - y_j)$ are easy to control and observe and therefore should be prioritized to be included in the nominal model whereas subsystems which have a lower value of $\phi(\hat{R}_{\Omega ij})$ indicates that the pair $(u_i - y_j)$ is more difficult to control and observe. The suitability of the pairing and the performance of the designed controller structure depend on how large the total of $\phi(\hat{R}_{\Omega ij})$ is for all the subsystems in the nominal model. When the total of $\phi(\hat{R}_{\Omega ij})$ for the selected subsystems is large, the original model and nominal model are close to each other and the error is small. Referring to the participation matrix in (4.71), to construct the structure of the nominal model for completely decentralized control only one element per row and one element per column can be selected. Selecting the pairs $(u_2, y_4), (u_1, y_1), (u_3, y_2)$ and (u_4, y_3) results in the following structure of the nominal model denoted as

$\mathcal{L}_n$ for implementing decentralized control:

$$struct(\mathcal{L}_n) = \begin{array}{c} \\ y_1 \\ y_2 \\ y_3 \\ y_4 \end{array} \begin{array}{c} \begin{array}{cccc} u_1 & u_2 & u_3 & u_4 \end{array} \\ \begin{bmatrix} * & 0 & 0 & 0 \\ 0 & 0 & * & 0 \\ 0 & 0 & 0 & * \\ 0 & * & 0 & 0 \end{bmatrix} \end{array}$$

This structure is associated with $\phi(\hat{R}_{\Omega 11}) + \phi(\hat{R}_{\Omega 42}) + \phi(\hat{R}_{\Omega 23}) + \phi(\hat{R}_{\Omega 34}) = 2.9353 + 19.2396 + 0.0499 + 3.2555 = 25.4803$ and a simple controller structure which is proposed is:

$$struct(C) = struct(\mathcal{L}_n^{-1}) = \begin{array}{c} \\ y_1 \\ y_2 \\ y_3 \\ y_4 \end{array} \begin{array}{c} \begin{array}{cccc} u_1 & u_2 & u_3 & u_4 \end{array} \\ \begin{bmatrix} * & 0 & 0 & 0 \\ 0 & 0 & 0 & * \\ 0 & * & 0 & 0 \\ 0 & 0 & * & 0 \end{bmatrix} \end{array}$$

If practically it is possible to use more complicated control structures other than completely decentralized control, y_4 can be commanded from u_1 then we will obtain $\phi(\hat{R}_{\Omega 11}) + \phi(\hat{R}_{\Omega 23}) + \phi(\hat{R}_{\Omega 34}) + \phi(\hat{R}_{\Omega 42}) + \phi(\hat{R}_{\Omega 41}) = 2.9353 + 19.2396 + 0.0499 + 3.2555 + 8.9006 = 34.3809$. The structure of the nominal model will then be:

$$struct(\mathcal{L}_n) = \begin{array}{c} \\ y_1 \\ y_2 \\ y_3 \\ y_4 \end{array} \begin{array}{c} \begin{array}{cccc} u_1 & u_2 & u_3 & u_4 \end{array} \\ \begin{bmatrix} * & 0 & 0 & 0 \\ 0 & 0 & * & 0 \\ 0 & 0 & 0 & * \\ * & * & 0 & 0 \end{bmatrix} \end{array}$$

A simple partially decentralized controller structure proposed is:

$$struct(C) = struct(\mathcal{L}_n^{-1}) = \begin{array}{c} \\ y_1 \\ y_2 \\ y_3 \\ y_4 \end{array} \begin{array}{c} \begin{array}{cccc} u_1 & u_2 & u_3 & u_4 \end{array} \\ \begin{bmatrix} * & 0 & 0 & 0 \\ * & 0 & 0 & * \\ 0 & * & 0 & 0 \\ 0 & 0 & * & 0 \end{bmatrix} \end{array}$$

iv Finally we compare the computational efficiency of the proposed method which requires solving only two Sylvester equation for each element of the participation matrix with the method in [88] which requires solving four Lyapunov equations for each element of the participation matrix. The time taken to solve all of the Sylvester equations to form the elements of the participation matrix using the proposed method is compared with the time taken to solve all of the Lyapunov equations to form the elements of the participation matrix using the method in [88] which uses the frequency interval controllability and observability gramians in (4.11) and (4.12). The details of this comparison is presented in Table 4.1.

For $G(s)$ which is a 4×4 MIMO system, it can be observed that the simulation time required to solve 32 Sylvester equations (two Sylvester equation is required for each of the subsystems) is half of the time required to solve 64 Lyapunov equations (four Lyapunov equations are required for each of the subsystems). All simulations in this paper were performed using a standard PC installed with MATLAB R2014B and having an Intel Core i7 processor.

Table 4.1: No. of Equations to Solve and Simulation Times for Example 1

Method	No. of Equations	Equation Type	Time (Sec)
Proposed	32	Sylvester	0.0152
Previous	64	Lyapunov	0.0293

4.4.3.2 Example 2

The computational efficiency associated with the usage of the derived frequency interval cross gramians for the formation of the participation matrix as part of the control configuration selection procedure is more prevalent for large scale MIMO systems with many inputs and outputs and this is demonstrated by the following high order model example. For this example a MIMO system with an order of 578 and having 9 inputs and 9 outputs adapted from the Modified Nodal Analysis (MNA) benchmark example of model reduction for linear time invariant systems presented in the SLICOT working note [92] is considered. Since the objective of this numerical example is solely to demonstrate computational efficiency with regard to the computation of the participation matrix, for simplicity the original E matrix of the descriptor state space model in [92] has been substituted with an identity matrix of the same dimension and therefore in order to calculate the participation matrix the same procedure described in Example 1 is applied in this example. Firstly this MIMO system is decomposed into its 81 elementary subsystems denoted by the following state space matrices:

$$G_{ij}(s) = \{A, B_{u_i,y_j}, C_{u_i,y_j}\},$$
$$(i = 1, 2, 3, ...9, j = 1, 2, 3, ...9).$$

The frequency interval cross gramian matrices - $\hat{R}_{\Omega ij}$ for each of these elementary subsystems are obtained by using equation (4.36). In this example the frequency interval emphasized for the subsystems $G_{i1j}(s)$ is $\Omega_{i1j} = [1, 10]$, $G_{i2j}(s)$ is $\Omega_{i2j} = [5, 20]$, $G_{i3j}(s)$ is $\Omega_{i3j} = [20, 50]$, where $i1 = 1, 2, 3, i2 = 4, 5, 6, i3 = 7, 8, 9, j = 1, 2, 3, ...9$. Table 4.2 presents the details of the comparison between the time taken to calculate all of the elements of participation matrix using the proposed method with the time taken to calculate all of the elements using the existing method in [88] which uses the frequency interval controllability and observability gramians in (4.11) and (4.12).

Table 4.2: No. of Equations to Solve and Simulation Times for Example 2

Method	No. of Equations	Equation Type	Time (Sec)
Proposed	162	Sylvester	120.9
Previous	324	Lyapunov	241.5

4.4.4 Application of Frequency Interval Cross Gramians for the Control Configuration Selection of Bilinear Systems

In this section the computational efficiency associated with applying frequency interval cross gramians for bilinear systems derived in the previous sections is demonstrated by the construction of a participation matrix which is essential for the formation of a nominal model and subsequently solving the control configuration selection problem for bilinear systems. The procedure used for the control configuration selection using frequency interval cross gramians is consistent with previous works which use other types of bilinear gramian matrices [86,87] and is described in section 4.4.4.1 with the help of a numerical example.

4.4.4.1 Example 3

Considering the numerical example of a 3×3 MIMO bilinear system presented in [86]:

i Firstly this 3×3 MIMO bilinear system is decomposed into its 9 elementary SISO subsystems denoted by the state space matrices $\Sigma = \{A, B_{u_i,y_j}, C_{u_i,y_j}, N_1, N_2, N_3\}$, $(i = 1, 2, 3, j = 1, 2, 3)$ respectively:

$$\Sigma_{ij} = \begin{cases} \dot{x}(t) = Ax(t) + \sum_{j=1}^{3} N_j x(t)u_j(t) +, B_{u_i,y_j}u(t) \\ y(t) = C_{u_i,y_j}x(t) \end{cases} \tag{4.72}$$

$$\Sigma = \begin{array}{c} \\ y_1 \\ y_2 \\ y_3 \end{array} \begin{array}{c} \begin{array}{ccc} u_1 & u_2 & u_3 \end{array} \\ \begin{bmatrix} \Sigma_{11}(s) & \Sigma_{12}(s) & \Sigma_{13}(s) \\ \Sigma_{21}(s) & \Sigma_{22}(s) & \Sigma_{23}(s) \\ \Sigma_{31}(s) & \Sigma_{32}(s) & \Sigma_{33}(s) \end{bmatrix} \end{array}$$

ii Secondly the frequency interval cross gramian matrices - $\hat{R}_{\Omega ij}$ for each of these elementary subsystems are obtained by solving the Sylvester equation in (4.44) using the iterative numerical solution method described in section 4.3.4. In this example the frequency interval emphasized for the subsystems $\Sigma_{1j}(s)$ is $\Omega_{1j} = [1, 10]$, $\Sigma_{2j}(s)$ is $\Omega_{2j} = [5, 20]$, $\Sigma_{3j}(s)$ is $\Omega_{3j} = [20, 50]$, where $j = 1, 2, 3$.

iii Thirdly the norm of the frequency interval cross gramian matrices - $\phi(\hat{R}_{\Sigma ij})$ corresponding to each subsystems is calculated and the following participation matrix denoted as Σ_{GH} is formed as follows:

$$\Sigma_{GH} = \begin{array}{c} \\ y_1 \\ y_2 \\ y_3 \end{array} \begin{array}{c} \begin{array}{ccc} u_1 & u_2 & u_3 \end{array} \\ \begin{bmatrix} \phi(\hat{R}_{\Omega 11}) & \phi(\hat{R}_{\Omega 12}) & \phi(\hat{R}_{\Omega 13}) \\ \phi(\hat{R}_{\Omega 21}) & \phi(\hat{R}_{\Omega 22}) & \phi(\hat{R}_{\Omega 23}) \\ \phi(\hat{R}_{\Omega 31}) & \phi(\hat{R}_{\Omega 32}) & \phi(\hat{R}_{\Omega 33}) \end{bmatrix} \end{array}$$

$$\Sigma_{GH} = \begin{array}{c} \\ y_1 \\ y_2 \\ y_3 \end{array} \begin{array}{c} \begin{array}{ccc} u_1 & u_2 & u_3 \end{array} \\ \begin{bmatrix} 0.3119 & 0.0072 & 0.2638 \\ 0.0163 & 0.2099 & 0.2253 \\ 0.0275 & 0.0189 & 0.0211 \end{bmatrix} \end{array}$$

which suggests the following nominal model for decentralized control:

$$struct(\Sigma_n) = \begin{array}{c} \\ y_1 \\ y_2 \\ y_3 \end{array} \begin{array}{c} \begin{array}{ccc} u_1 & u_2 & u_3 \end{array} \\ \begin{bmatrix} * & 0 & 0 \\ 0 & 0 & * \\ 0 & * & 0 \end{bmatrix} \end{array}$$

This structure is associated with $\phi(\hat{R}_{\Omega 11})+\phi(\hat{R}_{\Omega 23})+\phi(\hat{R}_{\Omega 32}) = 0.3119+0.0189+0.2253 = 0.5561$ and a simple controller structure proposed is:

$$struct(C) = struct(\mathcal{L}_n^{-1}) = \begin{array}{c} \\ y_1 \\ y_2 \\ y_3 \end{array} \begin{array}{c} \begin{array}{ccc} u_1 & u_2 & u_3 \end{array} \\ \begin{bmatrix} * & 0 & 0 \\ 0 & 0 & * \\ 0 & * & 0 \end{bmatrix} \end{array}$$

If practically it is possible to use more complicated control structures than completely decentralized control, y_1 could be commanded from u_3 and then we will obtain $\phi(\hat{R}_{\Omega 11}) + \phi(\hat{R}_{\Omega 23}) + \phi(\hat{R}_{\Omega 32}) + \phi(\hat{R}_{\Omega 31}) = 0.3119 + 0.0189 + 0.2253 + 0.2638 = 0.8199$. The structure of the nominal model will then be:

$$struct(\Sigma_n) = \begin{array}{c} \\ y_1 \\ y_2 \\ y_3 \end{array} \begin{array}{c} \begin{array}{ccc} u_1 & u_2 & u_3 \end{array} \\ \begin{bmatrix} * & 0 & * \\ 0 & 0 & * \\ 0 & * & 0 \end{bmatrix} \end{array}$$

A simple partially decentralized controller structure proposed is:

$$struct(C) = struct(\mathcal{L}_n^{-1}) = \begin{array}{c} \\ y_1 \\ y_2 \\ y_3 \end{array} \begin{array}{c} \begin{array}{ccc} u_1 & u_2 & u_3 \end{array} \\ \begin{bmatrix} * & * & 0 \\ 0 & 0 & * \\ 0 & * & 0 \end{bmatrix} \end{array}$$

Finally the computational efficiency of the proposed method is compared with the method in [79] which uses the frequency interval controllability and observability gramians in (4.22) and (4.29) and the details of this comparison are presented in Table 4.3.

4.4.4.2 Example 4

The computational efficiency associated with the usage of the derived frequency interval cross gramians for the formation of the participation matrix as part of the

Table 4.3: No of Equations to Solve and Simulation Times for Example 3

Method	No. of Equations	Equation Type	Time (Sec)
Proposed	18	Sylvester	0.53892
Previous	32	Lyapunov	1.062263

control configuration selction procedure for bilinear systems is more prevalent for large scale MIMO bilinear systems and this is demonstrated by the following high order bilinear model example with $n = 200$ states, 3 inputs and 3 outputs. This bilinear system consists of the following state space matrices:

$$A = \begin{bmatrix} 1000 & 0 & 0 & \cdots & \cdots & \cdots & \cdots & 0 \\ 200 & 1000 & 0 & \ddots & & & & \vdots \\ 0 & 200 & 1000 & 0 & \ddots & & & \vdots \\ \vdots & \ddots & \ddots & \ddots & \ddots & \ddots & & \vdots \\ \vdots & & \ddots & \ddots & \ddots & \ddots & \ddots & \vdots \\ \vdots & & & \ddots & 200 & 1000 & 0 & 0 \\ \vdots & & & & \ddots & 200 & 1000 & 0 \\ 0 & \cdots & \cdots & \cdots & \cdots & 0 & 200 & 1000 \end{bmatrix}$$

$$B = \begin{bmatrix} 1 & 1 & 1 \\ 0_{(n-1)\times 1} & 0_{(n-1)\times 1} & 0_{(n-1)\times 1} \end{bmatrix}$$

$$N_1 = N_2 = N_3 = \begin{bmatrix} -0.1 & 0 & 0 & 0 & 0 \\ 0 & \ddots & 0 & 0 & 0 \\ 0 & 0 & \ddots & 0 & 0 \\ 0 & 0 & 0 & \ddots & 0 \\ 0 & 0 & 0 & 0 & -0.1 \end{bmatrix}$$

$$C = B^T,$$

The same procedure described in Example 3 is used to calculate the participation

matrix of this system in which this 3×3 MIMO system is decomposed into its 9 elementary subsystems denoted by the state space matrices:

$$\Sigma_{ij} = \{A, B_{u_i,y_i}, C_{u_i,y_i}, N_1, N_2, N_3\},$$
$$(i = 1, 2, 3, j = 1, 2, 3)$$

respectively. The frequency interval cross gramian matrices - $\hat{R}_{\Omega ij}$ for each of these elementary subsystems are obtained by solving equation (4.44) using the iterative numerical solution method described in section 4.3.4. In this example the frequency interval emphasized for the subsystems $\Sigma_{1j}(s)$ is $\Omega_{1j} = [1, 10]$, $\Sigma_{2j}(s)$ is $\Omega_{2j} = [5, 20]$, $\Sigma_{3j}(s)$ is $\Omega_{3j} = [20, 50]$, where $j = 1, 2, 3$. Table 4.4 presents the details of the comparison between the time taken to calculate all of the elements of participation matrix using the proposed method with the time taken to calculate all of the elements using the existing method in [79] which uses the frequency interval controllability and observability gramians in (4.22) and (4.29).

Table 4.4: No of Equations to Solve and Simulation Times for Example 4

Method	No. of Equations	Equation Type	Time (Sec)
Proposed	18	Sylvester	41.365
Previous	32	Lyapunov	81.762

4.4.5 Formation of a Participation Matrix for Non - Square Linear and Bilinear Systems

The results in the previous sections can be extended to be applicable in the formation of the participation matrix of non-square linear and bilinear systems by incorporating the Moore-Penrose pseudo-inverse. Considering the 4×1 linear system obtained from the the stable subsystem of the state space model presented in section 6 of [29]

and calculating the norm of the frequency interval cross gramian - $\hat{R}_{\Omega ij}$ for each elementary subsystem using the same procedure as described in Example 1 yields the following non-square participation matrix:

$$\Sigma_{GH} = \begin{matrix} \\ y_1 \end{matrix} \begin{matrix} \begin{bmatrix} u_1 & u_2 & u_3 & u_4 \end{bmatrix} \\ \begin{bmatrix} 0.0343 & 0.0015 & 0.091 & 0.1440 \end{bmatrix} \end{matrix}$$

which suggests the following nominal model for decentralized control:

$$struct(\mathcal{L}_n) = \begin{matrix} \\ y_1 \end{matrix} \begin{matrix} \begin{bmatrix} u_1 & u_2 & u_3 & u_4 \end{bmatrix} \\ \begin{bmatrix} 0 & 0 & 0 & * \end{bmatrix} \end{matrix}$$

This structure is associated with $\phi(\hat{R}_{\Omega 14}) = 0.1440$. A simple controller is proposed by finding the Moore-Penrose pseudoinverse as follows:

$$struct(C) = struct(\mathcal{L}_n^{\dagger}) = \begin{matrix} \\ y_1 \\ y_2 \\ y_3 \\ y_3 \end{matrix} \begin{matrix} \begin{bmatrix} u_1 \end{bmatrix} \\ \begin{bmatrix} 0 \end{bmatrix} \\ \begin{bmatrix} 0 \end{bmatrix} \\ \begin{bmatrix} 0 \end{bmatrix} \\ \begin{bmatrix} * \end{bmatrix} \end{matrix}$$

The superscript '†' denotes the Moore-Penrose pseudoinverse. The same methodology is applicable for non-square bilinear systems.

4.5 Conclusion

New Sylvester equations for obtaining the frequency interval cross gramians are derived for both linear and bilinear SISO systems. The frequency interval cross gramians for both linear and bilinear SISO systems are then used to obtain the elements of a participation matrix in which the highly controllable and observable states can be identified and retained in the nominal model. A suitable controller structure can then be identified based on the nominal model obtained. The proposed method can also be applied to non-square MIMO systems by applying the

Moore-Penrose pseudo-inverse. The developed method is computationally more efficient compared to existing gramian based frequency interval control configuration selection techniques since the frequency interval cross gramians contains information regarding both controllability and observability in a single matrix and therefore half the number of equations are required to be solved as compared to existing methods resulting in faster simulation times that can be achieved especially for high order MIMO systems with many inputs and outputs.

Chapter 5

Frequency Interval Balanced Truncation of Discrete-Time Bilinear Systems

5.1 Introduction

Model reduction which is of fundamental importance in many modelling and control applications deals with the approximation of a higher order model by a lower order model such that the input-output behavior of the original system is preserved to a required accuracy. The balanced truncation model reduction technique originally developed by Moore for continuous-time linear systems is one of the most widely applied model reduction techniques [1]. In recent years many variations to this original balanced truncation technique have been developed [93–96].

One of the further developments to the original balanced truncation technique was the work by Gawronski and Juang which involved the development of frequency interval controllability and observability gramians [29]. The significance of emphasizing particular frequency intervals of interest in a variety of control engineering problems have led to extensive theoretical developments in robust control techniques which emphasize particular frequency intervals of interest which have been presented

in [49–51, 53, 97–99].

In the context of discrete-time systems, digital systems are designed to work with signals with known frequency characteristics, therefore it is essential to have model reduction techniques which generate reduced order models which function well with signals which have specified frequency characteristics. The works by Horta et al. [100], Wang and Zilouchian [101] and more recently by Imran and Ghafoor [54] described the formulation of frequency interval gramians for discrete-time systems.

In many control engineering applications the system being analyzed exhibits non-linear behaviour. In general methods for analyzing non-linear systems are limited compared to methods for analyzing linear systems. Standard linearization methods performed on non-linear systems may not be sufficient to capture the characteristics of the non-linear system. Bilinear systems are an important category of non-linear systems which have well established theories [38, 39, 63, 87, 102]. Many non-linear systems in various branches of engineering can be well represented by bilinear systems. The balanced truncation technique for continuous-time bilinear systems has been presented by Zhang and Lam in [40] whereas the balanced truncation technique for discrete-time bilinear systems has been presented by Zhang et al. in [64]. More recently further developments have been carried out to the original balanced truncation technique for continuous-time bilinear systems in order to reduce the approximation error between the outputs of the original bilinear model and reduced order bilinear model by incorporating time and frequency interval techniques [56, 103].

The contributions of this chapter are as follows. Firstly new generalized frequency interval controllability and observability gramians are defined for discrete-time bilinear systems. Secondly it is shown that these frequency interval controllability and observability gramians are solutions to a pair of new generalized Lyapunov equations. Thirdly conditions for solvability of these new generalized Lyapunov equation are proposed together with a numerical solution method for solving these new Lyapunov equations. Finally numerical examples are provided to demonstrate

the performance of the proposed method relative to existing techniques.

The notation used in this paper is as follows. M^* refers to the transpose of the matrix M if $M \in \mathbb{R}^{n\times m}$ and complex conjugate transpose if $M \in \mathbb{C}^{n\times m}$. The $\otimes$ symbol denotes a Kronecker product.

5.2 Preliminaries

5.2.1 Controllability and Observability Gramians of Discrete-Time Linear Systems

Considering the following time invariant and asymptotically stable discrete-time linear system (A, B, C):

$$\begin{aligned} x(k+1) &= Ax(k) + Bu(k) \\ y(k) &= Cx(k) \end{aligned} \tag{5.1}$$

where $u \in \mathbb{R}^p$, $y \in \mathbb{R}^q$, $x \in \mathbb{R}^n$ are the input, output and states respectively. $A \in \mathbb{R}^{n\times n}$, $B \in \mathbb{R}^{n\times p}$, $C \in \mathbb{R}^{q\times n}$ are matrices with appropriate dimensions.

Definition 5.1: The discrete-time domain controllability and observability gramian definitions are given by:

$$P = \sum_{k=0}^{\infty} A^k BB^* (A^*)^k \tag{5.2}$$

$$Q = \sum_{k=0}^{\infty} (A^*)^k C^* C A^k \tag{5.3}$$

Remark 5.1: It is established that (5.2) and (5.3) satisfy the following Lyapunov equations:

$$APA^* - P + BB^* = 0 \tag{5.4}$$

$$A^*QA - Q + C^*C = 0 \tag{5.5}$$

Remark 5.2: By applying a direct application of Parseval's theorem to (5.2) and (5.3), the controllability and observability gramians in the frequency domain are given by:

$$P = \frac{1}{2\pi}\int_{-\pi}^{\pi}(e^{j\theta}I - A)^{-1}BB^{*}(e^{-j\theta}I - A^{*})^{-1}d\theta \tag{5.6}$$

$$Q = \frac{1}{2\pi}\int_{-\pi}^{\pi}(e^{-j\theta}I - A^{*})^{-1}C^{*}C(e^{j\theta}I - A)^{-1}d\theta \tag{5.7}$$

where I is an identity matrix.

5.2.2 Frequency Interval Controllability and Observability Gramians of Discrete-Time Linear Systems

Definition 5.2: The frequency interval controllability and observability gramians for discrete-time systems are defined as [100]:

$$P_{cf} = \frac{1}{2\pi}\int_{\delta\theta}(e^{j\theta}I - A)^{-1}BB^{*}(e^{-j\theta}I - A^{*})^{-1}d\theta \tag{5.8}$$

$$Q_{cf} = \frac{1}{2\pi}\int_{\delta\theta}(e^{-j\theta}I - A^{*})^{-1}C^{*}C(e^{j\theta}I - A)^{-1}d\theta \tag{5.9}$$

where $\delta\theta = [\theta_1, \theta_2]$ is the frequency range of operation and $0 \leq \theta_1 < \theta_2 \leq \pi$. Due to the symmetry of the discrete Fourier transform, the integration is carried out throughout the frequency intervals $[\theta_1, \theta_2]$ and $[-\theta_2, -\theta_1]$ [100]. Therefore the gramians P_{cf} and Q_{cf} in (5.8) and (5.9) will always be real.

Remark 5.3: It has been shown that the frequency interval controllability and observability gramians defined in (5.8) and (5.9) are the solutions to the following Lyapunov equations [101]:

$$AP_{cf}A^{*} - P_{cf} + X_{cf} = 0 \tag{5.10}$$

$$A^{*}Q_{cf}A - Q_{cf} + Y_{cf} = 0 \tag{5.11}$$

where

$$X_{cf} = F_{cf}BB^* + BB^*F_{cf}^* \tag{5.12}$$

$$Y_{cf} = F_{cf}^*C^*C + C^*CF_{cf} \tag{5.13}$$

and

$$F_{cf} = \frac{-(\theta_2 - \theta_1)}{2\pi}I + \frac{1}{2\pi}\int_{\delta\theta}(I - Ae^{-j\theta})^{-1}d\theta \tag{5.14}$$

5.2.3 Controllability and Observability Gramians of Discrete-Time Bilinear Systems

Considering the following discrete-time bilinear system represented by:

$$x(k+1) = Ax(k) + \sum_{j=1}^{m} N_j x(k)u_j(k) + Bu(k) \tag{5.15}$$

$$y(k) = Cx(k) \tag{5.16}$$

where $x(k) \in \mathbb{R}^{n\times n}$ is the state vector, $u(k) \in \mathbb{R}^{m\times m}$ is the input vector and $u_j(k)$ is the corresponding jth element of $u(k)$, $y(k) \in \mathbb{R}^{q\times q}$ is the output vector and A, B, C and N_j are matrices with suitable dimensions. This bilinear system is denoted as (A, N_j, B, C).

The controllability gramian for this system is defined as [64]:

$$P = \sum_{i=1}^{\infty}\sum_{k_i=0}^{\infty}\cdots\sum_{k_1=0}^{\infty} P_i P_i^* \tag{5.17}$$

where

$$P_1(k_1) = A^{k_1}B$$

$$P_i(k_1, ...k_i) = A^{k_i}\begin{bmatrix} N_1P_{i-1} & N_2P_{i-1}\ldots N_mP_{i-1}\end{bmatrix}, i \geq 2$$

whereas the observability gramian is defined as [64]:

$$Q = \sum_{i=1}^{\infty}\sum_{k_i=0}^{\infty}\cdots\sum_{k_1=0}^{\infty} Q_i^* Q_i \tag{5.18}$$

where

$$Q_1(k_1) = CA^{k_1}$$

$$Q_i(k_1, ...k_i) = \begin{bmatrix} Q_{i-1}N_1 \\ Q_{i-1}N_2 \\ \vdots \\ Q_{i-1}N_m \end{bmatrix}$$

The controllability and observability gramians defined in (5.17) and (5.18) are the solution to the following generalized Lyapunov equations [64]:

$$APA^* - P + \sum_{j=1}^{\infty} N_j P N_j^* + BB^* = 0 \tag{5.19}$$

$$A^*QA - Q + \sum_{j=1}^{\infty} N_j^* Q N + C^*C = 0 \tag{5.20}$$

The generalized Lyapunov equations corresponding to the controllability and observability gramians in (5.19) and (5.20) can be solved iteratively. The controllability gramian can be obtained by [64]:

$$P = \lim_{i \to \infty} \hat{P}_i \tag{5.21}$$

where

$$\begin{aligned} &A\hat{P}_1 A^* - \hat{P}_i + BB^* = 0, \\ &A\hat{P}_i A^* - \hat{P} + \sum_{j=1}^{\infty} N_j \hat{P}_{i-1} N_j^* + BB^* = 0, i \geq 2 \end{aligned} \tag{5.22}$$

whereas the observability gramian can be obtained by [64]

$$Q = \lim_{i \to \infty} \hat{Q}_i \tag{5.23}$$

where

$$\begin{aligned} &A^*\hat{Q}_1 A - \hat{Q}_i + C^*C = 0, \\ &A^*\hat{Q}_i A - \hat{Q} + \sum_{j=1}^{\infty} N_j^* \hat{Q}_{i-1} N_j + C^*C = 0, i \geq 2 \end{aligned} \tag{5.24}$$

5.3 Main Work

5.3.1 Frequency Interval Controllability and Observability Gramians of Discrete-Time Bilinear Systems

For a particular discrete-time frequency interval $\Omega = [\gamma_1, \gamma_2]$, we define the frequency interval controllability and observability gramians as follows:

Definition 5.3: The generalized frequency interval controllability gramian for discrete-time bilinear systems is defined as:

$$\hat{P}(\theta) := \sum_{i=1}^{\infty} \frac{1}{(2\pi)^i} \int_{\delta\theta} \cdots \int_{\delta\theta} \hat{P}_i(\theta_1, ..., \theta_i) \hat{P}_i^*(\theta_1, ..., \theta_i) d\theta_1 \ldots d\theta_i \tag{5.25}$$

where $\delta\theta = [\gamma_1, \gamma_2]$ and

$$\hat{P}_1(\theta_1) = (e^{j\theta_1} I - A)^{-1} B$$

$$\vdots$$

$$\hat{P}_i(\theta_1, ..., \theta_i) = (e^{j\theta_i} I - A)^{-1} \begin{bmatrix} N_1 \hat{P}_{i-1} & N_2 \hat{P}_{i-1} \ldots N_m \hat{P}_{i-1} \end{bmatrix}$$

Similarly the generalized frequency interval observability gramian is defined as:

$$\hat{Q}(\theta) := \sum_{i=1}^{\infty} \frac{1}{(2\pi)^i} \int_{\delta\theta} \cdots \int_{\delta\theta} \hat{Q}_i^*(\theta_1, ..., \theta_i) \hat{Q}_i(\theta_1, ..., \theta_i) d\theta_1 \ldots d\theta_i \tag{5.26}$$

where $\delta\theta = [\gamma_1, \gamma_2]$ and

$$\hat{Q}_1(\theta_1) = C(e^{-j\theta_1} I - A^*)^{-1}$$

$$\vdots$$

$$\hat{Q}_i(\theta_1, ..., \theta_i) = \begin{bmatrix} N_1 \hat{Q}_{i-1} \\ N_2 \hat{Q}_{i-1} \\ \vdots \\ N_m \hat{Q}_{i-1} \end{bmatrix} (e^{-j\theta_i} I - A^*)^{-1}$$

These gramians defined in (5.25) and (5.26) are the solution to a pair of new generalized Lyapunov equations which is presented in the following Theorem 5.1. Lemma

5.1,5.2 and 5.3 together with Theorem 5.1 presented in the following sections are interrelated such that Lemma 5.1 and Lemma 5.2 are required as part of proving Lemma 5.3 whereas Lemma 5.3 is required for proving Theorem 5.1.

Lemma 5.1: Let A be a square matrix which is also stable and let M be a matrix with the appropriate dimension. If X satisfies the following equation:

$$X = \sum_{i=o}^{+\infty} A^i M (A^i)^* \tag{5.27}$$

It follows that X is the solution to:

$$AXA^* - X + M = 0 \tag{5.28}$$

Proof: Since $X = \sum_{i=0}^{+\infty} A^i M (A^i)^*$ and A is stable, it follows that:

$$AXA^* - X = A \sum_{i=0}^{+\infty} A^i M (A^i)^* (A^i)^* - \sum_{i=0}^{+\infty} A^i M (A^i)^*$$
$$= \sum_{i=0}^{+\infty} A^{i+1} M (A^*)^{i+1} - \sum_{i=0}^{+\infty} A^i M (A^i)^*$$

Since $\sum_{i=0}^{+\infty} A^{i+1} M (A^*)^{i+1} = \sum_{i=1}^{+\infty} A^i M (A^*)^i$

$$AXA^* - A = \sum_{i=1}^{+\infty} A^i M (A^*)^i - \sum_{i=0}^{+\infty} A^i M (A^*)^i = -M.$$

■

Lemma 5.2: Let A be a square matrix which is also stable and let R be a matrix with the appropriate dimension. If Y satisfies the following

$$Y = \sum_{i=o}^{+\infty} (A^i)^* R (A^i) \tag{5.29}$$

It follows that Y is the solution to

$$A^* Y A - Y + R = 0 \tag{5.30}$$

Proof: Similar to the proof of Lemma 5.1 and is therefore omitted for brevity. ■

Lemma 5.3: Let M and R be matrices with the appropriate dimensions and let A be stable, if $\hat{P}_{cf}$ and $\hat{Q}_{cf}$ satisfy:

$$\hat{P}_{cf} = \frac{1}{2\pi}\int_{\delta\theta}(e^{j\theta}I - A)^{-1}M(e^{-j\theta}I - A^*)^{-1}d\theta \tag{5.31}$$

$$\hat{Q}_{cf} = \frac{1}{2\pi}\int_{\delta\theta}(e^{-j\theta}I - A^*)^{-1}R(e^{j\theta}I - A)^{-1}d\theta \tag{5.32}$$

then $\hat{P}_{cf}$ and $\hat{Q}_{cf}$ are the solution to the following generalized Lyapunov equations:

$$A\hat{P}_{cf}A^* - \hat{P}_{cf} = X_{cf} \tag{5.33}$$

$$A^*\hat{Q}_{cf}A - \hat{Q}_{cf} = Y_{cf} \tag{5.34}$$

where

$$X_{cf} = -FM - MF^* \tag{5.35}$$

$$Y_{cf} = -F^*R - RF \tag{5.36}$$

and

$$F = \frac{(\theta_1 - \theta_2)}{2\pi}I + \frac{1}{2\pi}\int_{-\theta_2}^{\theta_2}(I - Ae^{-j\theta})^{-1}d\theta - \frac{1}{2\pi}\int_{-\theta_1}^{\theta_1}(I - Ae^{-j\theta})^{-1}d\theta \tag{5.37}$$

Proof: In this part we will prove that (5.31) is the solution to (5.33). This proof is a further development of the proof of equation 4.1a in [101]. The proof that (5.32) is the solution to (5.34) can then be obtained similarly by using lemma 5.2 and therefore is omitted for brevity. Firstly (5.28) can be re-written as follows:

$$-(e^{j\theta}I - A)X(e^{-j\theta}I - A^*) + X(e^{-j\theta}I - A^*)e^{j\theta}I + (e^{j\theta}I - A)Xe^{-j\theta}I = M \tag{5.38}$$

Multiplying (5.38) from the left by $(e^{j\theta}I - A)^{-1}$ and from the right by $(e^{-j\theta}I - A^*)^{-1}$ followed by integrating both sides by $\frac{1}{2\pi}\int_{\delta\theta}d\theta$ yields:

$$\begin{aligned}
&\frac{1}{2\pi}\int_{\delta\theta}(e^{j\theta}I - A)^{-1}M(e^{-j\theta}I - A^*)^{-1}d\theta \\
&= -\frac{1}{2\pi}\int_{\delta\theta}Xd\theta + \frac{1}{2\pi}\int_{\delta\theta}(e^{j\theta}I - A)^{-1}Xe^{j\theta}d\theta + \frac{1}{2\pi}\int_{\delta\theta}Xe^{-j\theta}(e^{-j\theta}I - A^*)^{-1}\theta \\
&= -\frac{1}{2\pi}\int_{\delta\theta}Xd\theta + \left(\frac{1}{2\pi}\int_{\delta\theta}(I - e^{-j\theta}IA)^{-1}d\theta\right)X + X\left(\frac{1}{2\pi}\int_{\delta\theta}(I - e^{-j\theta}IA)^{-1}d\theta\right)^*
\end{aligned} \tag{5.39}$$

Denoting $K_1 = \frac{1}{2\pi}\int_{\delta\theta}(I - e^{-j\theta}IA)^{-1}d\theta$, (5.39) can be re-written as:

$$\hat{P}_{cf} = -\frac{1}{2\pi}\int_{\delta\theta} Xd\theta + K_1X + XK_1^* \tag{5.40}$$

Substituting (5.40) into the left hand side of (5.33) yields:

$$A\left[-\frac{1}{2\pi}\int_{\delta\theta} Xd\theta + K_1X + XK_1^*\right]A^* - \left[-\frac{1}{2\pi}\int_{\delta\theta} Xd\theta + K_1X + XK_1^*\right] = X_{cf} \tag{5.41}$$

It has been shown in [101] that the property $AK_1 = K_1A$ and $AK_1^* = K_1^*A$ holds true. As a result (5.41) can be re-written as

$$\begin{aligned} X_{cf} &= -\frac{1}{2\pi}\int_{\delta\theta} 1d\theta I[AXA^* - X] + K_1[AXA^* - X] + [AXA^* - X]K_1^* \\ &= \left(\frac{1}{2\pi}\int_{\delta\theta} 1d\theta I\right)(M) - K_1M - MK_1^* \\ &= -\left(-\frac{1}{4\pi}\int_{\delta\theta} 1d\theta I + K_1\right)(M) - (M)\left(-\frac{1}{4\pi}\int_{\delta\theta} 1d\theta I + K_1\right)^* \end{aligned} \tag{5.42}$$

(5.42) is equivalent to the right hand side of (5.35). By comparing both expressions we have

$$F = -\frac{1}{4\pi}\int_{\delta\theta} 1d\theta I + K_1 \tag{5.43}$$

Due to the symmetry of the discrete Fourier transform, the integrations are carried out throughout the frequency intervals $[\theta_1, \theta_2]$ and $[-\theta_2, -\theta_1]$ ([100]). Therefore we have

$$F = \frac{(\theta_1 - \theta_2)}{2\pi}I + \frac{1}{2\pi}\int_{-\theta_2}^{\theta_2}(I - Ae^{-j\theta})^{-1}d\theta - \frac{1}{2\pi}\int_{-\theta_1}^{\theta_1}(I - Ae^{-j\theta})^{-1}d\theta$$

■

Lemma 5.3 derived previously is now applied as part of the proof of Theorem 5.1 as follows.

Theorem 5.1: The frequency interval controllablity and observability gramians $\hat{P}(\theta)$ and $\hat{Q}(\theta)$ defined in (5.25) and (5.26) are the solutions to the following generalized

Lyapunov equations:

$$A\hat{P}(\theta)A^* - \hat{P}(\theta) + F\left(\sum_{j=1}^{m} N_j\hat{P}(\theta)N_j^*\right) + \left(\sum_{j=1}^{m} N_j\hat{P}(\theta)N_j^*\right)F^* + FBB^* + BB^*F^* = 0 \tag{5.44}$$

$$A^*\hat{Q}(\theta)A - \hat{Q}(\theta) + F^*\left(\sum_{j=1}^{m} N_j^*\hat{Q}(\theta)N_j\right) + \left(\sum_{j=1}^{m} N_j^*\hat{Q}(\theta)N_j\right)F + F^*C^*C + C^*CF = 0 \tag{5.45}$$

Proof:

The proof that the frequency interval controllability gramian $\hat{P}(\theta)$ defined in (5.25) is the solution to the generalized Lyapunov equation in (5.44) is presented in this section. The proof that the frequency interval observability gramian $\hat{Q}(\theta)$ defined in (5.26) is the solution to the generalized Lyapunov equation in (5.45) can be obtained in a similar manner and therefore is omitted for brevity. Firstly let:

$$\tilde{P}_1(\theta) = \frac{1}{2\pi}\int_{\delta\theta} \hat{P}_1(\theta)\hat{P}_1^*(\theta)d\theta_1 \tag{5.46}$$

$$\vdots$$

$$\tilde{P}_i(\theta) = \frac{1}{2\pi}\int_{\delta\theta}\cdots\int_{\delta\theta} \hat{P}_i(\theta_1,\theta_2,...,\theta_i)\hat{P}_i^*(\theta_1,\theta_2,...,\theta_i)d\theta_1...d\theta_i \tag{5.47}$$

we have

$$\hat{P}(\theta) = \sum_{i=1}^{\infty}\tilde{P}_i(\theta) \tag{5.48}$$

Using Lemma 5.3 with $M = BB^*$, it is observed that $\tilde{P}_1(\theta)$ is the solution to

$$A\tilde{P}_1(\theta)A^* - \tilde{P}_1(\theta) + FBB^* + BB^*F^* = 0 \tag{5.49}$$

For $\tilde{P}_2(\theta)$ we have

$$\begin{aligned}
\tilde{P}_2(\theta) &= \frac{1}{(2\pi)^i}\int_{\delta\theta}\int_{\delta\theta}\hat{P}_2(\theta_1,\theta_2)\hat{P}_2^*(\theta_1,\theta_2)d\theta_1 d\theta_2 \\
&= \frac{1}{(2\pi)^i}\int_{\delta\theta}\int_{\delta\theta}(e^{j\theta}I - A)\left[N_1\hat{P}_1 \dots N_m\hat{P}_1\right]\begin{bmatrix}\hat{P}_1^*N_1^* \\ \vdots \\ \hat{P}_1^*N_m^*\end{bmatrix}(e^{-j\theta}I - A^*)d\theta_1 d\theta_2 \\
&= \frac{1}{2\pi}\int_{\delta\theta}(e^{j\theta}I - A)^{-1}\left(\sum_{j=1}^{m}N_j\left(\frac{1}{2\pi}\int_{\delta\theta}\hat{P}_1(\theta)\hat{P}_1^*(\theta)d\theta_1\right)N_j^*\right)(e^{-j\theta}I - A^*)^{-1}d\theta_2 \\
&= \frac{1}{2\pi}\int_{\delta\theta}(e^{j\theta}I - A)^{-1}\left(\sum_{j=1}^{m}N_j\tilde{P}_1(\theta)N_j^*\right)(e^{-j\theta}I - A^*)^{-1}d\theta_2
\end{aligned}$$

Denoting $M = \sum_{j=1}^{m}N_j\tilde{P}_1(\theta)N_j^*$, Lemma 5.3 applies and as a result $\tilde{P}_2(\theta)$ will be the solution to:

$$A\tilde{P}_2(\theta)A^* - \tilde{P}_2(\theta) + F\left(\sum_{j=1}^{m}N_j\tilde{P}_1(\theta)N_j^*\right) + \left(\sum_{j=1}^{m}N_j\tilde{P}_1(\theta)N_j^*\right)F^* = 0 \qquad (5.50)$$

Similarly according to Lemma 5.3, $\tilde{P}_i(\theta)$ will be the solution to

$$A\tilde{P}_i(\theta)A^* - \tilde{P}_i(\theta) + F\left(\sum_{j=1}^{m}N_j\tilde{P}_{i-1}(\theta)N_j^*\right) + \left(\sum_{j=1}^{m}N_j\tilde{P}_{i-1}(\theta)N_j^*\right)F^* = 0 \quad (5.51)$$

Adding (5.51) to (5.49) and applying a summation to infinity as in the right hand side of (5.48) yields

$$\begin{aligned}
&A\sum_{i=1}^{\infty}\tilde{P}_i(\theta)A^* - \sum_{i=1}^{\infty}\tilde{P}_i(\theta) + F\left(\sum_{j=1}^{m}N_j\sum_{i=2}^{\infty}\tilde{P}_{i-1}(\theta)N_j^*\right) + \dots \\
&\left(\sum_{j=1}^{m}N_j\sum_{i=2}^{\infty}\tilde{P}_{i-1}(\theta)N_j^*\right)F^* + FBB^* + BB^*F^* = 0 \qquad (5.52)
\end{aligned}$$

Equivalently we have

$$\begin{aligned}
&A\sum_{i=1}^{\infty}\tilde{P}_i(\theta)A^* - \sum_{i=1}^{\infty}\tilde{P}_i(\theta) + F\left(\sum_{j=1}^{m}N_j\sum_{i=1}^{\infty}\tilde{P}_i(\theta)N_j^*\right) + \dots \\
&\left(\sum_{j=1}^{m}N_j\sum_{i=1}^{\infty}\tilde{P}_i(\theta)N_j^*\right)F^* + FBB^* + BB^*F^* = 0 \qquad (5.53)
\end{aligned}$$

Finally applying the property in (5.48) to (5.53)

$$A\hat{P}(\theta)A^* - \hat{P}(\theta) + F\left(\sum_{j=1}^{m} N_j\hat{P}(\theta)N_j^*\right)... \\ + \left(\sum_{j=1}^{m} N_j\hat{P}(\theta)N_j^*\right)F^* + FBB^* + BB^*F^* = 0$$

■

5.3.2 Conditions for Solvability of the Lyapunov Equations Corresponding to Frequency Interval Controllability and Observability Gramians

In this section, the condition for solvability of the generalized Lyapunov equation in (5.44) which corresponds to the frequency interval controllability gramian defined in (5.25) is presented herewith in Theorem 5.2. The condition for solvability of the generalized Lyapunov equation in (5.45) which corresponds to the frequency interval observability gramian defined in (5.26) can be derived in a similar manner and is therefore omitted for brevity.

Theorem 5.2: The generalized Lyapunov equation in (5.44) is solvable and has a unique solution if and only if

$$W = (A \otimes A) - (I \otimes I) + (N_j \otimes FN_j) + (FN_j \otimes N_j) \tag{5.54}$$

is non-singular.

Proof:

Let $vec(.)$ be an operator which converts a matrix into a vector by stacking the columns of the matrix on top of each other. This operator has the following useful property [90]

$$vec(M_1, M_2, M_3) = (M_3^* \otimes M_1)vec(M_2) \tag{5.55}$$

Applying $vec(.)$ on (5.44) together with the property in (5.54) yields

$$\left\{(A\otimes A)-(I\otimes I)+\left(\sum_{j=1}^{m}N_j\otimes FN_j\right)+\left(\sum_{j=1}^{m}FN_j\otimes N_j\right)\right\}vec(\hat{P}(\theta))$$

$$=-vec(FBB^*+BB^*F) \tag{5.56}$$

The generalized Lyapunov equation in (5.44) is solvable provided that this equation presented in (5.56) is solvable and has a unique solution. It follows that (5.56) is solvable and has a unique solution if and only if

$$W=(A\otimes A)-(I\otimes I)+(N_j\otimes FN_j)+(FN_j\otimes N_j)$$

is non-singular. ■

5.3.3 Numerical Solution Method for the Lyapunov Equations Corresponding to the Frequency Interval Controllability and Observability Gramians

The iterative procedure for solving bilinear Lyapunov equations in previous studies can also be applied to obtain the solution to the generalized Lyapunov equation in (5.44) - $\hat{P}(\theta)$ as follows [40, 56, 64, 103]:

$$\hat{P}(\theta)=\lim_{i\to+\infty}\tilde{P}_i(\theta) \tag{5.57}$$

where

$$A\tilde{P}_1(\theta)A^*-\tilde{P}_1(\theta)+FBB^*+BB^*F^*=0 \tag{5.58}$$

$$A\tilde{P}_i(\theta)A^*-\tilde{P}_i(\theta)+F\left(\sum_{j=1}^{m}N_j\tilde{P}_{i-1}(\theta)N_j^*\right)+...$$

$$\left(\sum_{j=1}^{m}N_j\tilde{P}_{i-1}(\theta)N_j^*\right)F^*+FBB^*+BB^*F^*=0,\ \ i\geq 2 \tag{5.59}$$

The iterative procedure can be applied to solve the generalized Lyapunov equation corresponding to the frequency interval observability gramian in (5.45).

5.4 Numerical Examples

Considering the following 5th order discrete-time bilinear system originally presented by Hinamoto and Maekawa [104] which has also been used by Zhang et al [64].

$$x(k+1) = Ax(k) + \sum_{j=1}^{m} N_j x(k) u_j(k) + Bu(k)$$
$$y(k) = Cx(k) \tag{5.60}$$

where

$$A = \begin{bmatrix} 0 & 0 & 0.024 & 0 & 0 \\ 1 & 0 & -0.26 & 0 & 0 \\ 0 & 1 & 0.9 & 0 & 0 \\ 0 & 0 & 0.2 & 0 & -0.06 \\ 0 & 0 & 0.15 & 1 & 0.5 \end{bmatrix}, \quad B = \begin{bmatrix} 0.8 \\ 0.6 \\ 0.4 \\ 0.2 \\ 0.5 \end{bmatrix}, \quad N = \begin{bmatrix} 0.1 & 0 & 0 & 0 & 0 \\ 0 & 0.2 & 0 & 0 & 0 \\ 0 & 0 & 0.3 & 0 & 0 \\ 0 & 0 & 0 & 0.4 & 0 \\ 0 & 0 & 0 & 0 & 0.5 \end{bmatrix}$$
$$C = \begin{bmatrix} 0.2 & 0.4 & 0.6 & 0.8 & 1.0 \end{bmatrix}$$

The proposed technique involves firstly obtaining the frequency interval controllability and observability gramians defined in Theorem 5.1 and subsequently using these gramians as part of the balanced truncation technique [1, 40, 64]. This 5th order model $\{A, N, B, C\}$ is reduced to the following 2nd order model $\{A_{r1}, N_{r1}, B_{r1}, C_{r1}\}$ in the form of (5.60) by using the proposed technique for the frequency interval $\Omega = [0.04\pi, 0.3\pi]$

$$A_{r1} = \begin{bmatrix} 0.8247 & -0.2446 \\ 0.2394 & 0.5495 \end{bmatrix}, \quad B_{r1} = \begin{bmatrix} 1.2986 \\ -0.7881 \end{bmatrix}, N_{r1} = \begin{bmatrix} 0.3214 & 0.1276 \\ 0.0878 & 0.2862 \end{bmatrix}$$
$$C_{r1} = \begin{bmatrix} 1.2974 & 0.7789 \end{bmatrix}$$

Similarly by applying the proposed technique for the frequency interval $\Omega = [0, 0.1\pi]$ to this 5th order model $\{A, N, B, C\}$, a 3rd order discrete-time bilinear system with

the following system matrices $\{A_{r2}, N_{r2}, B_{r2}, C_{r2}\}$ in the form of (5.60) is obtained

$$A_{r2} = \begin{bmatrix} 0.7588 & -0.1963 & 0.0881 \\ 0.1932 & 0.4929 & 0.2810 \\ 0.0947 & -0.2836 & 0.2436 \end{bmatrix} \qquad B_{r2} = \begin{bmatrix} 1.4647 \\ -1.0558 \\ -0.6156 \end{bmatrix},$$

$$N_{r2} = \begin{bmatrix} 0.3260 & 0.1387 & 0.0108 \\ 0.0998 & 0.3008 & -0.1865 \\ -0.0108 & -0.0910 & 0.3204 \end{bmatrix}$$

$$C_{r2} = \begin{bmatrix} 1.4583 & 1.0710 & -0.5848 \end{bmatrix}$$

For comparison, we apply the method by Zhang et al [64] which yields the following second and third order discrete-time bilinear systems with the following system matrices $\{A_{r3}, N_{r3}, B_{r3}, C_{r3}\}$ and $\{A_{r4}, N_{r4}, B_{r4}, C_{r4}\}$ in the form of (5.60)

$$A_{r3} = \begin{bmatrix} 0.8032 & -0.2445 \\ 0.1692 & 0.6050 \end{bmatrix}, B_{r3} = \begin{bmatrix} 1.3335 \\ -0.8717 \end{bmatrix}, N_{r3} = \begin{bmatrix} 0.3387 & 0.1301 \\ 0.1075 & 0.2851 \end{bmatrix},$$

$$C_{r3} = \begin{bmatrix} 1.3615 & 0.7053 \end{bmatrix}$$

and

$$A_{r4} = \begin{bmatrix} 0.8032 & -0.2445 & 0.0373 \\ 0.1692 & 0.6050 & 0.3500 \\ 0.0732 & -0.3154 & 0.3499 \end{bmatrix}, \quad B_{r4} = \begin{bmatrix} 1.3335 \\ -0.8717 \\ -0.4052 \end{bmatrix}$$

$$N_{r4} = \begin{bmatrix} 0.3387 & 0.1301 & 0.0221 \\ 0.1075 & 0.2851 & -0.1982 \\ -0.0315 & -0.0857 & 0.3059 \end{bmatrix}, \quad C_{r4} = \begin{bmatrix} 1.3615 & 0.7053 & -0.2884 \end{bmatrix}$$

Figure 5.1 shows the step responses of the original 5th order model, 2nd order model obtained using the proposed method for a frequency interval $\Omega = [0.04\pi, 0.3\pi]$ and a 2nd order model obtained using the method by Zhang et al [64]. Table 5.1 shows the exact values for $y(k)$ for the discrete times $k = 20, 21, 22, 23, 24, 25$ from Figure 5.1. E1 and E2 denote the absolute error between the value of $y(k)$ of the original

model and the value of $y(k)$ obtained using the proposed method and the method by Zhang et al [64] respectively.

On the other hand Figure 5.2 shows the step responses of the original 5th order model, 3rd order model obtained using the proposed method for a frequency interval $\Omega = [0, 0.1\pi]$ and a 3rd order model obtained using the method by Zhang et al [64]. Table 5.2 shows the exact values for $y(k)$ for the discrete times $k = 20, 21, 22, 23, 24, 25$ from Figure 5.2. E1 and E2 denote the absolute error between the value of $y(k)$ of the original model and the value of $y(k)$ obtained using the proposed method and the method by Zhang et al. [64] respectively. From both Figure 5.1, Figure 5.2, Table 5.1 and Table 5.2 it is shown that applying the proposed technique yields a reduced order model which is a closer approximation to the original model compared to the method by Zhang et al. [64].

5.5 Conclusion

In this paper, a new model reduction method for discrete time bilinear systems based on balanced truncation is developed. The frequency interval controllability and observability gramians for discrete time bilinear systems are introduced and are shown to be solutions to a pair of new generalized Lyapunov equations. The conditions for solvability of these new Lyapunov equations are provided and the numerical solution method used to solve these equations are explained. Numerical results show that the proposed method yields reduced order models which is a closer approximation to the original models as compared to existing techniques.

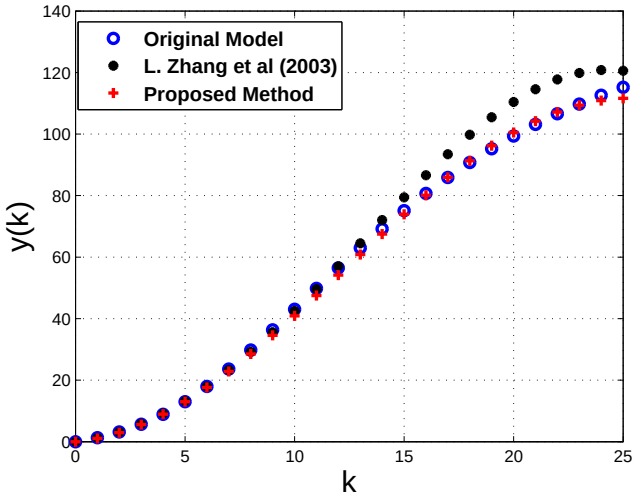

Figure 5.1: Step responses of the original model, 2nd order reduced model obtained using the method by [64] and 2nd order reduced model obtained using the proposed technique for a frequency $\Omega = [0.04\pi, 0.3\pi]$

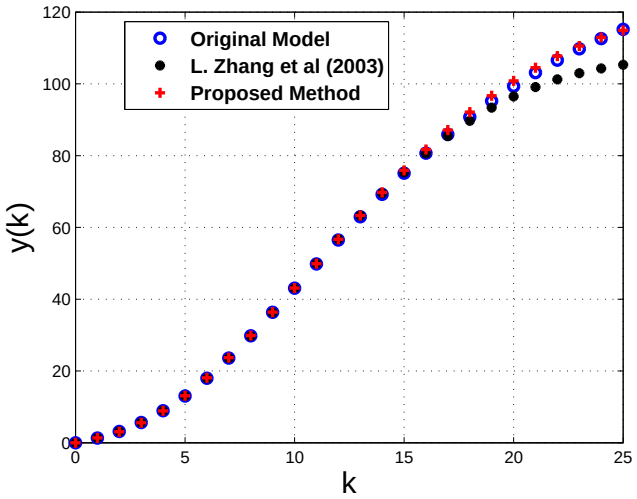

Figure 5.2: Step responses of the original model, 3rd order reduced model obtained using the method by [64] and 3rd order reduced model obtained using the proposed technique for a frequency $\Omega = [0, 0.1\pi]$

Table 5.1: Exact Values of $y(k)$ from Figure 5.1

k	y(k)				
	Original	Proposed	Zhang et al (2003)	E1	E2
20	99.35	**100.5**	110.4	**1.150**	11.050
21	103.1	**104.2**	114.6	**1.1**	11.5
22	106.6	**107.2**	117.7	**0.6**	11.1
23	109.7	**109.4**	119.9	**0.3**	10.2
24	112.6	**110.9**	120.8	**1.7**	8.2
25	115.2	**111.6**	120.6	**3.6**	5.4

Table 5.2: Exact Values of $y(k)$ from Figure 5.2

k	y(k)				
	Original	Proposed	Zhang et al (2003)	E1	E2
20	99.35	**100.8**	96.49	**1.45**	2.86
21	103.1	**104.5**	99.1	**1.4**	4
22	106.6	**107.7**	101.2	**1.1**	5.4
23	109.7	**110.5**	102.9	**0.8**	6.8
24	112.6	**112.9**	104.3	**0.3**	8.3
25	115.2	**114.9**	105.3	**0.3**	9.9

Chapter 6

Time Weighted Model Reduction of Flat Plate Solar Collectors

6.1 Introduction

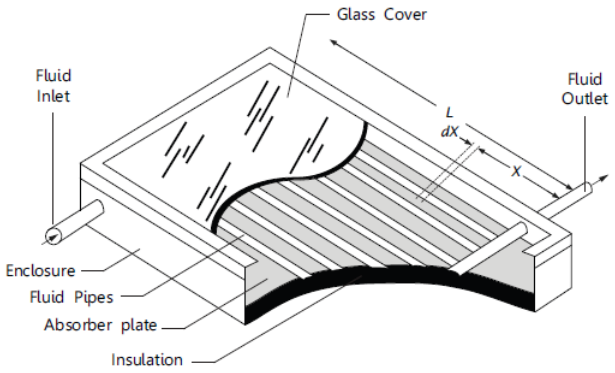

Figure 6.1: Elements of a Flat Plate Solar Collector (Image from [105, 106]).

The elements of a typical flat plate solar collector are shown in Figure 6.1. It consists of a metal box with a glass cover on top and a dark coloured absorber plate at the bottom. Solar radiant energy is transformed to heat as a result of incident sunlight which passes through the glass cover to the absorber plate where accumulation of heat occurs in the absorber plate. This accumulated heat is then transfered to a storage tank through a fluid medium such as water or air which circulates through the fluid pipes [107]. Although the principle of operation of a

flat plate solar collector is relatively straight forward, the resulting mathematical modelling framework of a flat plate solar collector may result in a high order model which can be an obstacle for simulations and model based predictive control.

Model reduction is a branch of control theory which deals with approximating a high order model with an equivalent low order model while preserving essential properties of the system such as stability and passivity. Balanced truncation originally developed by Moore is one of the most widely used model reduction methods [1]. Enns first introduced the application of frequency weightings onto the balanced truncation algorithm [25]. Improvements to the original frequency weighted balanced truncation by Enns have been described in [108–110].

Schelfhout and Moor pointed out that many specifications and robustness requirements yield natural frequency domain weighting functions but in other cases time domain weighting functions are more appropriate which led to the introduction of time weighted controllability and observability gramians for the balanced truncation algorithm which can be obtained by using recursive techniques [111]. Sreeram had defined the frequency response error bounds for time weighted balanced truncation [112]. More recently Shaker and Tahavori had introduced time weighted balanced stochastic truncation and singular perturbation approximation which also similarly involves the usage of recursive techniques [113, 114].

Cross gramians matrices contain information regarding both controllability and observability of a system in a single matrix [80, 115]. Instead of computing two separate gramians for controllability and observability, states which are the least controllable and observable can be identified from a single cross gramian matrix and these states can be truncated. The computation of a single cross gramian matrix instead of a pair of controllability and observability gramians is advantageous to increase the computational efficiency of recursive techniques. However cross gramians are only suitable for SISO and MIMO systems with symmetric transfer functions. The state space model of the flat plate solar collector under consideration is a SISO

model therefore usage of cross gramians is feasible.

In this chapter, time weighted model reduction using cross gramians is defined and applied to the SISO mathematical model of a flat plate solar collector which was originally derived in [116] and later on formulated in a state space representation in [105] and [106]. For benchmarking the resulting output obtained using the proposed time weighted model reduction method using cross gramians is compared with the output obtained by applying standard balanced truncation.

6.2 Mathematical Modelling and State Space Model Formulation

The flat plate solar collector as shown in Figure 6.1 can be modelled by using the following partial differential equations in (6.1) and (6.2) representing the instantaneous thermal balance of a differential element of length along the absorber plate together with the absorber to heat convection process. Complete details of the derivation of the partial differential equations in (6.1) and (6.2) from a heat transfer perspective can be found in [116].

$$\frac{\delta T_p}{\delta t}(t,x) = \frac{1}{\tau_d}\left[-\frac{1}{N_L}\frac{\delta T_p}{\delta t}(t,x) - T_p(t,x) + u(t)\right] \tag{6.1}$$

$$\frac{\delta T_f}{\delta t}(t,x) = N_c\left[T_p(t,x) - T_f(t,x)\right] \tag{6.2}$$

The variables and constants in (6.1) and (6.2) are defined as follows. The solar radiant energy input to the flat plate solar collector is represented by $u(t)$ in (6.1) which is a polynomial as a function of time t which approximates weather variations in a day [105, 106, 116]. T is the normalized temperature given by:

$$T = \frac{(\theta - \theta_a)}{\theta_e - \theta_a}$$

where θ is the temperature in $^\circ C$, θ_a is the ambient air temperature and θ_e is the equilibrium temperature. T_f is the temperature of the fluid flowing through the

fluid pipes whereas T_p is the temperature of the plate. With reference to Figure 6.1, x represents the ratio of the distance X to the length L of the plate and is given by:

$$x = \frac{X}{L}, \quad 0 \leq x \leq L$$

N_L and N_c represent the heat loss number and the convection number respectively and are defined by:

$$N_L = \frac{UWL}{\dot{m}c_f}$$
$$N_c = \frac{hWL}{\dot{m}c_f}$$

where $\dot{m}$ is the fluid mass flow rate (kg/sec), W is the width of the collector, L is the length of the collector, c_f is the specific heat of the fluid (J/kg$^\circ C$), c_p is the specific heat of the plate (J/kg$^\circ C$), h is the fluid heat convection coefficient ($W/m^{2\circ}C$) and U is the overall collector heat loss coefficient ($W/m^{2\circ}C$).

τ_d represents the discharge time taken by the flowing fluid in removing the heat stored by the flat plate collector and is given by:

$$\tau_d = \frac{\dot{m}_p c_p}{UW}$$

The finite difference method is applied to the partial differential equations in (6.1) and (6.2) as follows. Time and space discretization is performed simultaneously to obtain the state space model representing the partial differential equations in (6.1) and (6.2). Space is discretized by M grid points $\{x_1, x_2, x_3, ...x_M\}$ whereas time is discretized by L grid points $\{t_1, t_2, t_3, ...t_L\}$ and both discretizations are performed with uniform spacing. Applying a two point backward difference approximation to the partial differential operators $\frac{\delta T_p}{\delta t}(t,x)$, $\frac{\delta T_f}{\delta t}(t,x)$ in (6.1) and (6.2) yields:

$$\frac{\delta T_p}{\delta t}(t,x) \approx L[T_p(t_l, x_m) - T_p(t_{l-1}, x_m)] \tag{6.3}$$
$$\frac{\delta T_f}{\delta t}(t,x) \approx M[[T_f(t_l, x_m) - T_f(t_l, x_{m-1})] \tag{6.4}$$

Substituting (6.3) and (6.4) into (6.1) and (6.2) gives the following difference equa-

tions:

$$\left(L+\frac{1}{\tau_d}\right)T_p(t_l,x_m)=LT_p(t_{l-1},x_m)+\frac{M}{N_L\tau_d}T_f(t_l,x_{m-1})-\frac{M}{N_L\tau_d}T_f(t_l,x_m)+\frac{1}{\tau_d}u(t) \tag{6.5}$$

$$(M+N_c)T_f(t_l,x_m)=MT_f(t_l,x_{m-1})+N_cT_p(t_l,x_m) \tag{6.6}$$

State variables $z_p(k)$ and $z_f(k)$ are defined as follows:

$$z_p(k)\triangleq\begin{bmatrix}T_p(t_l,x_1)\\T_p(t_l,x_2)\\T_p(t_l,x_3)\\\vdots\\T_p(t_l,x_M)\end{bmatrix},z_f(k)\triangleq\begin{bmatrix}T_f(t_l,x_1)\\T_f(t_l,x_2)\\T_f(t_l,x_3)\\\vdots\\T_f(t_l,x_M)\end{bmatrix} \tag{6.7}$$

It follows that $z_p(k-1)$ and $z_f(k-1)$ are defined as

$$z_p(k-1)\triangleq\begin{bmatrix}T_p(t_{l-1},x_1)\\T_p(t_{l-1},x_2)\\T_p(t_{l-1},x_3)\\\vdots\\T_p(t_{l-1},x_M)\end{bmatrix},z_f(k-1)\triangleq\begin{bmatrix}T_f(t_{l-1},x_1)\\T_f(t_{l-1},x_2)\\T_f(t_{l-1},x_3)\\\vdots\\T_f(t_{l-1},x_M)\end{bmatrix} \tag{6.8}$$

Replacing these state variables $z_p(k)$ and $z_f(k)$ into the difference equations in (6.5) and (6.6) yields the following discrete time descriptor state space system:

$$\begin{bmatrix}(L+\frac{1}{\tau_d})I_M & A_{12}\\N_cI_M & A_{22}\end{bmatrix}\begin{bmatrix}z_p(k)\\z_f(k)\end{bmatrix}=\begin{bmatrix}LI_M & 0\\0 & 0\end{bmatrix}\begin{bmatrix}z_p(k-1)\\z_f(k-1)\end{bmatrix}+\begin{bmatrix}B_1\\0\end{bmatrix}u(k) \tag{6.9}$$

where:

$$B_1 = \begin{bmatrix} \frac{1}{\tau_d} \\ \frac{1}{\tau_d} \\ \frac{1}{\tau_d} \\ \vdots \\ \frac{1}{\tau_d} \end{bmatrix}, A_{12} = \frac{-M}{N_L \tau_d} \begin{bmatrix} -1 & 0 & \dots & 0 \\ 1 & -1 & \dots & 0 \\ \vdots & \ddots & \ddots & \vdots \\ 0 & \dots & 1 & -1 \end{bmatrix},$$

$$A_{22} = \begin{bmatrix} (M+N_c) & 0 & \dots & 0 \\ -M & (M+N_c) & \dots & 0 \\ \vdots & \ddots & \ddots & \vdots \\ 0 & \dots & -M & (M+N_c) \end{bmatrix}$$

(6.9) is a typical discrete time descriptor state space model having the form:

$$Ez(k+1) = Az(k) + Bu(k+1) \tag{6.10}$$

$$y(k) = Cz(k)$$

It follows from (6.9) that:

$$E = \begin{bmatrix} (L + \frac{1}{\tau_d}) I_M & A_{12} \\ N_c I_M & A_{22} \end{bmatrix}$$

$$A = \begin{bmatrix} L I_M & 0 \\ 0 & 0 \end{bmatrix}$$

$$B = \begin{bmatrix} B_1 \\ 0 \end{bmatrix}$$

The output y of the descriptor state space model in (6.10) can be either the fluid temperature at a specific position x_m along the flat plate solar colector - $T_f(t_l, x_m)$ or the plate temperature at a specific position x_m along the flat plate solar collector - $T_p(t_l, x_m)$.

The E matrix for this model is a nonsingular matrix, therefore the model reduction techniques for standard state space systems are applicable. For mathematical models

having an E matrix which is singular, the methods described in [117] need to be used instead. Since the E matrix in non-singular, (6.10) can be written in the following standard state space form:

$$z(k+1) = (E^{-1}A)z(k) + E^{-1}Bu(k+1)$$
$$y(k) = Cz(k) \tag{6.11}$$

The solar radiant energy input to the flat plate solar collector is defined by the polynomial as a function of discrete time $u(k)$ described here in (6.12). This polynomial serves as an approximation of weather variations in the 24 hours of a day [105, 106, 116].

$$u(k) = 0.5091k - 0.10019k^2 + 0.009118k^3 - 0.000326k^4 \tag{6.12}$$

The dimensions of the E,A and B matrix are as follows. In this paper space is discretized by $M = 200$ discretization points which results in 200 state variables representing the plate temperature $\{T_p(t_{l,1}), T_p(t_{l,1}), T_p(t_{l,1}), ...T_p(t_{l,200})\}$ and another 200 state variables $\{T_f(t_{l,1}), T_f(t_{l,1}), T_f(t_{l,1}), ...T_f(t_{l,200})\}$ representing the fluid temperature. Therefore both $z_p(k)$ and $z_f(k)$ representing the state variables in (6.9) have 200 rows respectively. As a result the dimension of the matrices are $E : 400 \times 400$, $A : 400 \times 400$ and $B : 400 \times 1$. The output y of the descriptor state space model in (6.11) can be either the fluid temperature at a specific cross section x_m along the flat plate solar colector - $T_f(t_l, x_m)$ or the absorber plate temperature at a specific cross section x_m along the flat plate solar collector - $T_p(t_l, x_m)$. The elements of the C matrics are adjusted accordingly according to the desired output. The matrix C has 1 row and 400 columns. The first 200 columns represent the plate temperature along the collector from the inlet to the outlet - $\{T_p(t_l, x_1), T_p(t_l, x_2), T_p(t_l, x_3), ...T_p(t_l, x_{200})\}$ whereas the next 200 columns represent fluid temperature along the collector from the inlet to the outlet - $\{T_f(t_l, x_1), T_f(t_l, x_2), T_f(t_l, x_3), ...T_f(t_l, x_{200})\}$. Suppose the fluid temperature at the outlet of the collector is the desired output - $T_f(t_{l,200})\}$, the corresponding C

matrix is:

$$C = \begin{bmatrix} 0 & 0 & 0 & \dots & 1 \end{bmatrix}$$

Suppose the fluid temperature at another cross section along the collector just before the outlet - is desired $T_f(t_{l,199})$. The corresponding C matrix is then:

$$C = \begin{bmatrix} 0 & 0 & \dots & 1 & 0 \end{bmatrix}$$

The matrix E for this model is a nonsingular matrix, therefore the model reduction techniques for standard state space systems are applicable. For mathematical models having an E matrix which is singular, the methods described in [117] can be used instead.

6.3 Time Weighted Model Reduction

All SISO systems have symmetric transfer functions [89]. Considering the discrete time case a linear discrete time n^{th} order system $S(A, B, C)$ defined by:

$$x(k+1) = Ax(k) + Bu(k) \qquad y(k) = Cx(k) \tag{6.13}$$

The discrete time symmetric transfer function in (6.13) fulfils the condition $H(z) = H^T(z)$ [89] as shown below.

$$D + C(zI - A)^{-1}B = D^T + B^T((zI - A)^T)^{-1}C^T \tag{6.14}$$

6.3.1 Time Weighted Cross Gramians: Discrete Time Case

Although there has not been many examples of the practical applications of time weighted balanced truncation, the theory behind time weighted balanced truncation indicates that the resulting approximation error obtained between the original and reduced order models can be reduced by a piecewise polynomial function [111–114]. For linear time invariant discrete time systems the controllability gramian -

P, observability gramian - Q and cross gramian - R are defined by:

$$P = \sum_{k=0}^{k=\infty} A^k B B^* (A^*)^k \tag{6.15}$$

$$Q = \sum_{k=0}^{k=\infty} (A^*)^k C^* C A^k \tag{6.16}$$

$$R = \sum_{k=0}^{k=\infty} A^k B C A^k \tag{6.17}$$

and are the solutions to the following Lyapunov and Sylvester equations:

$$APA^* - P + BB^* = 0 \tag{6.18}$$

$$A^*QA - Q + C^*C = 0 \tag{6.19}$$

$$ARA - R + BC = 0 \tag{6.20}$$

In addition to obtaining the controllability, observability and cross gramians using (6.18),(6.19) and (6.20), another approach for computing the gramians which is computationally efficient is by using recursive techniques [118–120]. The fundamental property which relates the gramians for systems with symmetric transfer functions has been defined in [80]:

$$R^2 = PQ \tag{6.21}$$

Theorem 6.1

The time weighted cross gramian R_{r+1} is defined as:

$$R_{r+1} = \sum_{k=0}^{k=\infty} \frac{(k+1)!}{k!} A^k B C A^k \;\; r = 0, 1, 2.. \tag{6.22}$$

and is related to the time weighted controllability and observability P_{r+1} and Q_{r+1} gramians such that

$$R_{r+1}^2 = P_{r+1} Q_{r+1} \tag{6.23}$$

Proof

The time weighted controllability and observability gramians have been defined in

[111] as follows:

$$P_{r+1} = \sum_{k=0}^{k=\infty} \frac{(k+1)!}{k!} A^k B B^* (A^*)^k \;\; r = 0, 1, 2... \tag{6.24}$$

$$Q_{r+1} = \sum_{k=0}^{k=\infty} \frac{(k+1)!}{k!} (A^*)^k C^* C A^k \;\; r = 0, 1, 2.. \tag{6.25}$$

By taking into consideration that the transfer function of the system is symmetric, Theorem 6.1 can be proved by replacing (6.22) into the left hand side of (6.23) and both (6.24) and (6.25) into the right hand side of (6.23). ■

It follows that the time weighted cross gramian, controllability gramian and observability gramian in (6.22),(6.24) and (6.25) can be solved recursively as in [111–114, 118] and are defined as follows:

$$AR_{r+1}A - R_{r+1} + R_r = 0 \;\; r = 0, 1, 2... \tag{6.26}$$

$$AP_{r+1}A^* - P_{r+1} + P_r = 0 \;\; r = 0, 1, 2... \tag{6.27}$$

$$A^*Q_{r+1}A - Q_{r+1} + Q_r = 0 \;\; r = 0, 1, 2... \tag{6.28}$$

where

$$R_0 = BC$$

$$P_0 = BB^*$$

$$Q_0 = C^*C$$

6.3.2 Computational Procedure for Time Weighted Model Reduction Using Cross Gramians

The computational procedure for time weighted model reduction using cross gramians is as follows:

1. For a given discrete state space system (A, B, C) as defined in (6.13), the time weighted cross gramian R_{r+1} is determined by solving (6.26) recursively

2. Using eigenvalue decomposition, obtain a matrix U which diagonalizes the time weighted cross gramian matrics, R_{r+1} resulting in a diagonal matrix S. Due to

the property described in (6.23), the elements along the diagonal of the matrix S obtained in (6.29) below are equal to the square root of the eigenvalues of the product of the time weighted controllability and observability gramians such that $\lambda(R_{r+1}) = \sqrt{\lambda(P_{r+1}Q_{r+1})}$.

$$S = U^{-1}R_{r+1}U \tag{6.29}$$

3. The diagonal entries of the matrix S in the previous step need to be arranged in decending order to reflect the controllability and observability of each state. If the diagonal entries of the matrix S are not in descending order permutation matrices are used to reorder the states of the model as described in [89].

4. Similarity transformation is applied onto A, B and C using the transformation matrics U obtained from the diagonalization of the time weighted cross gramian as and the least controllable and observable states are truncated.

6.4 Numerical Example and Simulation Results

To demonstrate the described computational procedure by a numerical example, the following values are inserted into the state space model in (6.11) - number of space discretization grid points M=200, number of time discretization grid points L=100, convection number N_c= 16.6, heat loss number N_L=0.5 and discharge time $\tau_d = 4$. Two examples are considered. In the first example the fluid temperature at the outlet of the collector $T_f(t_l, x_{200})$ or $x = 1$ is considered (please refer to Figure 6.1). In the second example the fluid temperature at the middle of the collector is considered $T_f(t_l, x_{100})$ (or at $x = 0.5$) (please refer to Figure 6.1). In both examples the described computational procedure is applied to the state space model of the flat plate solar collector where the original model with an order $N = 400$ is reduced to a model with the reduced order of $N_r = 1$. For the first example, in order to find the fluid temperature at the outlet of the collector $T_f(t_{l,200})$ or $x = 1$, the response of

the original high order model, the reduced first order models obtained by balanced truncation $H_1(z)$ and the reduced order model obtained by time weighted model reduction $H_2(z)$ to the input polynomial function representing weather variations in (6.12) is calculated and shown in (6.30) and (6.31)

$$H_1(z) = \frac{0.00296}{z - 0.9932} \tag{6.30}$$

$$H_2(z) = \frac{0.00392}{z - 0.9895} \tag{6.31}$$

Figure 6.1 shows the fluid temperature at $T_f(t_l, x_{200})$ or $x = 1$ (please refer to Figure 1) obtained by finding the response of the original high order model, (6.30) and (6.31) to the polynomial function in (6.12) representing weather variations.

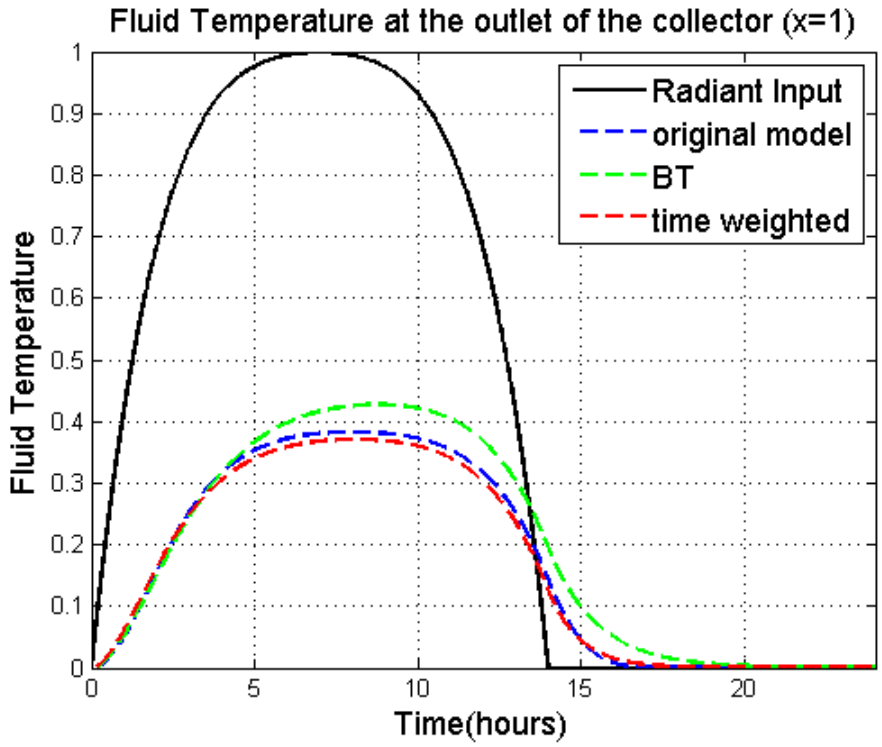

Figure 6.1: Response of Original and Reduced Order Models to the Polynomial in (6.12)

For the second example, suppose instead of the fluid temperature at the outlet of the collector we are interested in the fluid temperature at the middle of the collector - $T_f(t_{l,100})$ or at $x = 0.5$ (please refer to Figure 1). Modifying the C matrix to represent the fluid temperature cross section at the middle of the collector and

applying both balanced truncation and time weighted model reduction gives the following transfer functions $H_3(z)$ in (6.32) and $H_4(z)$ in (6.33). Figure 2 shows the fluid temperature obtained by finding the response of the models to the polynomial input in (6.12) representing weather variations.

$$H_3(z) = \frac{0.002969}{z - 0.9875} \tag{6.32}$$

$$H_4(z) = \frac{0.003837}{z - 0.982} \tag{6.33}$$

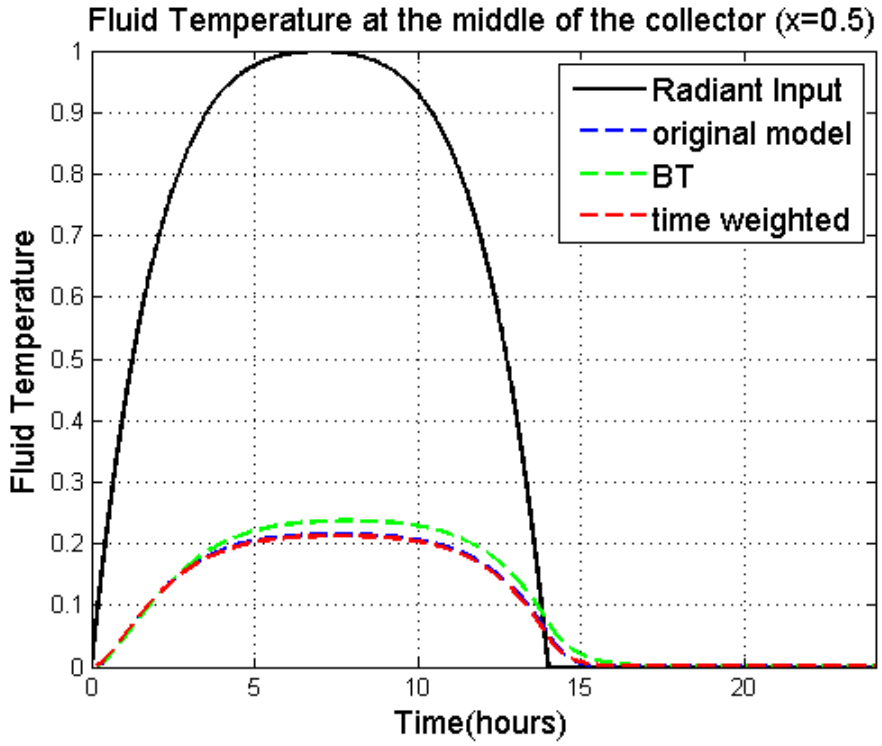

Figure 6.2: Response of Original and Reduced Order Models to the Polynomial in (6.12)

It is shown in Figure 6.1 and 6.2 that the reduced order models obtained using cross gramian based time weighted model reduction in (6.31) and (6.33) give a fluid temperature response which is closer to the original high order model compared to the reduced order models obtained using balanced truncation in (6.30) and (6.32). By comparing Figure 6.1 and Figure 6.2 it can be clearly observed that the fluid temperature nearer to the inlet is the lower and fluid temperature will increase with increased distance of x from the inlet to the outlet. This result agrees with the

theory of flat plate solar collectors where more heat is accumulated as the fluid flows from the inlet to the outlet.

6.5 Discussion and Conclusion

In this chapter the application of the time weighted model reduction method as previously described in [111,112] is applied onto the mathematical model representing the thermal behaviour of a flat plate solar collector. Numerical results show that a significant order reduction from $N = 400$ to $N_r = 1$ is possible with a close approximation to the original model. The results presented in this chapter is an indicator of the potential application of cross gramian based time weighted model reduction to state space models generated from finite difference method and possibly finite element method for usage in applications such as model predictive control and simulations. The computation of a single cross gramian matrix instead of a pair of controllability and observability gramians is advantageous to increase the computational efficiency of recursive techniques. In conclusion, the application of cross gramian based time weighted model reduction to a flat plate solar collector model obtained by finite differencing of a set of partial differential equations has been studied and significant order reduction is possible while achieving low approximation error. In terms of future work, nonlinear partial differential equations representing more detaliled dynamics of flat plate solar collectors can be considered for cross gramian based time weighted model reduction.

Chapter 7

Generalized Gramian Based Frequency Interval Model Reduction for Unstable Systems

7.1 Introduction

Controllability and observability gramians matrices have been applied in a broad range of applications such as for the input-output pairing methods in control configuration selection [42], sensitivity analysis of biochemical reaction networks [121] and the model order reduction of large scale dynamical systems and systems with complex hyperbolic networks [122]. Many problems which involve the computation of gramians are inherently frequency dependent [49, 50, 53, 57, 99]. Shaker had applied frequency limited controllability and observability gramians for input-output interactions for control configuration selection and also for the measurement of control reconfigurability in the context of fault tolerant control systems [88, 123].

For particular systems which are unstable or do not fulfill the solvability conditions of the standard Lyapunov equations, generalized controllability and observability gramians which are applicable to these systems have been described by Zhou, Salomon and Wu [124]. Inspired by this work, Shaker had introduced the gener-

alized cross gramian to obtain the cross gramians for systems where the Sylvester equation is not solvable [125]. This generalization is based on the techniques by Zhou, Salomon and Wu and also the alternative definition of the gramians defined by Fernando and Nicholson [80, 124].

In this chapter we propose a model reduction method based on solving a pair of generalized frequency interval controllability and observability gramians to deal with systems which do not have a solution to the standard frequency interval controllability and observability gramians in [29]. This approach is inspired by the method by Zhou, Salomon and Wu [124] and also the method by Gawronski and Juang [29].

7.2 Preliminaries

7.2.1 Controllability and Observability Gramians for Continuous-Time Systems

Consider the following continuous-time system

$$G(s) = C(sI - A)^{-1}B + D \tag{7.1}$$

where $\{A \in \mathbb{R}^{n\times n}, B \in \mathbb{R}^{n\times p}, C \in \mathbb{R}^{q\times n}, D \in \mathbb{R}^{p\times q}\}$ is its minimal realization. The equivalent time and frequency domain controllability and observability gramians are given as follows

$$P = \int_0^\infty e^{A\tau}BB^*e^{A^*\tau}d\tau \tag{7.2}$$

$$= \frac{1}{2\pi}\int_{-\infty}^{+\infty}(j\omega I - A)^{-1}BB^*(-j\omega I - A^*)^{-1}d\omega \tag{7.3}$$

$$= \frac{1}{2\pi}\int_{-\infty}^{+\infty}H(\omega)BB^*H^*(\omega)d\omega \tag{7.4}$$

$$Q = \int_0^{\infty} e^{A^*\tau} C^* C e^{A\tau} d\tau \tag{7.5}$$

$$= \frac{1}{2\pi} \int_{-\infty}^{+\infty} (-j\omega I - A^*)^{-1} C^* C (j\omega I - A)^{-1} d\omega \tag{7.6}$$

$$= \frac{1}{2\pi} \int_{-\infty}^{+\infty} H^*(\omega) C^* C H(\omega) d\omega \tag{7.7}$$

It is established that the gramians P and Q satisfy the following Lyapunov equations

$$AP + PA^* + BB^* = 0 \tag{7.8}$$

$$A^*Q + QA + C^*C = 0 \tag{7.9}$$

7.2.2 Frequency Interval Controllability and Observability Gramians for Linear Systems [29]

Definition 7.1 ([29]). The frequency interval controllability and observability gramians within the interval $\Omega = [\omega_1, \omega_2]$ for the stable linear system in (7.1) are defined as:

$$\hat{P}_\Omega = \hat{P}(\omega_2) - \hat{P}(\omega_1) \tag{7.10}$$

$$\hat{Q}_\Omega = \hat{Q}(\omega_2) - \hat{Q}(\omega_1), \tag{7.11}$$

where

$$\hat{P}(\omega) = \frac{1}{2\pi} \int_{-\omega}^{\omega} H(\omega) B B^* H^*(\omega) d\omega \tag{7.12}$$

$$= \frac{1}{2\pi} \int_{-\infty}^{+\infty} H(\mu) \left[S(\omega) B B^* + B B^* S^*(\omega) \right] H^*(\mu) d\mu$$

$$= S(\omega) P + P S^*(\omega) \tag{7.13}$$

$$\hat{Q}(\omega) = \frac{1}{2\pi} \int_{-\omega}^{\omega} H^*(\omega) C^* C H(\omega) d\omega \tag{7.14}$$

$$= \frac{1}{2\pi} \int_{-\infty}^{+\infty} H^*(\mu) \left[S(\omega) C^* C + C^* C S(\omega) \right] H(\mu) d\mu$$

$$= S^*(\omega) Q + Q S(\omega) \tag{7.15}$$

and

$$S(\omega) = \frac{1}{2\pi}\int_{-\omega}^{+\omega} H(\omega)d\omega$$
$$= \frac{1}{2\pi}\int_{-\omega}^{+\omega} (j\omega I - A)^{-1}d\omega \tag{7.16}$$
$$= \frac{j}{2\pi}\ln[(j\omega I + A)(-j\omega I + A)^{-1}] \tag{7.17}$$

It follows that $\hat{P}(\omega)$ and $\hat{Q}(\omega)$ are the solutions to the following Lyapunov equations [29]:

$$A\hat{P}(\omega) + \hat{P}(\omega)A^* + S(\omega)BB^* + BB^*S^*(\omega) = 0 \tag{7.18}$$

$$A^*\hat{Q}(\omega) + \hat{Q}(\omega)A + S^*(\omega)C^*C + C^*CS(\omega) = 0. \tag{7.19}$$

7.2.3 Controllability and Observability Gramians for Continuous-Time Unstable Systems [124]

The controllability and observability gramians defined in (7.2) and (7.5) are only valid for stable systems since for unstable systems the integrals will become unbounded. The Lyapunov equations in (7.8) and (7.9) however may still have solutions even though A is unstable provided that the matrix A does not have a pair of eigenvalues which are negatives of each other. If the matrix A has a pair of eigenvalues which are negatives of each other, then the Lyapunov equations in (7.8) and (7.9) will not have any solutions. For example consider the following system $G_1(s)$

$$G_1(s) = \left[\begin{array}{c|c} A & B \\ \hline C & D \end{array}\right] = \left[\begin{array}{cc|c} -1 & 0 & 0.1 \\ 0 & 1 & 1 \\ \hline 0 & 1 & 0 \end{array}\right] \tag{7.20}$$

Equations (7.8) and (7.9) will not have any solutions for the this system $G_1(s)$ since the A matrix of this system has a pair of eigenvalues which are negatives of each other.

Another constraint of using equations (7.8) and (7.9) to obtain the controllability and observability gramians is that even if (7.8) and (7.9) have solutions, the eigenvalues of the product of the controllability and observability gramians may be complex numbers which prohibits the use of the controllability and observability gramians in applications such as model order reduction and control configuration selection which require real numbered Hankel singular values. An example of a system which exhibits such a property is as follows:

$$G_2(s) = \left[\begin{array}{c|c} A & B \\ \hline C & D \end{array}\right] = \left[\begin{array}{cc|cc} -1 & 1 & 1 & 0 \\ 0 & 2 & 0 & 1 \\ \hline 1 & 0 & 0 & 0 \\ 0 & 1 & 0 & 0 \end{array}\right] \tag{7.21}$$

The eigenvalues of the product of the controllability and observability gramians calculated using (7.8) and (7.9) for this system $G_2(s)$ are a pair of complex conjugate numbers: $0.0625 + 0.2421i$ and $0.0625 - 0.2421i$

To overcome these constraints, Zhou, Salomon and Wu had defined the following generalized controllability and observability gramians for possibly unstable systems as follows [124]:

Suppose that (A, B) is stabilizable and (C, A) is detectable. Let X and Y be the stabilizing solutions to the following Riccati equations:

$$XA + A^*X - XBB^*X = 0 \tag{7.22}$$

$$AY + YA^* - XC^*CX = 0 \tag{7.23}$$

Let $F = -B^*X$ and $L = -YC^*$, the generalized controllability gramian P_F and observability gramian Q_F is the solution to the following modified Lyapunov equations:

$$A_F P_F + P_F A_F^* + BB^* = 0 \tag{7.24}$$

$$A_C^* Q_C + Q_C A_C + C^* C = 0 \tag{7.25}$$

where

$$A_F = A + BF \tag{7.26}$$

$$A_C = A + LC \tag{7.27}$$

In the form of integrals the solutions of (7.24) and (7.25) are:

$$P_F = \frac{1}{2\pi} \int_{-\infty}^{\infty} (j\omega I - A_F)^{-1} BB^* (-j\omega I - A_F^*)^{-1} d\omega \tag{7.28}$$

$$Q_C = \frac{1}{2\pi} \int_{-\infty}^{\infty} (-j\omega I - A_C^*)^{-1} C^* C (j\omega I - A_C)^{-1} d\omega \tag{7.29}$$

Remark 7.1: Suppose A is stable, it follows that $X = Y = 0$ and therefore P_F and Q_C in (7.24), (7.25), (7.28) and (7.29) are reduced to the standard controllability and observability gramians for stable systems as in (7.8),(7.9), (7.3) and (7.6).

7.3 Main Work

7.3.1 Generalized Frequency Interval Controllability and Observability Gramians for Unstable Systems

Definition 7.2: The frequency interval controllability gramian for an unstable system in the form of (7.1) is defined as follows

$$\hat{P}_\Omega = \hat{P}(\omega_2) - \hat{P}(\omega_1) \tag{7.30}$$

where $\hat{P}(\omega)$ satisfies

$$\hat{P}(\omega) = \frac{1}{2\pi} \int_{-\omega}^{\omega} (j\omega I - A_F)^{-1} BB^* (-j\omega I - A_F^*)^{-1} d\omega \tag{7.31}$$

Theorem 7.1: $\hat{P}(\omega)$ defined in (7.31) is the solution to the following Lyapunov equation

$$A_F\hat{P}(\omega) + \hat{P}(\omega)A_F^* + S_F(\omega)BB^* + BB^*S_F^*(\omega) = 0 \tag{7.32}$$

where

$$\begin{aligned} S_F(\omega) &= \frac{1}{2\pi}\int_{-\omega}^{+\omega}(j\omega I - A_F)^{-1}d\omega \\ &= \frac{1}{2\pi}\int_{-\omega}^{+\omega}H_F(\omega)d\omega \end{aligned} \tag{7.33}$$

Proof: Let

$$(j\omega I - A)^{-1}B = NM^{-1}$$

be such that M is inner, i.e. $M^{\sim}(s) = M^{-1}$. The co-prime factorization can then be obtained by using the following property described in [126]:

$$\begin{bmatrix} M \\ N \end{bmatrix} = \left[\begin{array}{c|c} A_F & B \\ \hline F & I \\ I & 0 \end{array}\right] \tag{7.34}$$

By using this property in (7.34), a generalized expression of $\hat{P}(\omega)$ in (7.12) can be written as follows

$$\begin{aligned} \hat{P}(\omega) &= \frac{1}{2\pi}\int_{-\omega}^{\omega}(j\omega I - A)^{-1}BB^*(-j\omega I - A^*)^{-1}d\omega \\ &= \frac{1}{2\pi}\int_{-\omega}^{\omega}N(j\omega)N^*(j\omega)d\omega \\ &= \frac{1}{2\pi}\int_{-\omega}^{\omega}(j\omega I - A_F)^{-1}BB^*(-j\omega I - A_F^*)^{-1}d\omega \end{aligned}$$

Taking into consideration that (7.24) can be re-written as

$$\begin{aligned} BB^* &= -A_FP_F - P_FA_F^* \\ &= (j\omega I - A_F)P_F + P_F(-j\omega I - A_F^*) \end{aligned}$$

Followed by substituting $BB^* = (j\omega I - A_F)P_F + P_F(-j\omega I - A_F^*)$ into (7.31) yields

$$\hat{P}(\omega) = \frac{1}{2\pi}\int_{-\omega}^{\omega}(j\omega I - A_F)P_F + P_F(-j\omega I - A_F^*)d\omega$$

Note that

$$S_F(\omega) = \frac{1}{2\pi}\int_{-\omega}^{+\omega}(j\omega I - A_F)^{-1}d\omega$$

Hence

$$\hat{P}(\omega) = S_F(\omega)P_F + P_F S_F^*(\omega) \tag{7.35}$$

Taking into consideration the following property [29, 30]

$$H_F(\omega_1)H_F(\omega_2) = H_F(\omega_2)H_F(\omega_1)$$

and substituting both (7.40) and (7.28) into (7.35) yields

$$\begin{aligned}
&\hat{P}(\omega) = \\
&\frac{1}{2\pi}\int_{-\omega}^{+\omega} H_F(\omega)d\omega \cdot \frac{1}{2\pi}\int_{-\infty}^{+\infty} H_F(\mu)BB^*H_F^*(\mu)d\mu + ... \\
&\frac{1}{2\pi}\int_{-\infty}^{+\infty} H_F(\mu)BB^*H_F^*(\mu)d\mu \cdot \frac{1}{2\pi}\int_{-\omega}^{+\omega} H_F^*(\omega)d\omega \\
&= \frac{1}{2\pi}\int_{-\infty}^{+\infty}\left(\frac{1}{2\pi}\int_{-\omega}^{+\omega} H_F(\omega)d\omega\right) H_F(\mu)BB^*H_F^*(\mu)d\mu + ... \\
&\frac{1}{2\pi}\int_{-\infty}^{+\infty} H_F(\mu)BB^*H_F^*(\mu)\left(\frac{1}{2\pi}\int_{-\omega}^{+\omega} H_F^*(\omega)d\omega\right)d\mu \\
&= \frac{1}{2\pi}\int_{-\infty}^{+\infty} H_F(\mu)\left(\frac{1}{2\pi}\int_{-\omega}^{+\omega} H_F(\omega)d\omega\right) BB^*H_F^*(\mu)d\mu + ... \\
&\frac{1}{2\pi}\int_{-\infty}^{+\infty} H_F(\mu)BB^*\left(\frac{1}{2\pi}\int_{-\omega}^{+\omega} H_F^*(\omega)d\omega\right) H_F^*(\mu)d\mu \\
&= \frac{1}{2\pi}\int_{-\infty}^{+\infty} H_F(\mu)\left[S_F(\omega)BB^* + BB^*S_F^*(\omega)\right] H_F^*(\mu)d\mu,
\end{aligned} \tag{7.36}$$

Since A_F is stable, we can conclude that $\hat{P}(\omega)$ expressed in the form of (7.36) is the solution to the following Lyapunov equation

$$A_F\hat{P}(\omega) + \hat{P}(\omega)A_F^* + S_F(\omega)BB^* + BB^*S_F^*(\omega) = 0.$$

■

Definition 7.3: The frequency interval observability gramian for an unstable system in the form of (7.1) is defined as follows

$$\hat{Q}_\Omega = \hat{Q}(\omega_2) - \hat{Q}(\omega_1) \tag{7.37}$$

where $\hat{Q}_\Omega$ satisfies

$$\hat{Q}_\Omega = \frac{1}{2\pi}\int_{-\omega}^{+\omega}(-j\omega I - A_C^*)^{-1}C^*C(j\omega I - A_C)^{-1}d\omega \tag{7.38}$$

Theorem 7.2: $\hat{Q}(\omega)$ defined in (7.37) is the solution to the following Lyapunov equation

$$A_C^*\hat{Q}(\omega) + \hat{Q}(\omega)A_C + S_C^*(\omega)C^*C + C^*CS_C(\omega) = 0. \tag{7.39}$$

where

$$\begin{aligned} S_C(\omega) &= \frac{1}{2\pi}\int_{-\omega}^{+\omega}(j\omega I - A_C)^{-1}d\omega \\ &= \frac{1}{2\pi}\int_{-\omega}^{+\omega}H_C(\omega)d\omega \end{aligned} \tag{7.40}$$

Proof: The proof of Theorem 7.2 is similar to the proof of Theorem 7.1 and is therefore ommited for brevity. ■

Algorithm 1: Given the system matrices $\{A, B, C, D\}$.

(a) **Step 1:** Check the stabilizability of the pair of matrices (A, B) and the detectability of the pair of matrices (C, A)

(b) **Step 2:** Obtain the stabilizing solutions - X and Y for the Riccati equations in (7.22) and (7.23)

(c) **Step 3:** Obtain the frequency interval controllability gramian $\hat{P}_\Omega$ and frequency interval observability gramian $\hat{Q}_\Omega$ by solving (7.30) and (7.37) respectively.

(d) **Step 4:** Obtain the similarity transformation matrix T which diagonalizes $\hat{P}_\Omega$ and $\hat{Q}_\Omega$ such that $T\hat{P}_\Omega T^* = (T^*)^{-1}\hat{Q}_\Omega T^{-1}$

(e) **Step 5:** Transform and partition to get a realization

$$\bar{A} = T^{-1}AT = \begin{bmatrix} A_{11} & A_{12} \\ A_{21} & A_{22} \end{bmatrix}, \quad \bar{B} = T^{-1}B = \begin{bmatrix} B_1 \\ B_2 \end{bmatrix}$$

$$\bar{C} = CT = \begin{bmatrix} C_1 & C_2 \end{bmatrix}$$

(f) **Step 6:** The matrices of the reduced order model are given by $A_r = A_{11}, B_r = B_1, C_r = C_1, D_r = D$

7.4 Numerical Examples

Considering the following 8th order continuous-time unstable system

$$A = \begin{bmatrix} A_1 & A_2 \end{bmatrix}$$

$$A_1 = \begin{bmatrix} -0.2625 & -5.1234 & 0 & 0 \\ 5.1234 & 0 & 0 & 0 \\ -0.1679 & -3.2777 & -0.0594 & -2.4376 \\ 0 & 0 & 2.4376 & 0 \\ -0.1679 & -3.2777 & -0.0368 & -1.5084 \\ 0 & 0 & 0 & 0 \\ 0 & 0 & 0 & 0 \\ 0 & 0 & 0 & 0 \end{bmatrix}$$

$$A_2 = \begin{bmatrix} 0 & 0 & 0 & 0 \\ 0 & 0 & 0 & 0 \\ 0 & 0 & 0 & 0 \\ 0 & 0 & 0 & 0 \\ -0.0076 & -0.8738 & 0 & 0 \\ 0.8738 & 0 & 0 & 0 \\ 0 & 1.1444 & 0 & 1.0000 \\ 0 & 0 & 1.0000 & 0 \end{bmatrix}$$

$$B = \begin{bmatrix} 1 & 0 & 1 & 0 & 1 & 0 & 0 & 0 \end{bmatrix}^T,$$

$$C = \begin{bmatrix} 0 & 0 & 0 & 0 & 0 & 0 & 0 & -2.1182 \end{bmatrix}, D = 0$$

The matrix A has a pair of eigenvalues which are negatives of each other (i.e. 1 and -1), therefore the controllability and observability gramians of this system cannot

be obtained by using the Lyapunov equations in (7.8) and (7.9). In addition many of the existing gramian based frequency weighted model reduction methods are not applicable for these type of systems [127–130].

In this section the original 8th order system is reduced to a 4th order system by using both the method by Zhou, Salomon and Wu [124] and also the proposed method. Figure 7.1 shows the magnitude responses of the original 8th order system, the magnitude response of the reduced 4th order system obtained using the method by Zhou, Salomon and Wu [124] and the magnitude response of the reduced 4th order system obtained using the proposed method (in which the range of the specified frequency interval is [0.2 rad/s, 1.5 rad/s]). Similarly, Figure 7.2 shows the magnitude responses of the original 8th order system, the magnitude response of the reduced 4th order system obtained using the method by Zhou, Salomon and Wu [124] and the magnitude response of the reduced 4th order system obtained using the proposed method (in which the range of the specified frequency interval is [3 rad/s, 9 rad/s])

From Figure 7.1 and Figure 7.2 it can be observed that although the reduced order model obtained by using the method by Zhou, Salomon and Wu [124] gives a closer approximation to the original model for the entire frequency region, the reduced order model obtained using the proposed method gives a closer approximation to the original model in the specified frequency interval.

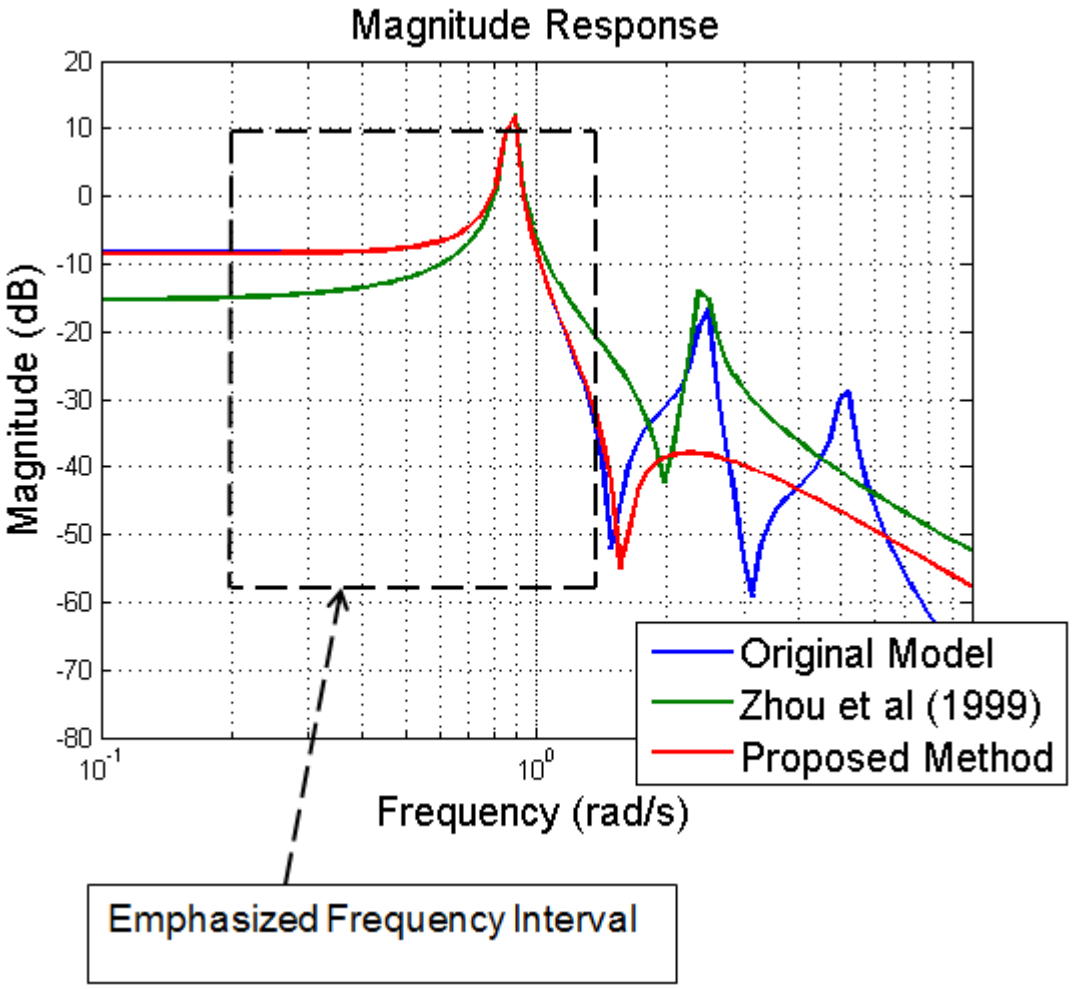

Figure 7.1: Magnitude response plot for the original 8th order model, 4th order model obtained using the method by Zhou et al. (1999) and 4th order model obtained using the proposed method

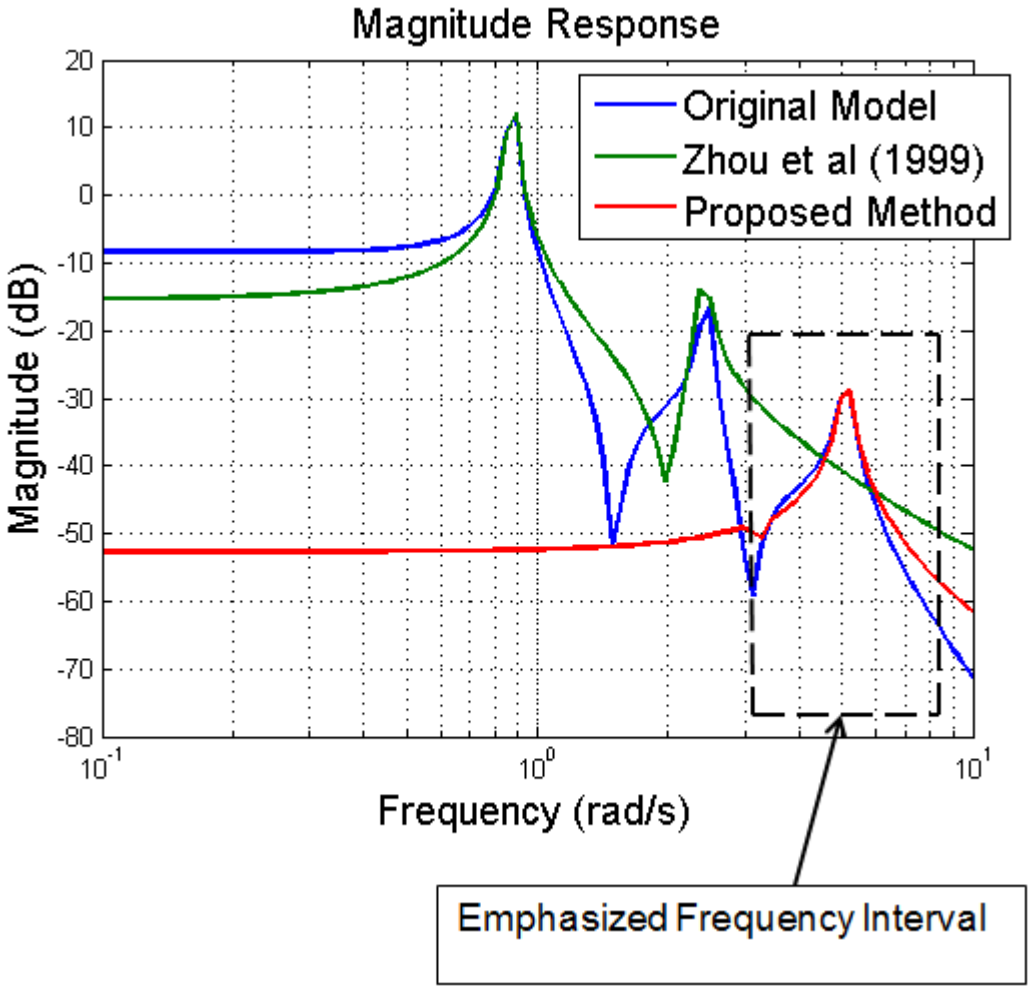

Figure 7.2: Magnitude response plot for the original 8th order model, 4th order model obtained using the method by Zhou et al. (1999) and 4th order model obtained using the proposed method

7.5 Conclusion

Generalized frequency interval controllability and observability gramians have been developed in order to obtain the frequency interval controllability and observability gramians for systems which do not have a solution to the standard Lyapunov equations. These gramians are used as part of the model reduction algorithm and numerical results demonstrate that the reduced order model obtained using the proposed method gives a closer approximation to the original model at the specified frequency interval.

Chapter 8

Partial Fraction Expansion Based Frequency Weighted Balanced Singular Perturbation Approximation Model Reduction Technique with Error Bounds

8.1 Introduction

Model reduction methods which emphasize particular frequency intervals continue to receive interest from the control theory community due to the importance of obtaining such reduced order models in a variety of applications ([50–52, 56, 79]). Frequency weighted model reduction methods based on the partial fraction expansion approach originally introduced by Saggaf and Franklin [131, 132] are an important category of model reduction methods which have been further developed to have desirable properties such as guaranteed stability for the case of double sided weightings and the existence of error bounds ([133–136]).

Sahlan and Sreeram presented a new model reduction approach based on the decomposition of the input-output augmented system using partial fraction expansion to form a new augmented system where the system matrix is block diagonal ([133, 134]). Standard balanced truncation by Moore [1] was then applied to the augmented system.

In this chapter, frequency weighted model reduction methods based on partial fraction expansion are firstly reviewed. A partial fraction expansion based frequency weighted model reduction algorithm is proposed to further improve the frequency weighted approximation error. In this algorithm, singular perturbation approximation originally proposed by Liu and Anderson [2] is applied to the framework of the method by Sahlan and Sreeram [133] in order to further improve the frequency weighted approximation error. Two free parameters α and β are also included in this algorithm in order to further minimize the frequency weighted approximation error. Error bounds are developed for the proposed method. Simulation results demonstrate that reduced frequency weighted approximation errors relative to the original method by Sahlan and Sreeram [133] can be obtained by using the proposed method.

8.2 Preliminaries

In this section, existing frequency weighted model reduction techniques are reviewed namely the methods by Enns [25], Sreeram and Anderson [135] and Sahlan and Sreeram [133]. An understanding of these techniques is required as a prerequisite for the material presented in this chapter.

Let $G(s)$ be the transfer function of a stable original system with the following minimal realization

$$G(s) = \left[\begin{array}{c|c} A & B \\ \hline C & D \end{array}\right]$$

Similarly let $V(s)$ and $W(s)$ be the transfer functions of stable input and output weights with the following minimal realizations

$$V(s) = \left[\begin{array}{c|c} A_V & B_V \\ \hline C_V & D_V \end{array}\right]$$

$$W(s) = \left[\begin{array}{c|c} A_W & B_W \\ \hline C_W & D_W \end{array}\right]$$

The state space realization of the augmented system $W(s)G(s)V(s)$ is then given by

$$\left[\begin{array}{c|c} \hat{A} & \hat{B} \\ \hline \hat{C} & \hat{D} \end{array}\right] = \left[\begin{array}{ccc|c} A_W & B_W C & B_W D C_V & B_W D D_V \\ 0 & A & B C_V & B D_V \\ 0 & 0 & A_V & B_V \\ \hline C_W & D_W C & D_W D C_V & D_W D D_V \end{array}\right] \tag{8.1}$$

The controllability and observability of the augmented realization $\{\hat{A}, \hat{B}, \hat{C}, \hat{D}\}$ is given as

$$\hat{P} = \begin{bmatrix} P_W & P_{12} & P_{13} \\ P_{12}^T & P_E & P_{23} \\ P_{13}^T & P_{23}^T & P_V \end{bmatrix}, \hat{Q} = \begin{bmatrix} Q_W & Q_{12} & Q_{13} \\ Q_{12}^T & Q_E & Q_{23} \\ Q_{13}^T & Q_{23}^T & Q_V \end{bmatrix} \tag{8.2}$$

such that both $\hat{P}$ and $\hat{Q}$ satisfy the following Lyapunov equations

$$\hat{A}\hat{P} + \hat{P}\hat{A}^T + \hat{B}\hat{B}^T = 0 \tag{8.3}$$

$$\hat{A}^T\hat{Q} + \hat{Q}\hat{A} + \hat{C}^T\hat{C} = 0 \tag{8.4}$$

Assuming that there are no pole-zero cancellations in $W(s)G(s)V(s)$, the augmented gramians $\hat{P}$ and $\hat{Q}$ are positive definite.

8.2.1 Enns Technique

The frequency weighted balanced truncation technique by Enns [25] is presented in this section. Expanding the (2,2) blocks respectively of equations (8.3) and (8.4)

yields the following equations

$$AP_E + P_E A^T + X_E = 0 \tag{8.5}$$

$$A^T Q_E + Q_E A + Y_E = 0 \tag{8.6}$$

where

$$X_E = BC_V P_{23}^T + P_{23} C_V^T B^T + BD_V D_V^T B^T \tag{8.7}$$

$$Y_E = C^T B_W^T Q_{12}^T + Q_{12}^T B_W C + C^T D_W^T D_W C \tag{8.8}$$

Simultaneously diagonalizing the weighted gramians P_E and Q_E, we get

$$T^T Q_E T = T^{-1} P_E T^{-T} = diag\{\sigma_1, \sigma_2, ...\sigma_n\} \tag{8.9}$$

where $\sigma_1 \geq \sigma_2 \geq ... \geq \sigma_r > \sigma_{r+1} \geq ... \geq \sigma_n > 0$. The order of the reduced order model is denoted by r whereas the order of the original model is denoted by n. Transforming and partitioning the original system we get

$$\hat{A} = T^{-1}AT = \begin{bmatrix} A_{11} & A_{12} \\ A_{21} & A_{22} \end{bmatrix}, \hat{B} = T^{-1}B = \begin{bmatrix} B_1 \\ B_2 \end{bmatrix}$$

$$\hat{C} = \begin{bmatrix} C_1 & C_2 \end{bmatrix}, \quad \hat{D} = D$$

The reduced order model is given by $G_r(s) = C_1(sI - A_{11})^{-1}B_1 + D$. The stability of the reduced order model obtained by using Enns technique is not guaranteed to be stable for the case of double sided input weighting.

8.2.2 Sreeram and Anderson's Partial Fraction Expansion Based Technique

The partial fraction expansion frequency weighted model reduction method which was first proposed by Saggaf and Franklin [131, 132] was only applicable to be used with single sided frequency weighting. Sreeram and Anderson [135] presented a generalization of the partial fraction expansion frequency weighted model reduction

method which is applicable for the case of double sided weighting. A frequency response error bound for this generalized technique was also presented by Sreeram and Anderson [135]. The main idea of this method is presented as follows.

The augmented system matrix in (8.1) is block diagonalized by the similarity transformation matrix $\tilde{T} = \begin{bmatrix} I & -Y & R \\ 0 & I & X \\ 0 & 0 & I \end{bmatrix}$ which yields

$$= \left[\begin{array}{ccc|c} A_W & B_W C & B_W D C_V & B_W D D_V \\ 0 & A & B C_V & B D_V \\ 0 & 0 & A_V & B_V \\ \hline C_W & D_W C & D_W D C_V & D_W D D_V \end{array}\right]$$

$$= \left[\begin{array}{c|c} \tilde{T}^{-1}\hat{A}\tilde{T} & \tilde{T}^{-1}\hat{B} \\ \hline \hat{C}\tilde{T} & \hat{D} \end{array}\right]$$

$$= \left[\begin{array}{ccc|c} A_W & X_{12} & X_{13} & X_1 \\ 0 & A & X_{23} & X_2 \\ 0 & 0 & A_V & B_V \\ \hline C_W & Y_1 & Y_2 & D_W D D_V \end{array}\right]$$

$$= \left[\begin{array}{ccc|c} A_W & 0 & 0 & X_1 \\ 0 & A & 0 & X_2 \\ 0 & 0 & A_V & B_V \\ \hline C_W & Y_1 & Y_2 & D_W D D_V \end{array}\right]$$

$$= \begin{bmatrix} A_W & X_1 \\ C_W & 0 \end{bmatrix} + \begin{bmatrix} A & X_2 \\ Y_1 & D_W D D_V \end{bmatrix} + \begin{bmatrix} A_V & B_V \\ Y_2 & 0 \end{bmatrix}$$

$$= W_{diag}(s) + G_{diag}(s) + V_{diag}(s)$$

where X, Y and R are obtained by solving the following matrix equations

$$X_{12} = YA - A_W Y + B_W C = 0 \tag{8.10}$$

$$X_{23} = AX - XA_V + BC_V = 0 \tag{8.11}$$

$$X_{13} = A_W R - RA_V + B_W CX + YAX + B_W DC_V + YBC_V - YXA_V = 0 \tag{8.12}$$

$$X_1 = B_W DD_V + YBD_V - YXB_V - RB_V \tag{8.13}$$

$$X_2 = BD_V - XB_V \tag{8.14}$$

$$Y_1 = D_W C - C_W Y \tag{8.15}$$

$$Y_2 = D_W CX + D_W DC_V + C_W R \tag{8.16}$$

$$\hat{D} = D_W DD_V \tag{8.17}$$

In this method the following gramians

$$P_{SA} = P_E - P_{23}X^T - XP_{23}^T + XP_V X^T \tag{8.18}$$

$$Q_{SA} = Q_E - Q_{12}Y - Y^T Q_{12}^T + Y^T Q_W Y \tag{8.19}$$

which satisfy the following Lyapunov equations

$$AP_{SA} + P_{SA}A^T + X_2 X_2^T = 0$$

$$A^T Q_{SA} + Q_{SA}A + Y_1^T Y_1 = 0$$

are simultaneously diagonalized.

Since the realization $\{A, X_2, Y_1\}$ is minimal and the gramians satisfy the Lyapunov equations, this partial fraction expansion based technique yields stable reduced order models for the case of double sided weightings.

8.2.3 Ghafoor and Sreeram's Partial Fraction Expansion Based Technique

Ghafoor and Sreeram [136] had further developed the original method by Sreeram and Anderson as follows. Instead of simultaneously diagonalizing the gramians P_{SA}

and Q_{SA} in (8.18) and (8.19) as with the method by Sreeram and Anderson [135], Ghafoor and Sreeram had simultaneously diagonalized the following new gramians

$$P_X = P + \alpha^2 P_{SA}$$

$$Q_X = Q + \beta^2 Q_{SA}$$

where α and β are real constants and both P and Q are the unweighted gramians satisfying

$$AP + PA^T + BB^T = 0$$

$$A^T Q + QA + C^T C = 0$$

The gramians P_X and Q_X satisfy the following Lyapunov equations

$$AP_X + P_X A^T + B_X B_X^T = 0$$

$$A^T Q_Y + Q_Y A + C_Y^T C_T = 0$$

where $B_X = [B \quad \alpha X_2]$ and $C_Y = \begin{bmatrix} C \\ \beta Y_1 \end{bmatrix}$.

8.2.4 Sahlan and Sreeram's Partial Fraction Expansion Based Technique

Sreeram and Sahlan [133] had also proposed a method based on decomposing the augmented system $W(s)G(s)V(s)$ to be equal to the summation of the elements of the decomposed system - $W_{diag}(s) + G_{diag}(s) + V_{diag}(s)$ by using partial fraction expansion where the system matrix is block diagonalized. The decomposed system $(W_{diag}(s) + G_{diag}(s) + V_{diag}(s))$ is then expressed as a new augmented system $\bar{W}(s)\bar{G}(s)\bar{V}(s)$ such that the system matrix of $W_{diag}(s) + G_{diag}(s) + V_{diag}(s)$ is the same as the system matrix of $\bar{W}(s)\bar{G}(s)\bar{V}(s)$ and is block diagonal such that

$$\begin{aligned} & W(s)G(s)V(s) \\ & = W_{diag}(s) + G_{diag}(s) + V_{diag}(s) \\ & = \bar{W}(s)\bar{G}(s)\bar{V}(s) \end{aligned} \tag{8.20}$$

where $\bar{G}(s) = \{A, \bar{B}, \bar{C}, \bar{D}\}$ is the new original system, $\bar{V}(s) = \{A_V, B_V, \bar{C}_V, \bar{D}_V\}$ and $\bar{W}(s) = \{A_W, \bar{B}_W, C_W, \bar{D}_W\}$ are the input and output weights respectively where

$$\bar{B}_W = \begin{bmatrix} B_W & A_W & I \end{bmatrix}, \bar{D}_W = \begin{bmatrix} D_W & C_W & 0 \end{bmatrix},$$

$$\bar{B} = \begin{bmatrix} B & -X & AX \end{bmatrix}, \bar{C} = \begin{bmatrix} C \\ -Y \\ YA \end{bmatrix}, \bar{D}_V = \begin{bmatrix} D_V \\ B_V \\ 0 \end{bmatrix},$$

$$\bar{D} = \begin{bmatrix} D & 0 & CX \\ 0 & 0 & R \\ YB & -R - YX & YAX \end{bmatrix}, \bar{C}_V = \begin{bmatrix} C_V \\ A_V \\ I \end{bmatrix}$$

The equations in (8.10) to (8.17) can then be factorized as follows:

$$X_{12} = \begin{bmatrix} B_W & A_W & I \end{bmatrix} \begin{bmatrix} C \\ -Y \\ YA \end{bmatrix} = \bar{B}_W \bar{C}$$

$$X_{23} = \begin{bmatrix} B & -X & AX \end{bmatrix} \begin{bmatrix} C_V \\ A_V \\ I \end{bmatrix} = \bar{B} \bar{C}_V$$

$$X_2 = \begin{bmatrix} B & -X & AX \end{bmatrix} \begin{bmatrix} D_V \\ B_V \\ 0 \end{bmatrix} = \bar{B} \bar{D}_V$$

$$Y_1 = \begin{bmatrix} D_W & C_W & 0 \end{bmatrix} \begin{bmatrix} C \\ -Y \\ YA \end{bmatrix} = \bar{D}_W \bar{C}$$

$$X_{13} = \begin{bmatrix} B_W & A_W & I \end{bmatrix} \begin{bmatrix} D & 0 & CX \\ 0 & 0 & R \\ YB & -R-YX & YAX \end{bmatrix} \begin{bmatrix} C_V \\ A_V \\ I \end{bmatrix} = \bar{B}_W \bar{D} \bar{C}_V$$

$$X_1 = \begin{bmatrix} B_W & A_W & I \end{bmatrix} \begin{bmatrix} D & 0 & CX \\ 0 & 0 & R \\ YB & -R-YX & YAX \end{bmatrix} \begin{bmatrix} D_V \\ B_V \\ 0 \end{bmatrix} = \bar{B}_W \bar{D} \bar{D}_V$$

$$Y_2 = \begin{bmatrix} D_W & C_W & 0 \end{bmatrix} \begin{bmatrix} D & 0 & CX \\ 0 & 0 & R \\ YB & -R-YX & YAX \end{bmatrix} \begin{bmatrix} C_V \\ A_V \\ I \end{bmatrix} = \bar{D}_W \bar{D} \bar{C}_V$$

$$\hat{D} = \begin{bmatrix} D_W & C_W & 0 \end{bmatrix} \begin{bmatrix} D & 0 & CX \\ 0 & 0 & R \\ YB & -R-YX & YAX \end{bmatrix} \begin{bmatrix} D_V \\ B_V \\ 0 \end{bmatrix} = \bar{D}_W \bar{D} \bar{D}_V$$

Standard balanced truncation can then be applied to the new original system $\bar{G}(s) = \{A, \bar{B}, \bar{C}, \bar{D}\}$ to obtain and r^{th} order reduced order model $\bar{G}_r(s) = \{A_r, \bar{B}_r, \bar{C}_r, \bar{D}_r\}$. The final reduced order model $G_r(s) = \{A_r, B_r, C_r, D_r\}$ is then obtained by deleting the extra rows in $\bar{C}_r$ and extra columns in $\bar{B}_r$ and both extra rows and columns in $\bar{D}_r$. The work presented by Sreeram et al. [134] is a further development to this method by Sahlan and Sreeram [133] by constructing an augmented system with zero cross terms.

8.3 Main Work

In the original partial fraction expansion method by Sahlan and Sreeram [133] described in the previous section, standard truncation by Moore [1] was applied to the augmented system $\bar{G}(s)$ in (8.20). In this section an algorithm is proposed to further reduce the frequency weighted approximation error. In this algorithm, singular perturbation approximation originally proposed by Liu and Anderson [2] is applied

to the framework of the method by Sahlan and Sreeram [133] in order to further improve the frequency weighted approximation error.

8.3.1 Proposed Algorithm

Step 1: Compute the matrices X and Y from (8.11) and (8.10) respectively.

Step 2: Calculate the fictitious input matrix $\bar{B}_{PF}$ and output matrix $\bar{C}_{PF}$ by using suitable values of the free parameters α and β as follows.

$$\bar{B}_{PF} = \begin{bmatrix} B & -\alpha X & AX \end{bmatrix}$$

$$\bar{C}_{PF} = \begin{bmatrix} C \\ -\beta Y \\ YA \end{bmatrix}$$

Step 3: Weighted controllability and observability gramians $\bar{P}_{PF}$ and $\bar{Q}_{QF}$ are obtained by solving the following Lyapunov equations.

$$A\bar{P}_{PF} + \bar{P}_{PF}A^T + \bar{B}_{PF}\bar{B}_{PF}^T = 0 \tag{8.21}$$

$$A^T\bar{Q}_{PF} + \bar{Q}_{PF}A + \bar{C}_{PF}^T\bar{C}_{PF} = 0 \tag{8.22}$$

Step 4: Calculate the transformation matrix T which simultaneously diagonalizes the matrices $\bar{P}_{PF}$ and $\bar{Q}_{PF}$ such that

$$T^T\bar{Q}_{PF}T = T^{-1}\bar{P}_{PF}T^{-T}$$

$$= diag\{\sigma_1, \sigma_2, ...\sigma_r, \sigma_{r+1}, ...\sigma_n\}$$

where $\sigma_i \geq \sigma_{i+1}, i = 1, 2, ..., n-1$ and $\sigma_r > \sigma_{r+1}$

Step 5: Compute the frequency weighted balanced realization.

$$\hat{A} = T^{-1}AT, \hat{B} = T^{-1}B, \hat{C} = CT$$

Step 6: Partition $\{\hat{A}, \hat{B}, \hat{C}\}$ as follows

$$\hat{A} = \begin{bmatrix} A_{11} & A_{12} \\ A_{21} & A_{22} \end{bmatrix}, \hat{B} = \begin{bmatrix} B_1 \\ B_2 \end{bmatrix}, \hat{C} = \begin{bmatrix} C_1 & C_2 \end{bmatrix}$$

where $A_{11} \in \mathbb{R}^{r\times r}, B_1 \in \mathbb{R}^{r\times p}, C_1 \in \mathbb{R}^{q\times r}$ and $r < n$

Step 7: The reduced order model is given by $G_{rspa}(s) = C_{spa}(sI - A_{spa})^{-1}B_{spa} + D_{spa}$, where

$$A_{spa} = A_{11} - A_{12}A_{22}^{-1}A_{21}$$

$$B_{spa} = B_1 - A_{12}A_{22}^{-1}B_2$$

$$C_{spa} = C_1 - C_2A_{22}^{-1}A_{21}$$

$$D_{spa} = D - C_2A_{22}^{-1}B_2$$

8.3.2 Error Bounds

In this section the error bounds for the reduced order models obtained using the proposed algorithm is derived. To establish the relationship between the input and output matrices (B and C), and the new fictitious input and output matrices ($\bar{B}_{PF}$ and $\bar{C}_{PF}$), we define two constant matrices, $K_{PF} = \begin{bmatrix} I/\alpha \\ 0 \end{bmatrix}$ and $L_{PF} = \begin{bmatrix} I/\beta & 0 \end{bmatrix}$ respectively where I is an identity matrix with the appropriate dimension. It follows that the following relationships hold true between the input and output matrices B and C and the fictitious input and output matrices $\bar{B}_{PF}$ and $\bar{C}_{PF}$

$$B = \bar{B}_{PF}K_{PF} \tag{8.23}$$

$$C = L_{PF}\bar{C}_{PF} \tag{8.24}$$

The relationships between the input and output matrices (B and C) and the new fictitious input and output matrices ($\bar{B}_{PF}$ and $\bar{C}_{PF}$) defined in (8.23) and (8.24) are used in Theorem 8.1 as follows.

Theorem 8.1: Let $G(s)$ be a stable and strictly proper transfer function whereas $V(s)$ and $W(s)$ are the input and output weights respectively. If $G_{spa}(s)$ is a reduced order model obtained by using the algorithm presented in Section 8.3.1, it follows that the following error bound holds true:

$$||W(s)(G(s) - G_{rspa}(s)V(s)||_\infty \leq \delta \sum_{k=r+1}^{n} \sigma_k \tag{8.25}$$

where $\delta = \frac{2}{\alpha\beta}||W(s)||_\infty||V(s)||_\infty$ and σ_k are the Hankel singular values of the system $\{A, \bar{B}_{PF}, \bar{C}_{PF}\}$.

Proof:

Upon partitioning the fictitious matrices $\bar{B}_{PF}$ and $\bar{C}_{PF}$ as $\bar{B}_{PF} = \begin{bmatrix} \bar{B}_{1PF} \\ \bar{B}_{2PF} \end{bmatrix}$ and $\bar{C}_{PF} = [\bar{C}_{1PF} \quad \bar{C}_{2PF}]$ respectively and substituting $B_1 = \bar{B}_{1PF}K_{PF}, B_2 = \bar{B}_{2PF}K_{PF}$ and $C_1 = L_{PF}\bar{C}_{1PF}, C_2 = L_{PF}\bar{C}_{2PF}$, we have

$$||W(s)[G(s) - G_{rspa}(s)]V(s)||_\infty$$

$$= ||W(s)[C(sI - A)^{-1}B + D - (C_{spa}(sI - A_{spa})^{-1}B_{spa} - D_{spa})]V(s)||_\infty$$

$$= ||W(s)[C(sI - A)^{-1}B + D - (C_1 - C_2A_{22}^{-1}A_{21})(sI - A_{spa})^{-1}(B_1 - A_{12}A_{22}^{-1}B_2) - ...$$

$$D + C_2A_{22}^{-1}B_2]V(s)||_\infty$$

$$= ||W(s)[L_{PF}\bar{C}_{PF}(sI - A)^{-1}\bar{B}_{PF}K_{PF} + L_{PF}\bar{C}_{2PF}A_{22}^{-1}\bar{B}_{2PF}K_{PF} - ...$$

$$L_{PF}(\bar{C}_{1PF} - \bar{C}_{2PF}A_{22}^{-1}A_{21})(sI - A_{spa})^{-1}(\bar{B}_{1PF} - A_{12}A_{22}^{-1}\bar{B}_{2PF})K_{PF}]V(s)||_\infty$$

$$= ||W(s)L_{PF}\{\bar{C}_{PF}(sI - A)^{-1}\bar{B}_{PF} - (\bar{C}_{1PF} - \bar{C}_{2PF}A_{22}^{-1}A_{21})(sI - A_{spa})^{-1} \times ...$$

$$(\bar{B}_{1PF} - A_{12}A_{22}^{-1}\bar{B}_{2PF}) + \bar{C}_{2PF}A_{22}^{-1}\bar{B}_{2PF}\}K_{PF}V(s)||_\infty$$

$$\leq ||W(s)L_{PF}||_\infty||\bar{C}_{PF}(sI - A)^{-1}\bar{B}_{PF} - (\bar{C}_{1PF} - \bar{C}_{2PF}A_{22}^{-1}A_{21})(sI - A_{spa})^{-1} \times ...$$

$$(\bar{B}_{1PF} - A_{12}A_{22}^{-1}\bar{B}_{2PF}) + \bar{C}_{2PF}A_{22}^{-1}\bar{B}_{2PF}||_\infty||K_{PF}V(s)||_\infty$$

$$\leq \frac{1}{\beta}||W(s)L_{PF}||_\infty||\bar{C}_{PF}(sI - A)^{-1}\bar{B}_{PF} - \bar{C}_{spa}(sI - A_{spa})^{-1}\bar{B}_{spa} + ...$$

$$\bar{C}_{2PF}A_{22}^{-1}\bar{B}_{2PF}||_\infty\frac{1}{\beta}||K_{PF}V(s)||_\infty$$

Since $\{A, \bar{B}_{PF}, \bar{C}_{PF}\}$ is a balanced realized model and $\{A_{spa}, \bar{B}_{spa}, \bar{C}_{spa}, -\bar{C}_{2PF}A_{22}^{-1}\bar{B}_{2PF}\}$ is its corresponding reduced order model, then from the derivations presented by Liu and Anderson [2], the following holds true

$$||\bar{C}_{PF}(sI - A)^{-1}\bar{B}_{PF} - \bar{C}_{spa}(sI - A_{spa})^{-1}\bar{B}_{spa} + \bar{C}_{2PF}A_{22}^{-1}\bar{B}_{2PF}||_\infty \leq 2\sum_{k=r+1}^{n}\sigma_k$$

it follows that

$$||W(s)(G(s) - G_{rspa}(s)V(s)||_\infty \leq \delta\sum_{k=r+1}^{n}\sigma_k$$

with $\delta = \frac{2}{\alpha\beta}||W(s)L_{PF}||_\infty||K_{PF}V(s)||_\infty$ ■

Corollary 8.1: The error bounds when only input or output weights are used are as follows:

$$||(G(s) - G_{rspa}(s)V(s)||_\infty \leq \frac{2}{\alpha}||K_{PF}V(s)||_\infty \sum_{k_i=r+1}^{n} \sigma_{ki}$$

and

$$||W(s)(G(s) - G_{rspa}(s)||_\infty \leq \frac{2}{\beta}||W(s)L_{PF}||_\infty \sum_{k_o=r+1}^{n} \sigma_{ko}$$

where σ_{ki} and σ_{ko} are the Hankel singular values of the systems $\{A, \bar{B}_{PF}, C\}$ and $\{A, B, \bar{C}_{PF}\}$ respectively.

8.4 Numerical Example

Considering the 4th order system originally from Enns [25]

$$A = \begin{bmatrix} -1 & 0 & 0 & 0 \\ 0 & -2 & 0 & 0 \\ 0 & 0 & -3 & 0 \\ 0 & 0 & 0 & -4 \end{bmatrix}, B = \begin{bmatrix} 0 & -5/2 \\ 1/2 & -3/2 \\ 1 & -5 \\ -1/2 & 1/6 \end{bmatrix}$$

$$C = \begin{bmatrix} 1 & 0 & 1 & 0 \\ 4/15 & 1 & 0 & 1 \end{bmatrix}, D = \begin{bmatrix} 0 & 0 \\ 0 & 0 \end{bmatrix}$$

and the 2nd order input and output weighting functions as

$$A_V = A_W = \begin{bmatrix} -4.5 & 0 \\ 0 & -4.5 \end{bmatrix}, B_V = B_W = \begin{bmatrix} 3 & 0 \\ 0 & 3 \end{bmatrix},$$

$$C_V = C_W = \begin{bmatrix} 1.5 & 0 \\ 0 & 1.5 \end{bmatrix}, D_V = D_W = \begin{bmatrix} 1 & 0 \\ 0 & 1 \end{bmatrix}$$

Table 8.1 shows the results of the weighted approximation errors - $||W(s)[G(s) - G_r(s)]V(s)||_\infty$ for the existing methods by Enns, Lin and Chiu, Wang et al. and

Table 8.1: Weighted Approximation Error Obtained by Various Techniques

Order	Enns	Lin and Chiu's	Wang et al		Imran et al
	W.E.	W.E.	W.E.	E.B.	W.E
1	2.1291	2.5744	2.1213	7.2898	2.1234
2	0.2660	0.5607	0.2720	1.4895	0.2424
3	0.1131	0.1645	0.1151	0.3228	0.1075

Imran et al. [25–27, 127] for benchmarking. Weighted approximation error and error bounds are denoted as W.E and E.B. respectively. Table 8.2 shows the weighted approximation error obtained using both methods described by Ghafoor and Sreeram [136]. W.E. 1 and W.E. 2 denote the weighted approximation errors obtained using method 1 and method 2 by Ghafoor and Sreeram [136]. Table 8.3 shows the results obtained by using the method by Sreeram and Sahlan [133]. Applying the proposed method with various values of the parameters α and β yields the results in Table 8.4. It can be observed that the proposed approach gives reduced frequency weighted approximation error relative to the method by [133]. The values of the free parameters α and β in Tables 8.2 to 8.4 are selected such that the minimum weighted approximation error is obtained. Figure 8.1 shows the variation of the frequency weighted approximation error relative to the variation of the free parameters α and β for a first order controller using the proposed method.

Table 8.2: Weighted Approximation Error Obtained by [136]

Order	Ghafoor and Sreeram's Method				
	α	β	W.E. 1	W.E 2	Error Bound
1	0.4	0.4	2.1126	1.4564	3.4848
	0.4	0.5	2.1165	1.4877	3.6212
	0.5	0.4	2.1131	1.4833	3.6229
2	0.8	2.9	0.2709	0.3116	2.3312
	0.9	2.7	0.2710	0.3238	2.3242
	0.7	0.7	0.2784	0.2543	0.8949
3	0.4	0.4	0.1009	0.0668	0.1589
	0.8	0.5	0.1084	0.0714	0.1786
	1	0.6	0.1117	0.0750	0.1942

Table 8.3: Weighted Approximation Error Obtained by [133, 134]

Order	Sreeram and Sahlan's Method			
	α	β	Weighted Error	Error Bound
1	8.1	6.7	2.1158	13.922
	8.2	6.9	2.1161	13.488
	8.0	7.0	2.1201	13.580
2	180	110	0.3149	0.5290
	90	110	0.3219	0.5686
	147.5	32.5	0.3166	0.6996
3	103.9	35.8	0.1081	0.3104
	105.7	35.7	0.1082	0.3092
	105.3	35.3	0.1082	0.3120

Table 8.4: Weighted Approximation Error Obtained Using the Proposed Method

Order	Proposed technique			
	α	β	Weighted Error	Error Bound
1	0.1	0.1	**1.2361**	**6.9011**
	0.2	0.1	**1.2363**	**6.9040**
	0.2	0.2	**1.2375**	**6.9112**
2	4.9	4.9	**0.2430**	**2.4105**
	4.5	4.5	**0.2432**	**2.1981**
	5.5	5.5	**0.2433**	**2.7572**
3	6.0	2.0	**0.0614**	**0.5388**
	7.0	3.0	**0.0648**	**0.6221**
	5.0	1.0	**0.0719**	**0.4599**

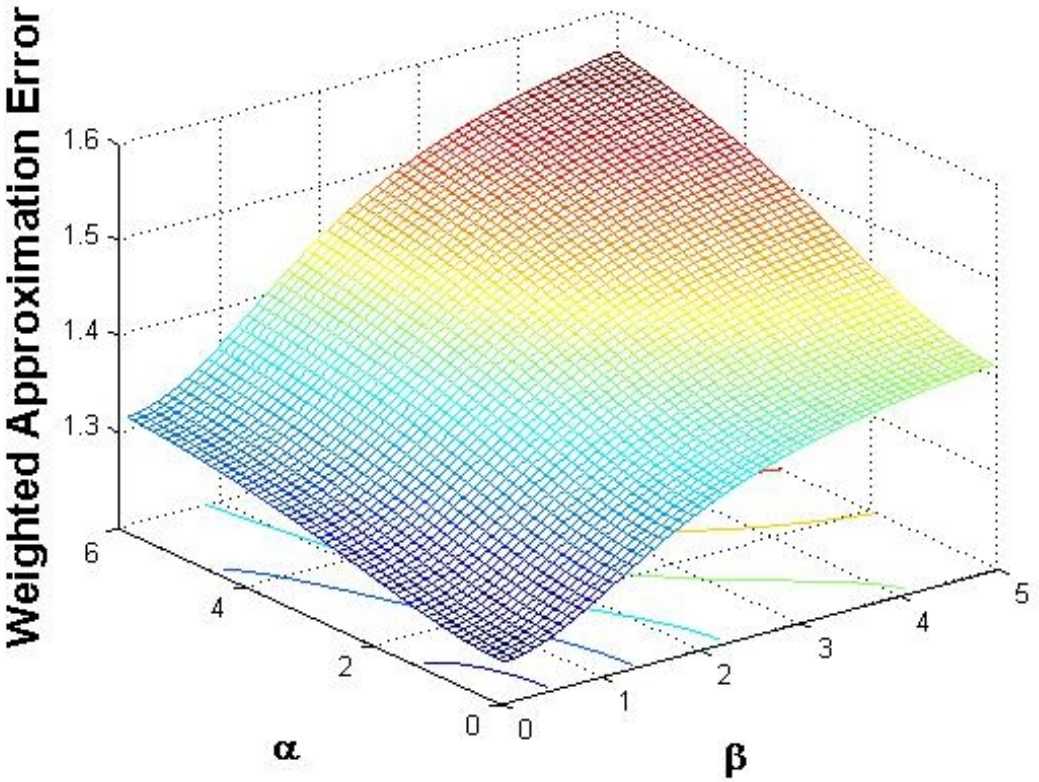

Figure 8.1: Variation of Weighted Approximation Error due to Variation of α and β for 1st order models obtained using the proposed

8.5 Conclusion

In this chapter, a frequency weighted balanced singular perturbation approximation model reduction method which belongs to the class of partial fraction expansion based model reduction method is developed which is a further development to the method proposed in [133]. By applying singular perturbation approximation instead of standard balanced truncation, it has been demonstrated that the frequency weighted approximation error can be reduced. An error bound has also been developed for the proposed technique.

Chapter 9

Conclusion

9.1 Overview of the Thesis

In this thesis various singular value decomposition based model order reduction techniques have been investigated.

In Chapter 2, we presented a comprehensive review of several important singular value decomposition based frequency and time weighted model reduction methods. The essential properties of these techniques have also been thoroughly discussed.

In Chapter 3, a solution to the controller reduction problem via a parameterized double-sided frequency weighted controller reduction technique has been developed for the feedback control of MIMO discrete time systems particularly for non-unity feedback control system configurations which have the controller located in the feedback path. New frequency weights which are a function of a free parameter matrix have been derived for the double sided frequency weighted model reduction problem. It has been demonstrated that the infinity norm of the approximation error between the original closed loop system and the closed loop system with a reduced order controller can be significantly reduced by varying this free parameter matrix. It has been demonstrated that the selection of an optimal value for this free parameter matrix which minimizes the infinity norm of the approximation error can be obtained by choosing a large value for the diagonal entries of this free parameter

matrix without the need to construct an approximating function.

In Chapter 4, frequency interval cross gramians have been derived for both linear and bilinear systems. New generalized Sylvester equations for calculating the frequency interval cross gramians are derived in order to be used to obtain information regarding controllability and observability within a single matrix. The usage of frequency interval cross gramians for the model reduction of bilinear SISO systems has been demonstrated. Frequency interval cross gramians have also been demonstrated to be advantageous in control configuration selection since by using frequency interval cross gramians only half of the number of equations need to be solved in order to obtain information regarding the controllability and observability of a system. Compared to existing techniques this leads to a more computationally efficient method. The computational efficiency of the proposed method based on frequency interval cross gramians relative to existing methods have been demonstrated through numerical examples.

In Chapter 5, a new model reduction method for discrete-time bilinear systems based on the balanced truncation framework has been developed. This method is based on solving a new pair of new generalized frequency interval controllability and observability gramians. The conditions for solvability of these new generalized Lyapunov equations have been presented together with a numerical solution method for solving these generalized Lyapunov equations. The performance of the proposed method has been demonstrated through numerical examples.

In Chapter 6, time weighted cross gramians have been developed and applied as part of the model reduction for a mathematical model which represents the dynamics of a flat plate solar collector. This mathematical model is obtained by the discretization of two partial differential equations resulting in a high order state space model. Model reduction based on time weighted cross gramians is then applied to this high order state space model. Numerical examples have been provided to demonstrate this proposed method based on time weighted cross gramians.

In Chapter 7, generalized frequency interval controllability and observability gramians have been developed in order to obtain the frequency interval controllability and observability gramians for continuous time linear systems which do not have a solution from the Lyapunov equations. The applicability of these generalized gramians to be used in model reduction has also been demonstrated.

In Chapter 8, a new frequency weighted partial fraction expansion based model reduction technique has been developed based on the partial fraction expansion approach. Singular perturbation approximation has been incorporated into the algorithm in order to reduce the frequency weighted approximation error. This technique results in stable reduced order models regardless if single sided or double sided weights are used. Error bounds have also been derived for the proposed method. For minimization of the frequency weighted approximation error, free parameters have been introduced into the algorithm. A numerical example has been provided to validate the proposed algorithm.

9.2 Future Work

The research carried out in this thesis does have possibilities for further development as follows:

1. The solution to the controller reduction problem via a parameterized double-sided frequency weighted controller reduction technique for MIMO discrete-time systems in the Linear Fractional Transformation (LFT) configuration has yet to be developed. The development of such a technique will be beneficial to a variety of control engineering problems which are formutaled in the form of an LFT configuration.

2. The derivation of a generalized Sylvester equation corresponding to the frequency interval cross gramians for bilinear discrete-time systems will be advantageous in the control configuration selection procedure of discrete-time

bilinear systems since the computational efficiency can be increased.

3. The development of new model order reduction techniques to reduce the order of high order models generated by discretizing the partial differential equations which represent the dynamics of solar collectors will be very useful in model predictive control and also for reducing simulation times. In addition to solar collectors, the partial differential equations representing building thermal dynamics which have non-linear characteristics will also benefit from the development of new model order reduction techniques.

4. The development of new generalized frequency interval controllability and observability gramians for discrete-time linear systems which do not have a solution to the discrete-time Lyapunov equations will be beneficial for the model order reduction of linear discrete-time systems.

Bibliography

[1] B.C. Moore. Principal component analysis in linear systems: Controllability, observability, and model reduction. *IEEE Transactions on Automatic Control*, Vol. AC-26, pp. 17-32, (1981).

[2] Y. Liu and B.D.O. Anderson. Singular perturbation approximation of balanced systems. *International Journal of Control*, Vol. 50, No. 4, pp. 1339-1405, (1989).

[3] K. Glover. All optimal Hankel-norm approximation of linear multivariable systems and their L_∞ - error bounds. *International Journal of Control*, Vol. 39, No.6, pp. 1115 - 1195, (1984).

[4] V. Sreeram and P. Agathoklis. Design of Linear-Phase IIR filters via Impulse-Response Gramians. *IEEE Transactions on Signal Processing*, Vol. 40, No.2, pp.389-394, (1992).

[5] V. Sreeram and P. Agathoklis. Discrete-Systems Reduction via Impulse Response Gramians and its Relation to q-Markov Covers. *IEEE Transactions on Automatic Control*, Vol. AC-37, No.5, pp.653-658, (1992).

[6] V. Sreeram and P. Agathoklis. The discrete-time q-Markov cover models with improved low-frequency approximation. *IEEE Transactions on Automatic Control*, Vol. 39, No.5, pp.1102-1105, (1994).

[7] S. Holford and P. Agathoklis. The Use of Model Reduction Techniques for Designing IIR Filters with Linear Phase in the Passband. *IEEE Transactions on Signal Processing*, Vol.44, No.10, pp. 2396-2404, (1996).

[8] C. Xiao and P. Agathoklis. Design and implementation of approximately linear phase two-dimensional IIR filters. *IEEE Transactions on Circuits and Systems II: Analog and Digital Signal Processing*, Vol. 45, No. 9, pp. 1279-1288, (1998).

[9] X.X. Huang, W.Y. Yan, and K.L.Teo. A New Approach to Frequency Weighted L-2 Optimal Model Reduction. *International Journal of Control*,Vol. 74, No.12, pp. 1239-1246, (2001).

[10] X.X. Huang, W.Y. Yan, and K.L.Teo. H-2 Near-optimal Model Reduction. *IEEE Transactions on Automatic Control*,Vol. 46, No.8, pp.1279-1284, (2001).

[11] A. Jazlan, V. Sreeram, R. Togneri and W. Mousa. A review on reduced order approximation for digital filters with complex coefficients using model reduction. In: *Proceedings of the 3rd Australian Control Conference*, pp. 79-84, (2013).

[12] S.O.R. Moheimani, H. R. Pota and I. R. Petersen. Spatial balanced model reduction for flexible structures. *Automatica*, Vol. 35, No. 2, pp.269-277, (1999).

[13] S. O. R. Moheimani, H. R. Pota and I. R. Petersen. Spatial balanced model reduction for flexible structures. In: *Proceedings of the 1997 American Control Conference*, Albuquerque, NM, Vol.5, pp. 3098-3102, (1997).

[14] H. Habibullah, H. R. Pota, I. R. Petersen and M. S. Rana. Tracking of Triangular Reference Signals Using LQG Controllers for Lateral Positioning of an AFM Scanner Stage. *IEEE/ASME Transactions on Mechatronics*, Vol. 19, No. 4, pp. 1105-1114, (2014).

[15] S. O. R. Moheimani, H. R. Pota and I. R. Petersen. Active control of noise and vibration in acoustic ducts and flexible structures-a spatial control approach. In: *Proceedings of the 1998 American Control Conference*, Philadelphia, PA, Vol.4, pp. 2601-2605, (1998).

[16] I.R. Petersen, H. R. Pota. Minimax LQG optimal control of a flexible beam. *Control Engineering Practice*, Vol. 11, No. 11, pp.1273-1287, (2003).

[17] W.R. Lee, L. Caccetta, K.L. Teo, and V. Rehbock. Optimal Design of Complex FIR Filters With Arbitrary Magnitude and Group Delay Responses. *IEEE Transactions on Signal Processing*, Vol. 54, No.5, pp. 1617-1628, (2006).

[18] B.K. Lau, V. Sreeram, Y.H. Leung and K.L. Teo. Design of Low Order Approximately Linear Phase IIR Filters. In *Proceedings of the IEEE Symposium on Advances in Digital Filtering and Signal Processing*, Victoria, BC, Canada, (1998).

[19] D.S. Naidu. Singular Perturbations and Time Scales in Control Theory and Applications: An Overview. *Dynamics of Continuous, Discrete and Impulsive Systems Series B: Applications and Algorithms*, Vol. 9, No. 2002, pp. 233-278, (2002).

[20] D.S. Naidu. Analysis of non-dimensional forms of singular perturbation structures for hypersonic vehicles. *Acta Astronautica*, Vol. 66, No. 3-4, pp. 577-586, (2010).

[21] H. M. Nguyen and D. S. Naidu. Singular Perturbation Analysis and Synthesis of Wind Energy Conversion Systems under Stochastic Environments. In: Proceedings of the 12th WSEAS International Conference on Advances in Systems Theory, Signal Processing and Computational Science, Turkey, (2012).

[22] Y. Zhang, D.S. Naidu, C. Cai and Y. Zou. Singular Perturbations and Time Scales in Control Theory and Applications: An Overview 2002-2012. *International Journal of Information and System Sciences*, Vol. 9, No. 1, pp. 1-36, (2014).

[23] Y. Zhang, D.S. Naidu, C. Cai and Y. Zou. Composite control of a class of nonlinear singularly perturbed discrete-time systems via D-SDRE. *International Journal Of Systems Science*, Vol. 47, No.11, pp. 2632-2641, (2016).

[24] B.D.O. Anderson and Y. Liu. Controller Reduction: Concepts and Approaches. *IEEE Transactions on Automatic Control*, Vol. 34, No. 8, pp.802-812, (1989).

[25] D. Enns. Model reduction with balanced realizations: An error bound and a frequency weighted generalization. In: *Proceedings of the 23rd IEEE Conference on Decision and Control, Las Vegas, USA*, pp. 127-132, (1984).

[26] C.A. Lin and T.Y. Chiu. Model Reduction via frequency weighted balanced realization. *Control Theory and Advanced Technology*, Vol. 8, pp. 341-451, (1992).

[27] G. Wang, V. Sreeram and W.Q. Liu. A new frequency weighted balanced truncation method and error bound. *IEEE Transactions on Automatic Control*, Vol. 44, No. 9, pp. 1734-1737, (1999).

[28] A. Varga and B.D.O. Anderson. Accuracy-enhancing methods for balancing related frequency weighted model and controller reduction. *Automatica*, Vol. 39, No. 5, pp. 919-927, (2003).

[29] W. Gawronski and J. Juang. Model reduction in limited time and frequency intervals. *International Journal of System Science*, Vol. 21, No. 2, pp. 349-376 (1990).

[30] S. Gugercin and A. C. Antoulas. A survey of model reduction by balanced truncation and some new results. *International Journal of Control*, Vol. 77, No. 8, pp.748-766 (2004).

[31] X. Du, A. Jazlan, V. Sreeram, R. Togneri, A. Ghafoor and S. Sahlan. A frequency limited model reduction technique for linear discrete systems, In: *Proceedings of the 3rd Australian Control Conference*, pp.421-426, (2013).

[32] S. Sahlan, A. Ghafoor, V. Sreeram. A new method for the model reduction technique via a limited frequency interval impulse response gramian. *Mathematical and Computer Modelling*, Vol. 55, No. 3-4, pp. 1034-1040 (2012).

[33] G. Schelfhout and B. De Moor. Time domain weighted balanced truncation. In: *Proceedings of the 3rd European Control Conference*, Vol. 3B, pp. 2187-2190, (1995).

[34] V. Sreeram. Frequency response error bounds for time-weighted balanced truncation. In: *Proceedings of the 41st IEEE Conference on Decision and Control*, Vol. 3, pp. 3330-3331, (2002).

[35] , M. Tahavori and H. Shaker. Relative error model reduction via time weighted balanced stochastic singular perturbation, *Journal of Vibration and Control*, Vol. 18, No. 13, pp. 2006-2016, (2011).

[36] S. Svoronos, G. Stephanopoulos and A. Aris. Bilinear approximation of general nonlinear dynamic systems with linear inputs. *International Journal of Control*, Vol. 31, No. 1, pp.109-126, (1980).

[37] J. Deutscher. Nonlinear model simplification using L2-optimal bilinearization, *Mathematical and Computer Modelling of Dynamical Systems*, Vol. 11, No.1, pp.1-19, (2005).

[38] H.T. Dorissen. Canonical forms for bilinear systems. *Systems and Control Letters*, Vol. 13, No. 2, pp.153-160, (1989).

[39] S. A. Al-Baiyat, M. Bettayeb and U. M. Al-Saggaf. New model reduction scheme for bilinear systems.*International Journal of Systems Science*, Vol. 25, No. 10, pp.1631-1642, (1994).

[40] L. Zhang and J. Lam. On H_2 Model reduction of bilinear systems. *Automatica*, Vol. 38, No. 2, pp. 205-216 (2002).

[41] D.D. Siljak. Decentralized control and computations: Status and prospects. *Annual Reviews in Control*, Vol. 20, pp.131-141 (1996).

[42] B. Moaveni and A. Khaki-Sedigh. *Control Configuration Selection for Multivariable Plants, Lecture Notes in Control and Information Sciences*, Vol. 391, Springer-Verlag, Berlin, Heidelberg (2009).

[43] W. Birk, M.C. Arranz and A. Johansson. An application software for visualization and control configuration selection of interconnected processes. *Control Engineering Practice*, Vol. 26, pp. 188-200 (2014).

[44] M.C. Arranz and W. Birk. New methods for interaction analysis of complex processes using weighted graphs. *Journal of Process Control*, Vol. 22, No. 1, pp. 280-295 (2012).

[45] H.R. Shaker and M. Komareji. Control Configuration Selection for Multivariable Nonlinear Systems. *Industrial and Engineering Chemistry Research*, Vol. 51, No. 25, pp. 8583-8587 (2012).

[46] B. Wittenmark and M. Salgado, Hankel-norm based interaction measure for input-output pairing. In: *Proceedings of the IFAC 15th Triennal World Congress*, Barcelona, Spain (2002).

[47] M. Salgado and A. Conley. MIMO interaction measure and controller structure selection. *International Journal of Control*, Vol. 77, No. 4, pp. 367-383 (2004).

[48] H.R. Shaker and J. Stoustrup. An interaction measure for control configuration selection for multivariable bilinear systems. *Nonlinear Dynamics*, Vol. 72, pp. 165-174 (2013).

[49] X. Li, C. Yu and H. Gao. Frequency limited H_∞ model reduction for positive systems.*IEEE Transactions on Automatic Control*, Vol. 60, No. 4, pp 1093-1098 (2015).

[50] D.W. Ding, X. Du, and X. Li. Finite-frequency model reduction of two-dimensional digital filters. *IEEE Transactions on Automatic Control*, Vol. 60, No. 6, pp. 1624-1629 (2015).

[51] X. Li, S. Yin, and H. Gao. Passivity-preserving model reduction with finite frequency approximation performance.*Automatica*, Vol. 50, No. 9, pp. 2294-2303 (2014).

[52] X. Du, and G. H. Yang, H_∞ Model reduction of linear continuous-time systems over finite frequency interval.*IET Control Theory and Applications*, Vol. 4, No. 3, pp. 499-508 (2010).

[53] M. Imran and A. Ghafoor. Model reduction of descriptor systems using frequency limited gramians. *Journal of the Franklin Institute*, Vol. 352, No. 1, pp. 33-51 (2015).

[54] M. Imran and A. Ghafoor. Stability preserving model reduction technique and error bounds using frequency-limited gramians for discrete-time systems. *IEEE Transactions on Circuits and Systems II: Express Briefs*, Vol. 61, No. 9, pp. 716-720 (2014).

[55] J. Shen and J. Lam. Improved results on H-infinity model reduction for continuous-time linear systems over finite frequency ranges. *Automatica*, vol. 53, pp. 79-84, (2015).

[56] H.R. Shaker, and M. Tahavori. Frequency interval model reduction of bilinear systems.*IEEE Transactions on Automatic Control*, Vol. 59, No. 7, pp. 1948-1953 (2014).

[57] X. Du, F. Fan, D. Ding and F. Liu. Finite-frequency model order reduction of discrete-time linear time-delayed systems. *Nonlinear Dynamics*, vol. 83, no. 49, pp. 2485-2496, (2016).

[58] V. Sreeram and S. Sahlan, Improved results on frequency-weighted balanced truncation and error bounds. *International Journal of Robust and Nonlinear Control*, Vol. 22, No. 11, pp. 1195-1211, (2012).

[59] V. Sreeram, S. Sahlan, W.M.W. Muda, T. Fernando and H.H.C. Iu. A generalised partial-fraction-expansion based frequency weighted balanced truncation technique, *International Journal of Control*, Vol. 86, No.5, pp. 833-843, (2013).

[60] J. Shen and J. Lam. H-infinity Model Reduction for Positive Fractional Order Systems. *Asian Journal of Control*, Vol.16, No. 2, pp. 441-450, (2014).

[61] H. Minh, C. Batlle and E. Fossas. A new estimation of the lower error bound in balanced truncation method, *Automatica*, Vol.50, No.8, pp. 2196-2198, (2014).

[62] X. Li, J. Lam, H. Gao and P. Li. Improved results on model reduction for Markovian jump systems with partly known transition probabilities, *Systems and Control Letters*, vol. 70, no. 2014, pp. 109-117, (2014).

[63] H.R. Shaker and M. Tahavori. Control configuration selection for bilinear systems via generalised Hankel interaction index array, *International Journal of Control*, vol.88, no.1, 2014, pp. 30-37, (2015).

[64] L. Zhang, J. Lam, B. Huang and G.H. Yang, On Gramians and Balanced Truncation of Discrete-Time Bilinear Systems, *International Journal of Control*, Vol. 76, No. 4, pp. 414-427 (2003).

[65] P. Houlis and V. Sreeram. A Parametrized Controller Reduction Technique, In: *Proceedings of the 45th IEEE Conference on Decision and Control, San Diego, USA*, pp. 3430-3435, (2006).

[66] P. Houlis and V. Sreeram. A Parametrized Controller Reduction Technique via a New Frequency Weighted Model Reduction Formulation, *IEEE Transactions on Automatic Control*, Vol. 54, No.5, pp.1087-1093, (2009).

[67] P. Houlis and V. Sreeram. A Parametrized Controller Reduction Technique, In: *Proceedings of the Joint 20th IEEE International Symposium on Intelligent Control (ISIC'05) and 13th Mediterranean Conference on Control and Automation (MED'05)*, Limassol, Cyprus, pp.537-542, (2005).

[68] P. Houlis and V. Sreeram. A generalized controller reduction technique using LFT framework. In: *10th International Conference on Control, Automation, Robotics and Vision, 2008. ICARCV 2008*, pp. 2130-2135, (2008).

[69] J.J. D'Azzo, C.H. Houpis and S.N. Sheldon. *Linear Control System Analysis and Design, Fifth Edition, Revised and Expanded*, CRC Press, 2003.

[70] B.L. Stevens and F.L. Lewis.*Aircraft Control and Simulation*, John Wiley and Sons, 2003.

[71] N.S. Nise. *Control Systems Engineering*, John Wiley and Sons, 2010.

[72] P. Houlis and V. Sreeram. A new double sided frequency weighted problem formulation. In: *Proceedings of the 2009 European Control Conference (ECC)*, pp. 1041-1046, (2009).

[73] B.D.O. Anderson and Y. Liu. Controller Reduction: Concepts and Approaches. *IEEE Transactions on Automatic Control*, Vol. 34, No. 8, pp.802-812, (1989).

[74] G. Obinata and B.D.O. Anderson. *Model Reduction for Control System Design*, London: Springer Verlag, 2001.

[75] M.S. Mahmoud and Y. Xia.*Applied Control System Design*, London: Springer-Verlag, 2012.

[76] G. Schelfhout and B.D. Moor. A note on closed-loop balanced truncation. *IEEE Transactions on Automatic Control*, Vol. 41, No. 10, pp. 1498-1500, (1996).

[77] A. Varga, A. Hansson and G. Puyou (Eds.), *Optimization Based Clearance of Flight Control Laws: A Civil Aircraft Application, Lecture Notes in Control and Information Sciences*, Vol. 416, Springer-Verlag: Berlin Heidelberg (2012).

[78] F. Wu and J. J. Jaramillo. Computationally efficient algorithm for frequency-weighted optimal H_∞ model reduction. *Asian Journal of Control*, Vol. 5, No. 3, pp. 341-349 (2003).

[79] H.R. Shaker and M. Tahavori. Frequency-interval control configuration selection for multivariable bilinear Systems. *Journal of Process Control*, Vol. 23, No. 6, pp. 894-904 (2013).

[80] K.V. Fernando and H. Nicholson. On the fundamental property of the cross-gramian matrix. *IEEE Transactions on Circuits and Systems*, Vol. 21, No. 2, pp. 349-376 (1984).

[81] C. Himpe and M. Ohlberger. Cross-gramian-based combined state and parameter reduction for large-scale control systems. *Mathematical Problems in Engineering*, Vol. 2014, No. 843869, pp.1-13 (2014).

[82] W.Q. Liu, V. Sreeram and K.L. Teo. Model Reduction for State-Space Symmetric Systems. *Systems and Control Letters*,Vol. 34, No.4, pp.209215, (1998).

[83] V. Sreeram and P. Agathoklis. On the computation of the Gram matrix in time domain and its application. *IEEE Transactions on Automatic Control*, Vol. 38, No.10, pp.1516-1520 (1993).

[84] V. Sreeram and P. Agathoklis. On the properties of Gram matrix. *IEEE Transactions on Circuits and Systems I: Fundamental Theory and Applications*, Vol. 41, No. 3, pp. 234-237 (1994).

[85] B. Moaveni and A. Khaki-Sedigh. Input-output pairing analysis for uncertain multivariable processes. *Journal of Process Control*, Vol. 18, No. 6, pp. 527-532 (2008).

[86] H.R. Shaker and M. Tahavori. Control configuration selection for bilinear systems via generalised hankel interaction index array. *International Journal of Control*, Vol. 88, No. 1, pp. 30-37 (2015).

[87] H.R. Shaker and M. Tahavori. Generalized hankel interaction index array for control structure selection for discrete-time MIMO bilinear processes and plants.

In: *Proceedings of the 53rd IEEE Conference on Decision and Control*, Los Angeles, California, USA, pp. 3149-3154 (2014).

[88] H.R. Shaker. Frequency-interval interaction measure for control configuration selection for multivariable processes. In: *Proceedings of the IEEE International Conference on Control Applications*, Hyderabad, India, pp. 889-893. (2013).

[89] L. Fortuna and M. Frasca. *Optimal and Robust Control: Advanced Topics with MATLAB*, CRC Press, Boca Raton (2012).

[90] A. Graham. *Kronecker Products and Matrix Calculus: With Applications, Ellis Horwood Series in Mathematics and its Applications*, Wiley, New York (1981).

[91] I. Alatiqi and L. Luyben. Control of a complex sidestream column/stripper distillation configuration. *Industrial and Engineering Chemistry Process Design and Development*, Vol. 25, No. 3, pp. 762-767 (1986).

[92] Y. Chahlaoui and P. V. Dooren. Benchmark examples for model reduction of linear time-invariant dynamical systems. In: P. Benner, V. Mehrmann and D.C. Sorensen (Eds.), *Dimension reduction of large-scale systems, Lecture Notes in Computer Science and Engineering*, Vol. 45, pp. 379-392, Springer-Verlag, Berlin, Heidelberg (2005).

[93] M. Opmeer and T. Reis, A lower bound for the balanced truncation error for MIMO systems, *IEEE Transactions on Automatic Control*, Vol.60, No.8, pp.2207-2212, (2015).

[94] H.B. Minh, C. Battle and E. Fossas, A new estimation of the lower error bound in balanced truncation method, *Automatica*, Vol.50 No.8, pp.2196-2198, (2014).

[95] H. Zhang, L. Wu, P. Shi and Y. Zhao, Balanced truncation approach to model reduction of Markovian jump time-varying delay systems, *Journal of the Franklin Institute*, Vol.352, No.10, pp.4205-4224, (2015).

[96] X. Li, C. Yu, H. Gao and L. Zhang. A new approach to H_∞ model reduction for positive systems, In: *Proceedings of the 19th IFAC World Congress*, (2014).

[97] X. Du, F. Fan, D.W. Ding and F. Liu. Finite-frequency model order reduction of discrete-time linear time-delayed systems. *Nonlinear Dynamics*, Vol.83, No.4, pp.24852496, (2016).

[98] D.W. Ding, X.J. Li, X. Du and X. Xie. Finite-Frequency Model Reduction of Takagi-Sugeno Fuzzy Systems. *IEEE Transactions on Fuzzy Systems*, Vol.PP No.81, pp.1-10, (2016).

[99] X.J. Li and G.H. Yang. Adaptive control in finite frequency domain for uncertain linear systems. *Information Sciences*, Vol.314 , No.1, pp.14-27, (2016).

[100] L.G. Horta, J.N. Juang and R.W. Longman. Discrete-time model reduction in limited frequency ranges. *Journal of Guidance, Control, and Dynamics*, vol. 16, no.6, pp. 1125-1130, (1993).

[101] D. Wang and A. Zilouchian. Model reduction of discrete linear systems via frequency-domain balanced structure. *IEEE Transactions on Circuits and Systems I: Fundamental Theory and Applications*, Vol. 47, No.6, pp. 830-837, (2000).

[102] P. D-Alessandro, A. Isidori and A. Ruberti. Realization and Structure Theory of Bilinear Dynamical Systems. *SIAM Journal on Control*, Vol.12, No.3, pp.517-535, (1974).

[103] H.R. Shaker and M. Tahavori. Time-interval model reduction of bilinear systems. *International Journal of Control*, Vol.87, No.8, pp.1487-1495, (2014).

[104] T. Hinamoto and S. Maekawa. Approximation of Polynomial State-Affine Discrete Time Systems. *IEEE Transactions on Circuits and Systems*, Vol.31, No.8, pp.713-721, (1984).

[105] M. Nabag, M.A. Al-Radhawi and M. Bettayeb, Model reduction of flat-plate solar collector using time-space discretization. In: *Proceedings of the 2010 IEEE International Energy Conference and Exhibition*, pp. 45-50, (2010).

[106] M.A. Al-Radhawi,M. Nabag and M. Bettayeb. Balanced Model Reduction of Flat-Plate Solar Collector using Descriptor State-Space Formulation, In: *Proceedings of the International Symposium on Environment Friendly Energies in Electrical Applications EFEEA*, pp. 1-6, (2010).

[107] G. Prakash and H.P. Garg. *Solar Energy: Fundamentals and Applications*, Tata McGraw-Hill Publishing Company, 2000.

[108] A. Ghafoor and V. Sreeram. Partial-Fraction Expansion Based Frequency Weighted Model Reduction Technique With Error Bounds. *IEEE Transactions on Automatic Control*, Vol.52, No.10, pp.1942-1948, (2007).

[109] V. Sreeram and S. Sahlan. Improved results on frequency-weighted balanced truncation and error bounds, *International Journal of Robust and Nonlinear Control*, Vol.22, No.11, pp. 1195-1211, (2012).

[110] V. Sreeram, S. Sahlan, W.M.W. Muda, T. Fernando and H.H.C Iu. A generalised partial-fraction-expansion based frequency weighted balanced truncation technique, *International Journal of Control*, Vol.86, No.5, pp. 833-843, (2013).

[111] G. Schelfhout and B. De Moor. Time Domain Weighted Balanced Truncation. In: *Proceedings of the 3rd European Control Conference,1995*, pp. 2187-2190, (1995).

[112] V. Sreeram. Frequency response error bounds for time-weighted balanced truncation, In: *Proceedings of the 41st IEEE Conference on Decision and Control*, pp. 3330-3331, (2002).

[113] M. Tahavori and H.R. Shaker. Relative error model reduction via time-weighted balanced stochastic singular perturbation. *Journal of Vibration and Control*, Vol. 18, No.13, pp. 1-11, (2012).

[114] M. Tahavori and H.R. Shaker. Time-weighted balanced stochastic model reduction. In: *50th IEEE Conference on Decision and Control and European Control Conference (CDC-ECC)*, pp. 7777-7781, (2011).

[115] K.V. Fernando and H. Nicholson. On the structure of balanced and other principal representations of SISO systems. *IEEE Transactions on Automatic Control*, Vol. 28, No.2, pp. 228-231, (1983).

[116] M.F. El-Refaie and M.A. Hashish. Temperature distributions in the flat-plate collector under actual unsteady insolation, *Applied Mathematical Modelling*, Vol. 4, No.3, pp. 181 - 186, (1980).

[117] T. Stykel. Gramian-Based Model Reduction for Descriptor Systems. *Mathematics of Control, Signals and Systems*, Vol. 16, No.4, pp. 297-319, (2004).

[118] V. Sreeram. Recursive technique for computation of gramians. *IEE Proceedings Part D, Control Theory and Applications*, Vol.140, No.3, pp.160-166, (1993).

[119] V. Sreeram and P. Agathoklis. Recursive technique for computation of Gramians. *IEE Proceedings Part D, Control Theory and Applications*, Vol.138, No.6, pp.529-534, (1991).

[120] K.C. Wan and V. Sreeram. Solution of the bilinear matrix equation using Astrom-Jury-Agniel algorithm, *IEE Proceedings Part D, Control Theory and Applications*, vol.142, pp.603-610, (1995).

[121] S. Streif, R. Findeisen and E. Bullinger. Relating Cross Gramians and Sensitivity Analysis in Systems Biology, In: *Proc. 17th Int. Symp. Math. Theory of Networks and Systems*, pp. 24-28, (2006).

[122] C. Himpe and M. Ohldberger. Model Reduction of Complex Hyperbolic Networks. In *Proceedings of the European Control Conference*, pp. 2739-2743, (2014).

[123] H.R. Shaker. Frequency-Interval Control Reconfigurability for Automated Processes. *Natural Hazards*, Vol.72, No.2, pp 1021-1027, (2014).

[124] K. Zhou, G. Salomon and E. Wu. Balanced realization and model reduction for unstable systems, *International Journal of Robust and Nonlinear Control*, Vol.9, No.3, pp. 183-198, (1999).

[125] H. Shaker. Generalized Cross Gramian for Linear Systems. In: *Proc. of the 7th IEEE Conference on Industrial Electronics and Applications (ICIEA)*, pp. 749-751, (2011).

[126] K. Zhou, J.C. Doyle and K. Glover *Robust and Optimal Control*, New Jersey: Prentice Hall, 1996.

[127] M. Imran, A. Ghafoor and V. Sreeram. A frequency weighted model order reduction technique and error bounds, *Automatica*, Vol.50, No.12 pp.3304 - 3309, (2014).

[128] S. Sahlan, A. Ghafoor and V. Sreeram. A new method for the model reduction technique via a limited frequency interval impulse response Gramian, *Mathematical and Computer Modelling*, Vol.55, No.3-4, pp.1034-1040, (2012).

[129] V. Sreeram, S. Sahlan, W.M.W Muda, T. Fernando and H.H.C. Iu. A generalised partial-fraction-expansion based frequency weighted balanced truncation technique. *International Journal of Control*, Vol.86, No.5, pp.883-843, (2013).

[130] V. Sreeram and S. Sahlan. Improved results on frequency-weighted balanced truncation and error bounds. *International Journal of Control*, Vol.22, No.11, pp.1195-1211, (2012).

[131] U.M. Saggaf and G.F. Franklin. On Model Reduction. In: *Proceedings of the 23rd IEEE Conference on Decision and Control*, pp.1064-1069, (1986).

[132] U.M. Saggaf and G.F. Franklin. Model reduction via balanced realization, *IEEE Transactions on Automatic Control*, Vol.AC-33, pp.687-692, (1988).

[133] S. Sahlan and V. Sreeram. New results on partial fraction expansion based frequency weighted balanced truncation. In: *Proceedings of the 2009 American Control Conference*, pp. 5695-5700, (2009).

[134] V. Sreeram, S. Sahlan, W.M.W Muda, T. Fernando and H.H.C. Iu, A generalised partial-fraction-expansion based frequency weighted balanced truncation technique, *International Journal of Control*, Vol.86, No.5, pp.833-843, (2013).

[135] V. Sreeram and B.D.O. Anderson, Frequency weighted balanced reduction technique: A generalization and an error bound. In: *Proceedings of the 34th IEEE Conference on Decision and Control*, pp.3576-3581, (1995).

[136] A. Ghafoor and V. Sreeram, Partial Fraction Expansion Based Frequency Weighted Model Reduction Techniquee with Error Bounds. *IEEE Transactions on Automatic Control*, Vol.52, No.10, pp.1942-1948, (2007).